



This is to certify that the

dissertation entitled

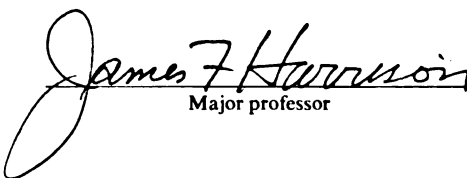
I. The Electronic and Geometric Structures of
Various Products of the $\text{Sc}^+ + \text{H}_2\text{O}$ and
 H_2S .

II. The Electronic and Geometric Structures
of $^+\text{ScSe}$ and $^+\text{ScSeH}$ presented by

Jeffrey Lee Tilson

has been accepted towards fulfillment
of the requirements for

~~Ph.D~~ degree in ~~Chemistry~~


Major professor

Date November 28, 1992



3 1293 01033 0425

LIBRARY
Michigan State
University

PLACE IN RETURN BOX to remove this checkout from your record.
TO AVOID FINES return on or before date due.

DATE DUE	DATE DUE	DATE DUE
_____	_____	_____
_____	_____	_____
_____	_____	_____
_____	_____	_____
_____	_____	_____
_____	_____	_____
_____	_____	_____

I. THE ELECTRONIC AND GEOMETRIC STRUCTURES OF
VARIOUS PRODUCTS OF THE $\text{Sc}^+ + \text{H}_2\text{O}$ AND H_2S
REACTIONS.

II. THE ELECTRONIC AND GEOMETRIC STRUCTURES OF
 $^+\text{ScSe}$ AND $^+\text{ScSeH}$

By

Jeffrey Lee Tilson

A DISSERTATION

Submitted to
Michigan State University
in partial fulfillment of the requirements
for the degree of

DOCTOR OF PHILOSOPHY

Department of Chemistry

1993

ABSTRACT

I. THE ELECTRONIC AND GEOMETRIC STRUCTURES OF
VARIOUS PRODUCTS OF THE $\text{Sc}^+ + \text{H}_2\text{O}$ AND H_2S
REACTIONS.

II. THE ELECTRONIC AND GEOMETRIC STRUCTURES OF
 $^+\text{ScSe}$ AND $^+\text{ScSeH}$

By

Jeffrey Lee Tilson

The products of the $\text{Sc}^+ + \text{H}_2\text{O}$ and H_2S reactions were investigated by constructing ab-initio MCSCF and MCSCF+1+2 wavefunctions for various states of ^+ScL , $^+\text{ScLH}$, Sc^+LH_2 , HSc^+LH and $\text{H}_2\cdots^+\text{ScL}$ (L=O and S). The energies were computed at the optimized geometries. A Mulliken population analysis was performed for each molecule. Where possible, comparisons to experimental data are made. The ground state product of the $\text{Sc}^+ + \text{H}_2\text{O}$ reaction is the insertion product, H^+ScOH which assumes a cis conformation and is 40 kcal/mol below the reactants. The two reaction products, $\text{H}_2\cdots^+\text{ScO}$ and H^+ScOH , are nearly degenerate ($\Delta E = 5$ kcal/mol) and

are both the result of an exoergic reaction. The $\text{H}_2 \cdots {}^+\text{ScO}$ product is the ground state ${}^+\text{ScO}$ molecule electrostatically bound to H_2 and is 35 kcal/mol below the reactants. The ground state of the reaction $\text{Sc}^+ + \text{H}_2\text{S}$ is the $\text{H}_2 \cdots {}^+\text{ScS}$ electrostatic species (34.5 kcal/mol below $\text{Sc}^+ + \text{H}_2\text{S}$) while the electrostatic product, Sc^+SH_2 , is exoergic by only 11.4 kcal/mol. The insertion product, $\text{H}-{}^+\text{ScSH}$, was examined and is not a minimum on the $\text{Sc}^+ + \text{H}_2\text{S}$ reaction surface.

The ${}^1\Sigma^+$, ${}^3\Delta$ and ${}^3\Sigma^+$ states of ${}^+\text{ScSe}$ and the ${}^2\Delta$ and ${}^2\Sigma^+$ states of ${}^+\text{ScSeH}$ were analyzed. The ground state ${}^+\text{ScSe}$ is a triply bonded species of ${}^1\Sigma^+$ symmetry with a bond strength of 84 kcal/mol. The ${}^3\Delta$ and ${}^3\Sigma^+$ excited states lie higher in energy at 31 and 28 kcal/mol, respectively. The ${}^+\text{ScSeH}$ molecule has a ${}^2\Delta$ ground state nearly degenerate with the excited ${}^2\Sigma^+$ state with both differentially stabilized by formation of the Se-H bond. This stabilization is consistent with the work on ${}^+\text{ScOH}$ and ${}^+\text{ScSH}$.

To Red, Joan, John, Nana and Herb

ACKNOWLEDGMENTS

I first want to sincerely thank Dr. James F. Harrison for accepting the job of being my mentor. His intellectual support, guidance, patients and stamina throughout my time in graduate school was second to none. No less important are the contributions of my guidance committee. In particular, Drs. George Leroi, Dan Nocera, Ned Jackson and John Allison for their advice and opinions. Thanks also to the faculty and staff of the Department of Chemistry (MSU) for help, advice and encouragement when it was needed and especially to Dr. K. Hunt and Dr. T. V. (TVA) Atkinson, for allowing me to frequently interrupt them to discuss the occasional intellectual curiosities of mine.

My time in graduate school would have been much less significant without the contributions of the expert service facilities and, of course, my friends.

Finally, I wish thank Michigan State University and the Department of Chemistry (MSU) for financial support during my graduate career.

TABLE OF CONTENTS

	Page
LIST OF TABLES	ix
LIST OF FIGURES	xii
KEYS TO SYMBOLS AND ABBREVIATIONS	xv
CHAPTER I	
INTRODUCTION	2
CHAPTER II	
THE ELECTRONIC AND GEOMETRIC STRUCTURES OF VARIOUS PRODUCTS OF THE $\text{Sc}^+ + \text{H}_2\text{O}$ AND H_2S REACTIONS.	
INTRODUCTION	5
BASIS SETS	6
FRAGMENT ENERGIES	7
MOLECULAR CODES	10
AB-INITIO CALCULATION OF ^+ScO AND ^+ScS	13
A. GENERAL CONSIDERATIONS	13
B. MCSCF RESULTS FOR ^+ScO	15
C. MCSCF RESULTS FOR ^+ScS	18
D. MCSCF+1+2 RESULTS FOR ^+ScO	20
E. MCSCF+1+2 RESULTS FOR ^+ScS	21
ELECTRONIC DISTRIBUTION	23
A. ^+ScO	23
B. ^+ScS	26
C. COMPARISON OF ^+ScO AND ^+ScS	28

	Page
D. DIFFERENCE DENSITY CONTOURS.....	30
AB-INITIO CALCULATIONS OF ^+ScOH AND ^+ScSH	32
A. ^+ScOH	32
B. ^+ScSH	37
C. COMPARISON OF ^+ScNH , ^+ScOH , AND ^+ScSH	41
REACTION PRODUCTS.....	42
A. $H-^+ScOH$	42
B. $^+ScOH_2$	45
C. COMPARISON WITH THE $^+Sc + NH_3$ SYSTEM.....	48
D. $^+Sc + SH_2$	51
E. H_2-^+ScS	54
F. $H-^+ScSH$	55
CHEMISTRY-PREDICTIONS.....	57
CONCLUSIONS.....	59
REFERENCES.....	66
 CHAPTER III	
THE ELECTRONIC AND GEOMETRIC STRUCTURES OF	
^+ScSe AND ^+ScSeH	
INTRODUCTION	71
BASIS SETS	72
MOLECULAR CODES	72
FRAGMENT ENERGIES	73
MCSCF FUNCTION FOR ^+ScSe	74
MCSCF+1+2 FUNCTION FOR ^+ScSe	79
ELECTRONIC STRUCTURE OF ^+ScSe	82
^+ScSeH GENERAL CONSIDERATIONS	91

	Page
ELECTRONIC STRUCTURE OF $^{+}\text{ScSeH}$	95
THERMOCHEMISTRY	101
SUMMARY	106
REFERENCES	108
APPENDIX A	
ELECTRONIC STRUCTURE THEORY: TECHNIQUES	
INTRODUCTION	111
HAMILTONIAN	112
CONSTRUCTION OF THE WAVEFUNCTION.....	116
SCF EQUATION	124
EXTENSIONS	126
REFERENCES.....	131
APPENDIX B	
LIST OF PUBLICATIONS	134

LIST OF TABLES

Table	Page
<u>CHAPTER II</u>	
1. Total Fragment Energies (au)	11
2. Dissociation Energies (kcal/mol).....	12
3. ^+ScS and ^+ScO Equilibrium energies (E_{min} , au), Vibrational frequencies (ω_e , cm^{-1}), Bond Lengths (r_e , au) and Dissociation Energies (D_e , kcal/mol)	19
4. Valence $^+ScO(H)$ MCSCF orbital populations at equilibrium.....	24
5. Valence $^+ScS(H)$ MCSCF orbital populations at equilibrium.....	27
6. MCSCF Gross atomic charges.....	29
7. $^+ScS(H)$ and $^+ScO(H)$ Equilibrium energies (au), Equilibrium bond lengths (au), and Dissociation energies (kcal/mol).....	39
8. Summary of MCSCF+1+2 $Sc^+ + SH$ and OH fragment energies (kcal/mol).....	44

Table	Page
9. H_2^+ScO and H^+ScOH Equilibrium Energies (au), Bond Lengths (au) and Angles (deg).....	46
10. $^3\text{A}_2$ and $^3\text{A}_1$ states of Sc^+SH_2 . Optimized Geometries and Total Energies.....	53
11. $\text{H}_2\cdots^+\text{ScS}$ Optimized geometry, Total Energy and Dissociation Energies.....	56
12. MCSCF+1+2 Dissociation Energies (D_e , kcal/mol).....	62
 <u>CHAPTER III</u>	
1. Fragment Total Energies (au)	75
2. Dissociation Energies (kcal/mol).....	76
3. $^+\text{ScSe}$, ^+ScS , and ^+ScO Equilibrium energies (E_{min} , au), Vibrational frequencies (ω_e , cm^{-1}), Bond Lengths (r_e , au) and Dissociation Energies (D_e , kcal/mol)	80
4. Valence $^+\text{ScSe}(\text{H})$ MCSCF orbital populations at equilibrium.....	83
5. Valence $^+\text{ScS}(\text{H})$ MCSCF orbital populations at equilibrium.....	86

Table	Page
6. Valence $^+ScO(H)$ MCSCF orbital populations at equilibrium.....	87
7. MCSCF Gross atomic charge distribution.....	89
8. $^+ScSe(H)$, $^+ScS(H)$, and $^+ScO(H)$ Equilibrium energies (au), Equilibrium bond lengths (au), and Dissociation energies (kcal/mol).....	93
9. Summary of MCSCF+1+2 $Sc^+ + H_2Se$, H_2S and H_2O fragment energies (kcal/mol).....	94

LIST OF FIGURES

Figure	Page
<u>CHAPTER II</u>	
1. MCSCF potential energies of the $1\Sigma^+$, 3Δ , and $3\Sigma^+$ states of ^+ScS and ^+ScO relative to the ground state asymptote.....	16
2. MCSCF+1+2 potential energies of the $1\Sigma^+$, 3Δ , and $3\Sigma^+$ states of ^+ScS and ^+ScO relative to the ground state asymptote.....	22
3. MCSCF Total density contours (TDCs) and Difference density contours (DDCs) for the $1\Sigma^+$, 3Δ and $3\Sigma^+$ states of ^+ScO	31
4. MCSCF Total density contours (TDCs) and Difference density contours (DDCs) for the $2\Sigma^+$ state of $^+\text{ScOH}$ and the $1\Sigma^+$ and $3\Sigma^+$ states of ^+ScO	34
5. MCSCF+1+2 relative energies (kcal/mol).....	36
6. MCSCF Total density contours (TDCs) and Difference density contours (DDCs) for the $2\Sigma^+$ state of $^+\text{ScSH}$ and the $1\Sigma^+$ and $3\Sigma^+$ states of ^+ScS	43

Figure	Page
7. Illustration of the energetics amongst the $\text{Sc}^+ + \text{SH}_2$ reaction products. Minima on the curve are MCSCF+1+2 optimized values.....	58
8. MCSCF+1+2 relative energies of the $\text{Sc}^+ + \text{OH}_2$ reaction.....	60
9. MCSCF+1+2 relative energies of the $\text{Sc}^+ + \text{SH}_2$ reaction.....	61

CHAPTER III

1. MCSCF potential energies of the $^1\Sigma^+$, $^3\Delta$ and $^3\Sigma^+$ states of $^+\text{ScSe}$, ^+ScS and ^+ScO relative to the ground state asymptote.....	78
2. MCSCF+1+2 potential energies of the $^1\Sigma^+$, $^3\Delta$ and $^3\Sigma^+$ states of $^+\text{ScSe}$, ^+ScS and ^+ScO relative to the ground state asymptote.....	81
3. Radial distribution function of the ground state ^+Sc (3D) Inner 1s core orbital not displayed.....	85
4. Orbital populations of ^+ScL and $^+\text{ScLH}$ (L=O, S, Se).....	90

Figure	Page
5. MCSCF Total density contours (TDCs) and Difference density contours (DDCs) for the $^2\Sigma^+$ state of $^+\text{ScSeH}$ and the $^1\Sigma^+$ and $^3\Sigma^+$ states of $^+\text{ScSe}$	97
6. MCSCF Total density contours (TDCs) and Difference density contours (DDCs) for the $^2\Sigma^+$ state of $^+\text{ScSH}$ and the $^1\Sigma^+$ and $^3\Sigma^+$ states of ^+ScS	98
7. MCSCF Total density contours (TDCs) and Difference density contours (DDCs) for the $^2\Sigma^+$ state of $^+\text{ScOH}$ and the $^1\Sigma^+$ and $^3\Sigma^+$ states of ^+ScO	99
8. Contours of the valence natural orbitals for the $^2\Sigma^+$ states of $^+\text{ScLH}$ at equilibrium.....	100
9. MCSCF+1+2 relative energies (kcal/mol) of selected $\text{Sc}^+ + \text{SeH}_2$ products.....	103
10. MCSCF+1+2 relative energies (kcal/mol) of selected $\text{Sc}^+ + \text{SH}_2$ products.....	104
11. MCSCF+1+2 relative energies (kcal/mol) of selected $\text{Sc}^+ + \text{OH}_2$ products.....	105

KEY TO SYMBOLS AND ABBREVIATIONS

<u>Symbol or Abbreviation</u>	<u>Meaning</u>
SCF	Self-Consistent-Field
GVB	Generalized Valence Bond
MCSCF	Multiconfiguration SCF
CI	Configuration Interaction
MCSCF+1+2	Single and double excitations from a MCSCF reference space
SCF+1+2	Single and double excitations from a SCF reference space
Ψ	Wavefunction
ϕ	Spatial or spin orbital
\mathcal{H}_e	Electronic hamiltonian
\mathcal{A}	Antisymmetrizing operator
∇^2	Laplace operator
\mathcal{F}/\mathbf{F}	Fock Operator/ Matrix
$\mathcal{J}_j(1) / \mathcal{K}_j(1)$	Coulomb/Exchange operator
J_{ij} / K_{ij}	Coulomb/Exchange energy
$\langle ij ij \rangle / \langle ij ji \rangle$	Coulomb/Exchange energy
au	Atomic Units Energy = hartree Distance = Bohrs (0.527 Ang.)
$\langle \rangle$	Bra-Ket Notation
R_e or R_{min}	Equilibrium distance
E_e or E_{min}	Equilibrium energy

<u>Symbol or Abbreviation</u>	<u>Meaning</u>
ω_e	Vibrational frequency (cm^{-1})
i, j	Electron index
k, p	Nuclear index
CSF	Configuration State Function
α, β	Spin functions (spinors)
Z_n	Atomic number of the n th nucleus
ϵ_i	Orbital (one-electron) energy
δ_{ij}	Kronecker Delta
χ_μ	μ th Basis function
p_x, p_y, p_z	Atomic (Real) p functions
$d_{x^2+y^2-2z^2}, d_{xy}, d_{xz}, d_{yz}, d_{x^2-y^2}$	Atomic (Real) d functions
TDC	Total density contour
DDC	Difference density contour

CHAPTER I

CHAPTER I

INTRODUCTION

The focus of the work presented in this dissertation is electronic structure calculations of transition metal (TM) containing species. The techniques employed are Multiconfiguration self-consistent-field (MCSCF) and configuration interaction calculations (CI). These methods are significantly more advanced than SCF calculations and are required to incorporate the important near degeneracy effects present in all TMs.

The work presented in Chapter II examines the possible products of the $\text{Sc}^+ + \text{H}_2\text{O}$ and H_2S reactions. Experimental data available for the $\text{Sc}^+ + \text{H}_2\text{O}$ reaction are compared. No experimental data are available for the SH_2 reaction. Many structural similarities exist between these two reactions, but the ground state reaction products are different.

Chapter III continues with a theoretical examination of $^+\text{ScSe}(\text{H})$, $^+\text{ScS}(\text{H})$, and $^+\text{ScO}(\text{H})$. The ligands (O, S, and Se) belong to Group VI and therefore have the same valence structure. This analysis allows us to make predictions for the reaction of $\text{Sc}^+ + \text{SeH}_2$. The filled 3d-shell of Se is found, as expected, to not significantly influence the bonding structure of $^+\text{ScSe}(\text{H})$ relative to $^+\text{ScO}(\text{H})$ and $^+\text{ScS}(\text{H})$.

Appendix A is included to outline the theoretical techniques used throughout this dissertation, with particular attention paid to the Hartree-Fock (HF) wavefunction and its extensions.

A listing of publications resulting from this work is presented in Appendix B.

CHAPTER II

CHAPTER II

THE ELECTRONIC AND GEOMETRIC STRUCTURES OF VARIOUS PRODUCTS OF THE $\text{Sc}^+ + \text{H}_2\text{O}$ AND H_2S REACTIONS.

INTRODUCTION

We are interested in characterizing the possible products of the gas phase reaction of the monovalent ions of the early transition metals with H_2O ¹ and H_2S .² In this dissertation the focus is on the simplest of these ions, Sc^+ , and this chapter reports the results of ab-initio electronic structure calculations on the systems ^+ScL in their $1\Sigma^+$, 3Δ and $3\Sigma^+$ states, the $^+\text{ScLH}$ 2Δ and $2\Sigma^+$ states and the reaction products $\text{H}-^+\text{ScLH}$, H_2^+ScL , and $^+\text{ScLH}_2$ where $L=\text{O}$ and S .

There has been extensive experimental and theoretical work on the reactions of transition metal ions with small ligands. Pertinent to this work are the ^+MO ($M=\text{Sc}$, Ti , etc.) bond strengths³ (in particular ^+ScO $D_0=159\pm 7$ kcal/mol) and the several experimental $^+\text{M-OH}$ and $^+\text{MO-H}$ ($M=\text{Sc}$, Ti , V , Cr , etc.) bond strengths.⁴ Recent results indicate a $^+\text{Sc-OH}$ bond strength of 87.8 kcal/mol and further suggests the reaction of Sc^+ with H_2O yields the product $\text{Sc}^+\cdots\text{OH}_2$ with an interaction energy (D_0) of 31.4 kcal/mol.⁵ There are no experimental data available for the $^+\text{ScS(H)}$ species.

The results of this work indicate that the bonding of H to the O in ^+ScO and the N in $^+\text{ScN}^6$ causes a differential strengthening of the Sc^+ to oxygen and nitrogen bonds of approximately 43 kcal/mol. This strengthening results from a ligand to metal sigma dative bond, formed in concert with the bond between N or O and the H atom. This added stabilization causes the $\text{Sc}^+ + \text{H}_2\text{O}$ ground state reaction product to be the insertion species,¹ HSc^+-OH , ($\Delta E = -40$ kcal/mol) with the electrostatic species, $^+\text{Sc}\cdots\text{OH}_2$, slightly higher⁷ ($\Delta E = -36.2$ kcal/mol). The analogous $^+\text{Sc} + \text{SH}_2$ reaction products were analyzed with emphasis placed on the strength and structure of the induced sigma dative bond.

The point groups employed in all calculations are either C_{2v} or C_s . This is possible because all the studied species are of the same or higher symmetry. It is always possible to use a less discriminating, i.e. lower, point group since it will fully contain all operations of the higher point group. This lowering of the point group order in a calculation will increase the amount of computational time but yields exactly the same results. The similarity of results allows us to interpret orbitals in terms of atomic type orbitals regardless of the selected point group. Throughout this dissertation the atomic, C_{2v} and C_s orbital symmetries will be used interchangeably.

BASIS SETS

The Scandium basis set used in this study consists of the (14s,9p,5d) basis from Wachters⁸ augmented with two diffuse p

functions (Dunning)⁹ and a diffuse d function as recommended by Hay.¹⁰ This set was contracted to (5s,4p,3d) following Raffennetti.¹¹

The Oxygen basis was the (11s,7p) set from Duijneveldt¹² augmented with a single diffuse d (exp=0.85) function and contracted to (4s,3p,1d) following Raffennetti.¹¹

The Sulfur basis was the (12s,9p) set from Huzinaga¹³ augmented with a diffuse s (exp = 0.60), a diffuse p (exp = 0.04) and a diffuse d (exp=0.31) function and contracted to (5s,5p,1d) following Raffennetti.¹¹

Two basis sets were used for the Hydrogen atom. The first consists of the Huzinaga¹³ (4s) augmented with a single p (exp=1.00) function and contracted to (2s,1p). This was the set chosen for the ^+ScOH , $H-^+ScOH$, ^+ScSH and $H-^+ScSH$ calculations. The second basis set consists of the above 4s basis augmented with a single s (exp=0.03) function and three p (exp=1.00, 0.33, 0.11) functions. This set was contracted to (3s,3p) and used in the $H_2 \cdots ^+ScO$ and $H_2 \cdots ^+ScS$ calculations. This basis was previously shown to adequately represent the polarizability of the H_2 molecule.¹⁴

FRAGMENT ENERGIES

Sc⁺

The ground state¹⁵ ($^3D, 3d^1 4s^1$) energy was computed using the SCF and SCF+1+2 (substitutions from only valence electrons) functions. The $Sc^{++}(^2D, 3d^1)$ SCF energy was also determined. The total energies plus the energy for the mixed state $Sc^+(^3B_2, 3d^1 3d\pi^1)$ are collected in Table 1.

S

The Sulfur $3P$ state¹⁵ was analyzed with MCSCF and MCSCF+1+2 wavefunctions. The MCSCF function was constructed from the in-out correlation (GVB) of the doubly occupied $3p\pi_x$ orbital plus all valence spin couplings. This results in 5 CSFs of 3B_2 symmetry. All valence single and double substitutions (of 3B_2 symmetry) from the MCSCF reference space result in the 619 CSF MCSCF+1+2 function. These energies are collected in Table 1.

SH

The $^2\Pi$ state of SH was examined by a 2B_1 17 configuration MCSCF function. This was constructed from all spin couplings of a GVB(2/4) function (correlating the π bond and the doubly occupied S $3p\pi_y$ orbital) and a 3,766 CSF MCSCF+1+2 constructed from all valence single and double substitutions (of 2B_1 symmetry) from the MCSCF reference space. The total energies are listed in Table 1 while the dissociation energy (D_e) is collected in Table 2.

H₂S

The energy and optimized geometry of H₂S was computed with a 37 CSF MCSCF function constructed to correlate in a GVB way the two bonding orbitals and the S doubly occupied out-of-plane orbital plus all spin couplings and a 23,922 CSF MCSCF+1+2 function derived from all valence single and double substitutions from the MCSCF reference space. The equilibrium energies are listed in Table 1 and the dissociation energies in Table 2.

O

The Oxygen $3P$ state¹⁵ was analyzed with MCSCF and MCSCF+1+2 wavefunctions. The MCSCF function was constructed

from the left-right correlation (GVB) of the doubly occupied $2p\pi_x$ orbital plus all valence spin couplings. This results in 5 CSFs of 3B_2 symmetry. All valence single and double substitutions (of 3B_2 symmetry) from the MCSCF reference space result in the 408 CSF MCSCF+1+2. These energies are collected in Table 1.

OH

The $^2\Pi$ state of OH was examined by a 2B_1 17 configuration MCSCF function. This was constructed from all spin couplings of a GVB(2/4) function (correlating the π bond and the doubly occupied O $2p\pi_y$ orbital) and a 2,729 CSF MCSCF+1+2 constructed from all valence single and double substitutions (of 2B_1 symmetry) from the MCSCF reference space. The total energies are listed in Table 1 while the dissociation energy (D_e) is collected in Table 2.

H₂O

The energy and optimized geometry of H₂O was computed with a 37 CSF MCSCF function (constructed from all spin couplings of a GVB(2/4) function) and an 18,410 CSF MCSCF+1+2 function derived from all valence single and double substitutions from the MCSCF reference space. The equilibrium energies are listed in Table 1, and the dissociation energies in Table 2.

H₂ and H

The H (2S)¹⁵ energy was computed with a SCF function using the (2s,1p) basis. This energy is collected in Table 1. The total energy of H₂ using the (3s,3p) basis was determined with a 3 CSF MCSCF and 120 CSF MCSCF+1+2 function constructed from all single and double excitations. The total energies and D_e are listed in Tables 1 and 2, respectively.

MOLECULAR CODES

All ab-initio calculations on the oxygen containing species were done on a FPS-164 jointly supported by the Michigan State University Chemistry Department and the Office of the Provost by using the Argonne National Laboratory collection of Quest-164 codes. The integrals were calculated using the program ARGOS written by Pitzer;¹⁶ the SCF and MCSCF calculations were done using GVB164 written by Bair¹⁷ and the UEXP program and related utility codes written by Shepard.¹⁸ The configuration interaction calculations were performed using the program UCI (and related utility codes) written by Lischka et al.¹⁹

Ab-initio calculations on the sulfur containing species were done on a Stardent TITAN computer located in the Michigan State University Chemistry Department using the Argonne National Laboratory collection of COLUMBUS codes.²⁰

All density and difference density contours were calculated with the MSUPLOT collection of codes written by Harrison, and all spectroscopic constants were determined by performing a Dunham analysis.²¹

Table 1: Total Fragment Energies (au)

Fragment	E_{\min} (MCSCF)	E_{\min} (MCSCF+1+2)
Sc ⁺ $^3D(4s^1 3d^1)$	-759.52848	-759.52906
Sc ⁺ $^3B_2(3d\pi^1 3d\delta^1)$	-759.48576	-759.49960
Sc ⁺⁺ $^2D(3d^1)$	-759.08187	
S 3P	-397.50318	-397.54525
O 3P	-74.82254	-74.87100
H 2S	-0.49928	
SH $^2\Pi$	-398.11446	-398.16883
SH ₂ 1A_1	-398.73762	-398.80756
OH $^2\Pi$	-75.46483	-75.52573
OH ₂ 1A_1	-76.14408	-76.21173
H ₂ $^1\Sigma_g^+(3s/3p)$	-1.14813	-1.16652

Table 2: Dissociation Energies (kcal/mol)

	MCSCF(D_e/D_0)	MCSCF+1+2(D_e/D_0)	Exp (D_0) ^a
$\text{SH}^2\Pi \rightarrow \text{S}^3\text{P} + \text{H}^2\text{S}$	70.3/69.4	78.0/77.0	81.4
$\text{OH}^2\Pi \rightarrow \text{O}^3\text{P} + \text{H}^2\text{S}$ ^b	89.7/84.5	97.6/92.2	101.0
$\text{H}_2^1\Sigma^+_g(3s/3p) \rightarrow 2\text{H}^2\text{S}$ ^b	93.8/87.7	105.4/99.3	103.3
$\text{SH}_2 \rightarrow \text{S}(^3\text{P})+2\text{H}(^2\text{S})$	148.0	165.5	
$\text{OH}_2 \rightarrow \text{O}(^3\text{P})+2\text{H}(^2\text{S})$ ^b	202.7	214.7	219.4

^a ref (24).

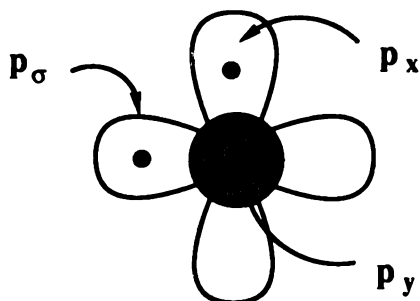
AB-INITIO CALCULATION OF ^+ScO AND ^+ScS A. GENERAL CONSIDERATIONS

In the following discussion only the oxygen-containing species will be discussed. In all cases, Sulfur may be substituted for Oxygen with the appropriate change in valence orbital level.

If the two valence electrons on Sc^+ form two bonds with the two unpaired electrons in the ground state of O, the resulting molecule is a singlet of Σ symmetry and can be represented by the Lewis structure

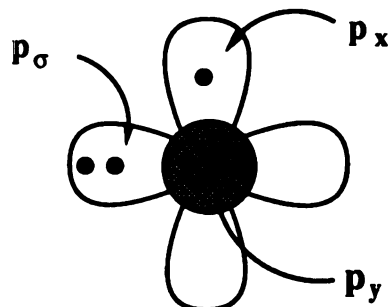


where we suppress the explicit representation of the O 2s electrons. The ground state oxygen atom may approach the Sc^+ in either of two orientations, according to whether the oxygen 2ps orbital is singly or doubly occupied.



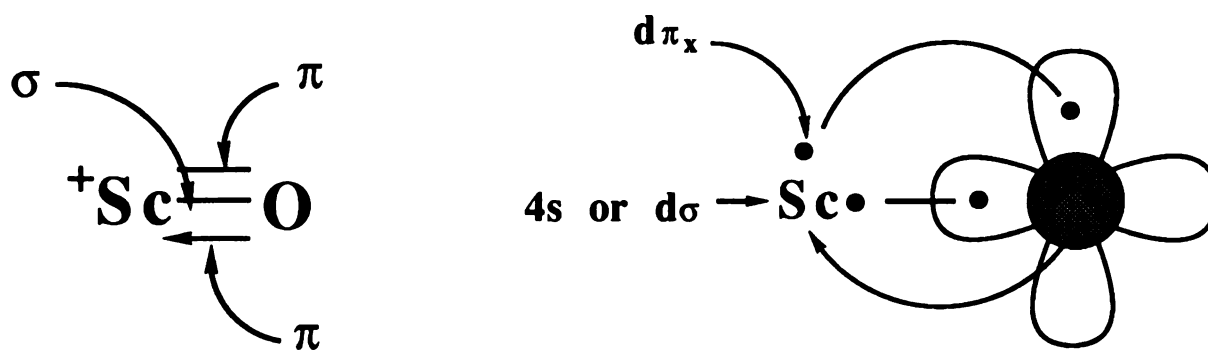
Π orientation

OR

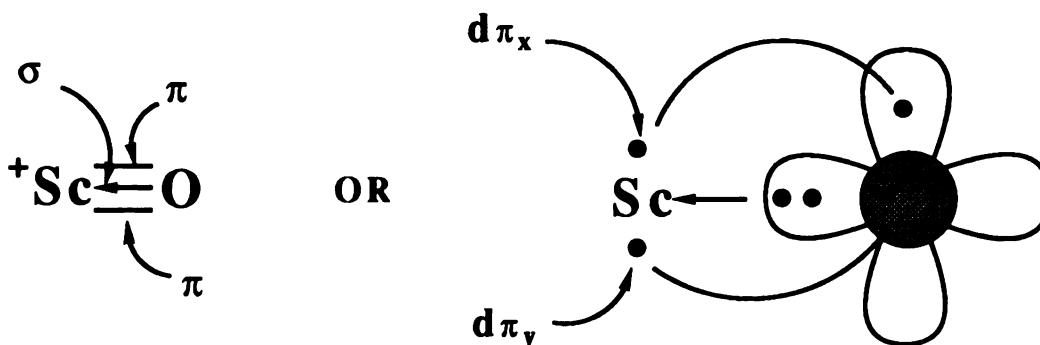


Σ^- orientation

The local symmetry of O in the first approach is Π and in the second, Σ^- . If O is in the Π orientation, Sc^+ must also be locally Π and this may be accomplished using either the ground $4s3d$ configuration ($4s3d\pi_x$ or $4s3d\pi_y$) or the low lying $3d^2$ configuration ($3d\sigma3d\pi_x$ or $3d\sigma3d\pi_y$). These options result in the Lewis structure



where one of the π bonds results from the singlet coupling of the Sc^+ $d\pi$ and O $2p\pi$ and the second π bond is a dative bond formed from the lone pair in the $2p\pi$ orbital on O and the empty $d\pi$ on Sc^+ . In the calculations the π bonds are of course equivalent. The Sc^+ σ electron is asymptotically either a $4s$ or $3d\sigma$. If, however, O is in the Σ^- orientation, Sc^+ must also be locally Σ^- . This may be achieved using the d^2 configuration, in particular $d\pi_x d\pi_y$. This results in the Lewis structure



where the σ electrons are formally from O. Clearly the equilibrium structure will be a mixture of the two Lewis structures.

B. MCSCF RESULTS FOR ^+ScO

The character of both Lewis structures may be incorporated into a 3 pair Generalized Valence Bond²² (GVB) wavefunction of the form

$$\Psi \sim (\text{core})^2 (8\sigma^2 - \lambda 9\sigma^2)(3\pi_x^2 - \nu 4\pi_x^2)(3\pi_y^2 - \nu 4\pi_y^2)$$

where the core electrons are suppressed for brevity but are always fully optimized in all calculations. An MCSCF function of this form which includes all possible spin couplings consists of 37 configuration state functions (CSFs). A function of this form allows the bonds to properly separate to the ground state atoms for large internuclear distances. In particular, the σ bond $(8\sigma^2 - \lambda 9\sigma^2)$ separates to the $Sc^+ 4s^1$ and $O 2p_z^1$ orbitals while the two π bonds together separate to the $Sc^+ 3d\pi^1$ and $O 2p\pi^4$ configurations. The energy predicted by this function is shown in Figure 1 as a function of Sc-O separation. This function predicts an equilibrium separation of 3.095 au and a dissociation energy, D_e , of 134 kcal/mol. Also shown in Figure 1 are various low lying triplet states. The $^3\Sigma^+$ state obtains by triplet coupling the σ bonding electrons in the $^1\Sigma^+$ state. The $d\delta_+$ symmetry orbitals were eliminated from the $^3\Sigma^+$ calculation to prevent collapsing to the δ_+ component of the lower energy $^3\Delta$ state.

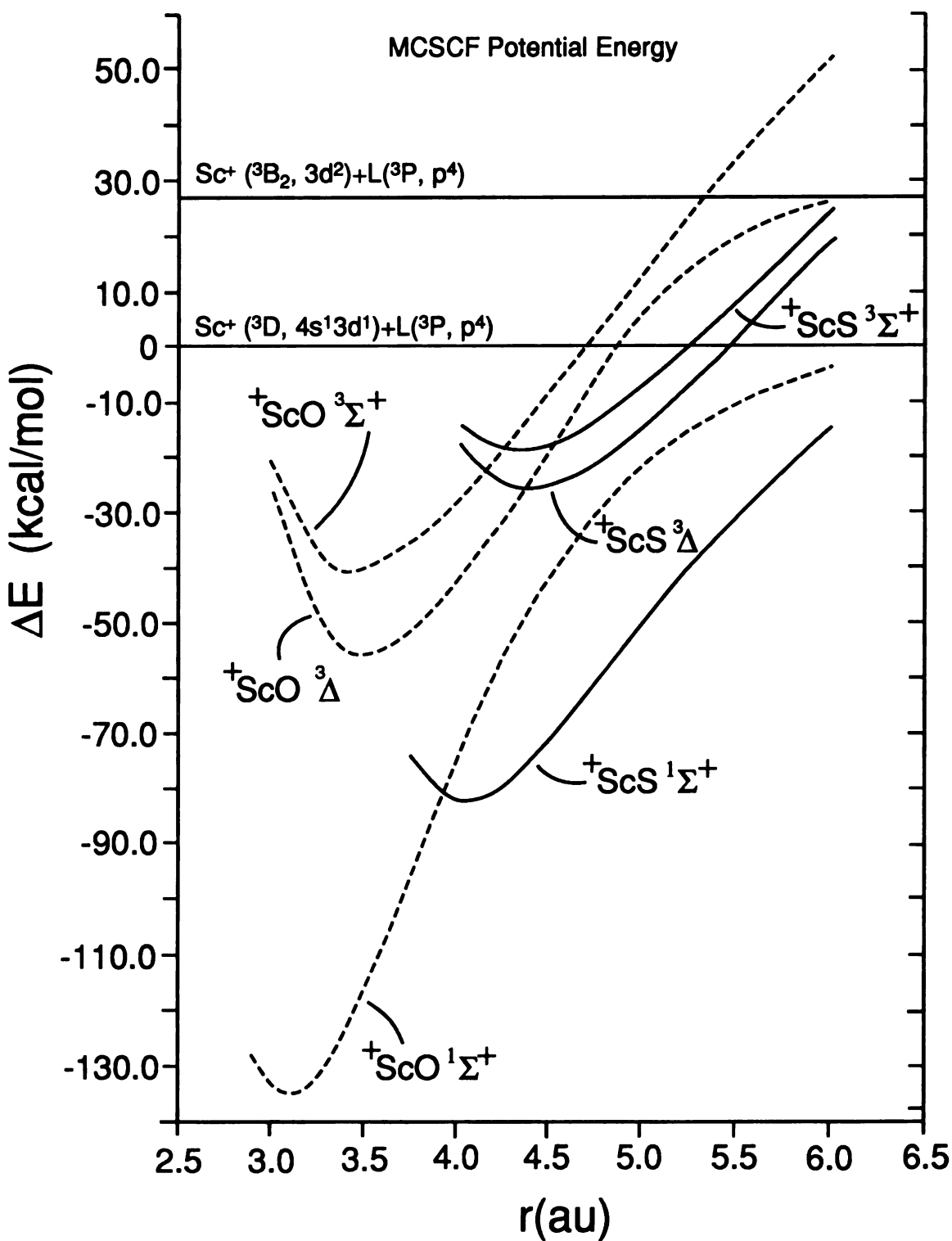


Figure 1. MCSCF potential energies of the ¹Σ⁺, ³Δ and ³Σ⁺ states of ⁺ScS and ⁺ScO relative to the ground state asymptote. Energy is in kcal/mol. The atomic structure at the asymptote is indicated by both atomic symmetry and valence configuration (L=O and S)

One of the triplet coupled electrons becomes localized on Sc^+ in an orbital of $3d\sigma$ symmetry with some $4s$ character while the companion electron settles into an oxygen $2p\sigma$ orbital.

The bond length in this state is longer than in the $^1\Sigma^+$ state (3.454 au versus 3.095 au) and the molecule contains two equivalent π bonds and no σ bond. This molecular state should dissociate to the ground¹⁵ 3D state of Sc^+ and the ground¹⁵ 3P state of O and its D_e relative to this asymptote is 39 kcal/mol. If we imagine forming this state from the asymptotic ground state fragments we must triplet couple the spatially extensive Sc^+ $4s$ and the O $2p\sigma$ electrons and singlet couple the Sc^+ $3d\pi$ and singly occupied O $2p\pi$ orbital. At large Sc-O separations the π,π bond would be very weak and the repulsive triplet coupling in the σ system dominant. Consequently we anticipate that this state would be repulsive at large separations and would have to overcome a barrier to obtain the electronic structure we see at equilibrium. This equilibrium structure obtains when this repulsive curve intersects the attractive $^3\Sigma^+$ curve which separates to the Sc^{++} (2D ; $3d\sigma$) + O^- (2P ; $2p\sigma$) asymptote. The second triplet is of $^3\Delta$ symmetry and is obtained from the $^3\Sigma^+$ by moving the unpaired σ electron on Sc into a δ orbital. The δ occupation forces dissociation to the higher energy asymptote seen in Figures 1 and 2. Both of these states have π,π bonds and no σ bond. Exciting an unpaired electron from the σ orbital on Sc^+ to its δ_- orbital puts more electron density on Sc^+ in the π region and weakens the π,π bonds. This results in the $^3\Delta$ bond length increasing to 3.50 au as compared to 3.45 au in the $^3\Sigma^+$ state. This σ to δ_- excitation also reduces the repulsion between the unpaired electron on Sc^+ and the O $2p\sigma$

electron. That the total energy of the $^3\Delta$ state drops by 15 kcal/mol relative to the $^3\Sigma^+$ state suggests the reduced repulsion more than compensates for the slight reduction in the π,π bond strength.

The absolute energies (E_{\min}), dissociation energies (D_e), bond lengths (r_e), and vibrational frequencies (ω_e) are collected in Table 3.

C. MCSCF RESULTS FOR ^+ScS

A MCSCF function that includes the two important configurations for ^+ScS is constructed as follows.

$$\Psi \sim (\text{core})^2 (10\sigma^2 - \lambda 11\sigma^2)(4\pi_x^2 - v 5\pi_x^2)(4\pi_y^2 - v 5\pi_y^2)$$

where the structural correlation is achieved with a GVB(3/6) function²² followed by all spin couplings. This results in 37 configuration state functions (CSFs) of $^1\Sigma^+$ symmetry under the C_{2v} point group. The σ bond ($10\sigma^2 - \lambda 11\sigma^2$) separates to the $\text{Sc}^+ 4s^1$ and S $3p_z^1$ orbitals while the two π bonds together separate to the $\text{Sc}^+ 3d\pi^1$ and S $3p\pi^4$ configurations for large internuclear distances

The energy predicted by this function is displayed in Figure 1 as a function of the Sc-S internuclear distance. The D_e relative to the ground state products is calculated to be 82 kcal/mol with an equilibrium separation of 4.048 au.

The $^3\Sigma^+$ MCSCF is obtained by triplet coupling the $^1\Sigma^+$ sigma valence electrons. The Sc δ_+ symmetry orbitals were eliminated to prevent collapse to the δ_+ component of the lower energy $^3\Delta$ state. This results in 25 CSFs. The equilibrium structure has two π,π bonds

Table 3: ${}^1\text{ScS}$ and ${}^1\text{ScO}$ Equilibrium Energies (E_{min})(au), Vibrational Frequencies (ω_e)(cm^{-1}), Bond Lengths (r_e)(au) and Dissociation Energies (kcal/mol).

State	Energy		r_e		ω_e		D_e		Exp.
	MCSCF	MCSCF+1+2	MCSCF	MCSCF+1+2	MCSCF	MCSCF+1+2	MCSCF	MCSCF+1+2	
${}^1\text{ScS}^1\Sigma^+$	-1157.16247	-1157.22884	4.0477	4.0802	587	574	82.1	96.9	
${}^1\text{ScS}^3\Delta$	-1157.07250	-1157.13827	4.3767	4.3797	450	445	25.6	40.1	
${}^1\text{ScS}^3\Sigma^+$	-1157.06154	-1157.11827	4.3152	4.5611	423	358	18.8	27.6	
${}^1\text{ScO}^1\Sigma^+$	-834.56442	-834.63270	3.0953	3.1196	1067	1134	134.2	146.0	159 ± 7^d
${}^1\text{ScO}^3\Delta$	-834.43800	-834.50591	3.5008	3.4941	743	734	54.8	66.4	
${}^1\text{ScO}^3\Sigma^+$	-834.41312	-834.47419	3.4537	3.4361	592	622	39.2	46.5	

^a ref (3)

with one of the triplet coupled sigma electrons localized in a Scandium $3d\sigma+\lambda 4s$ orbital and the other in a Sulfur $3p\sigma$ orbital.

The bond length increases relative to the $^1\Sigma^+$ state by 0.267 au to 4.315 au and the D_e relative to the ground state asymptote becomes 18.8 kcal/mol. We expect the long range Sc^+ to S interaction to be attractive (electrostatic) but as the two atoms approach along the $^3\Sigma^+$ curve we anticipate a repulsive interaction between the triplet coupled sigma electrons ($\text{Sc}^+ 4s + \text{S } 3p\sigma$) analogous to ^+ScO . The $^3\Delta$ function results from moving the $\text{Sc}^+ 3d\sigma+\lambda 4s$ electron to a $3d\delta_-$ orbital. This results in a 25 CSF MCSCF function giving rise to a π,π doubly bonded species with one electron localized in a $\text{Sc}^+ 3d\delta_-$ orbital and the other in a S $3p\sigma$. The bond length increases slightly to 4.377 au while the D_e relative to the ground state asymptote becomes 25.6 kcal/mol. The $^3\Delta$ and $^3\Sigma^+$ energies are displayed as a function of internuclear distance in Figure 1. The D_e , r_e and vibrational frequencies (ω_e) are collected in Table 3.

D. MCSCF+1+2 RESULTS FOR ^+ScO

The three states of ^+ScO described above were studied using multireference configuration interaction (CI) techniques. For each state we constructed a CI wavefunction containing all single and double substitutions from the MCSCF reference space. For example, the $^1\Sigma^+$ MCSCF space consisted of 37 CSFs. All single and double excitations from the space, consistent with the $^1\Sigma^+$ symmetry, result in 23,990 CSFs. Several experiments were performed to test the adequacy of this procedure. In the first we added an additional

active σ orbital to the MCSCF space and generated 81 CSFs. All singles and doubles from this reference space resulted in 40,996 CSFs. These additional configurations lowered the total energy of the $1\Sigma^+$ state by 10 millihartrees (mH) at the MCSCF level and 1 mH at the MCSCF+1+2 level, but had no appreciable effect on r_e or D_e .

In the second we examined the necessity of including the O 2s orbital to the MCSCF (CI) active space. The O 2s orbital was added to the MCSCF active space (generating 81 CSFs) followed by all valence single and double substitutions and resulted in 99,463 CSFs. We also constructed a CI function by allowing all valence single and double substitutions (including the O 2s) from the 37 CSF MCSCF reference space. This resulted in 76,659 CSFs. The total CI energy dropped by 60 mH for each function while the computed D_e remained essentially the same at 145.9 and 144.7 kcal/mol, respectively.

We conclude from these experiments that excitations from the O 2s orbital are not important in determining the relative energy and r_e of the low lying states of ^+ScO . The size of the triplet states constructed as all single and double excitations from the MCSCF reference space was 29,481 CSFs ($^3\Delta$) and 24,133 CSFs ($^3\Sigma^+$). The ^+ScO potential curves at the MCSCF+1+2 level are presented in Figure 2 and the calculated r_e , D_e and ω_e s are collected in Table 3.

E. MCSCF+1+2 RESULTS FOR ^+ScS

The three states of ^+ScS described above were also examined using multi-reference configuration interaction (MCSCF+1+2) techniques. The MCSCF+1+2 wavefunction for each state was

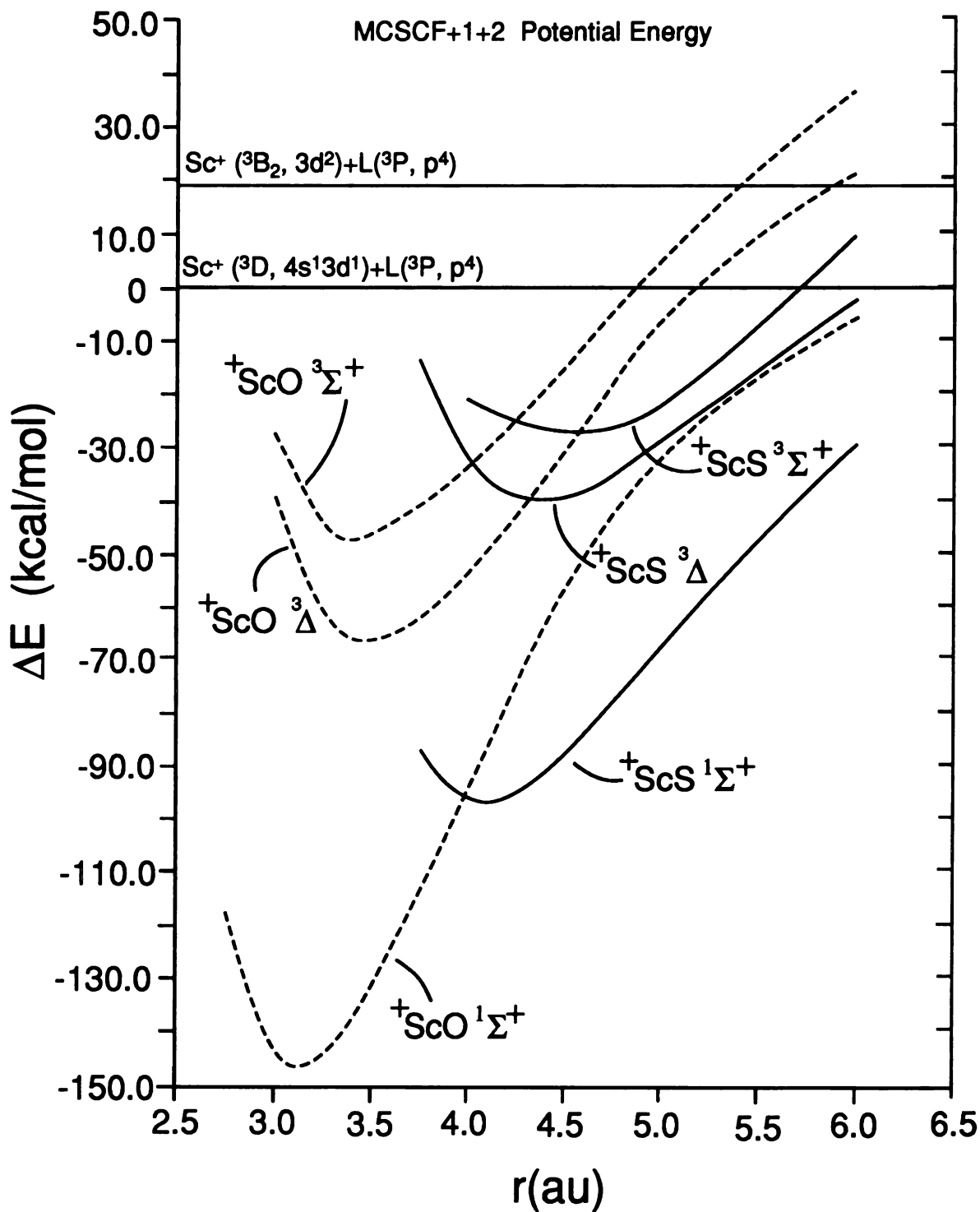


Figure 2. MCSCF+1+2 potential energies of the $1\Sigma^+$, 3Δ and $3\Sigma^+$ states of $+\text{ScS}$ and $+\text{ScO}$ relative to the ground state asymptote. Energy is in kcal/mol. The atomic structure at the asymptote is indicated by both atomic symmetry and valence configuration (L=O and S)

constructed by allowing all single and double excitations from the MCSCF reference space.

In particular, the triplet states resulted in 34,952 CSFs ($^3\Delta$) and 29,205 CSFs ($^3\Sigma^+$) and the ground state ($^1\Sigma^+$) was 28,337 CSFs. The predicted energies are displayed as a function of Sc-S distance in Figure 2. The inclusion of dynamic correlation accounted for by the MCSCF+1+2 function drops the total energy by around 60 mH but has only a small effect on the computed dissociation energies and no effect on the state orderings. The D_e , r_e and ω_e are collected in Table 3.

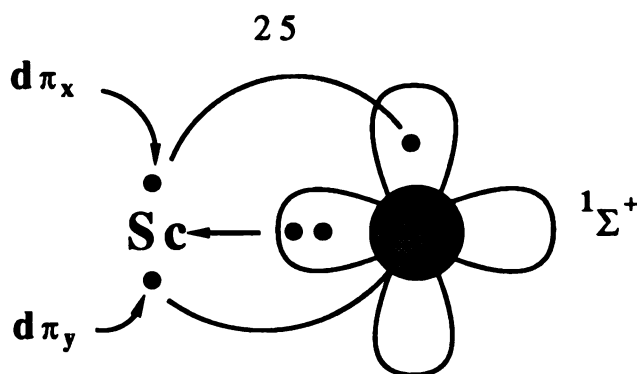
ELECTRONIC DISTRIBUTION

A. ^+ScO

Included in Table 4 are the valence orbital populations^{2 3} predicted by the MCSCF function for various states of ^+ScO . Note that in the $^1\Sigma^+$ state there is very little Sc^+ 4s character and the Sc^+ ion has lost electrons to neutral O. The charge distribution may be rationalized by imagining the in-situ Sc^+ ion in the $d\pi_x d\pi_y$ configuration interacting with the O atom in the $2p\sigma^2 2\pi_x 2\pi_y$ configuration. Oxygen first donates charge to the empty 3d σ on Sc^+ via the dative interaction of the doubly occupied O 2p. As charge leaves O in the σ system it returns in the π system.

Table 4: Valence ^+ScO (F) MCSCF orbital populations at equilibrium

State	Sc^+										O			$H(O)$
	4s	4p σ	4p $_x$	4p $_y$	3d σ	3d p_x	3d p_y	3d $_z$	2s	2p σ	2p $_x$	2p $_y$		
$^+ScO(^1\Sigma^+)$	0.02	0.19	0.05	0.05	0.55	0.43	0.43	-	1.80	1.44	1.52	1.52		
$^+ScO(^3\Delta)$	0.02	0.09	0.04	0.04	0.07	0.16	0.16	1.00	1.88	0.94	1.80	1.80		
$^+ScO(^3\Sigma^+)$	0.40	0.07	0.04	0.04	0.67	0.19	0.19	-	1.90	0.96	1.77	1.77		
$^+ScOH(^2\Delta)$	0.03	0.10	0.03	0.03	0.10	0.12	0.12	1.00	1.74	1.37	1.83	1.83	0.64	
$^+ScOH(^2\Sigma^+)$	0.48	0.08	0.03	0.03	0.61	0.16	0.16	-	1.76	1.42	1.80	1.80	0.67	



While the total charge on the Sc^+ ion in the $^3\Sigma^+$ state is similar to that in the $^1\Sigma^+$ state (+1.40 vs +1.28) the character of the electrons is very different. In particular, in the $^3\Sigma^+$ state there is a large 4s component and a significantly reduced 3d π occupation. We can rationalize this by noting that the $^3\Sigma^+$ may be formed from the $^1\Sigma^+$ by triplet coupling the σ bonding electrons. This localizes one electron in σ orbitals on Sc and the other in a 2p σ on O. As a result of this transfer the oxygen atom becomes more positive and attracts electrons into the 2p π orbitals, considerably reducing the Sc^+ 3d π occupation. The choice Sc^+ has to make is the relative amount of 4s and 3d σ character to allot to its unpaired electron. If the in-situ character of Sc was Sc^{++} we would expect the unpaired electron to be primarily 3d σ .¹⁵ The observed 40% 4s, 60% 3d σ reflects the intermediacy of the Sc^+ charge (greater than +1 but less than +2). The electron distribution in the $^3\Delta$ can be understood by noting that the $^3\Delta$ is formed from the $^3\Sigma^+$ by exciting the unpaired σ electron to a d orbital, precluding any 4s character.

B. ${}^+ScS$

The valence orbital populations²³ as predicted by the MCSCF functions for the ${}^+ScS$ states are collected in Table 5. We find that the Sc^+ 4s contribution to the ${}^1\Sigma^+$ state is small (0.17) though non-negligible and that Scandium has lost some electron density to S. The equilibrium structure is described as Sc^+ in a 3F ($3d\pi_x, 3d\pi_y$) state in-situ bonded to S with two π, π bonds and a (primarily) S $3p\sigma$ to Sc^+ $3d\sigma$ dative bond. This structure arises when S donates charge in the sigma system (sigma dative bond) followed by π density being transferred back from Sc^+ to S. The distribution of bonding electrons in the ${}^+ScS$ ${}^3\Delta$ and ${}^3\Sigma^+$ states are similar with both markedly different from the ${}^1\Sigma^+$ state. We find that precluding the sigma dative bond formation results in significantly more π density (approx. 0.30e per bond) being transferred from Sc^+ to S. When the sigma electrons are triplet coupled one becomes localized on Scandium and the other on Sulfur. This results in relatively less sigma electron density on S in the $3p\sigma$ orbital, causing a greater propensity to attract density into its $3p\pi$ orbitals thus reducing the Sc $3d\pi$ occupation.

The contribution of the Sc^+ 4s to the ${}^3\Sigma^+$ state is twice that for the ${}^1\Sigma^+$ state. This can be understood by realizing the ${}^3\Sigma^+$ state results from triplet coupling the sigma electrons in the ${}^1\Sigma^+$ with the localized electron on Sc^+ becoming of $3d\sigma + \lambda 4s$ character.

Table 5: Valence ^+ScS (H) MCSCF orbital populations at equilibrium

State	Sc^+										S			$H(S)$
	4s	4p σ	4p $_x$	4p $_y$	3d σ	3d p_x	3d p_y	3d δ	3s	3p σ	3p $_x$	3p $_y$		
$^+ScS(^1\Sigma^+)$	0.17	0.06	0.08	0.08	0.43	0.52	0.52	-	1.94	1.42	1.39	1.39		
$^+ScS(^3\Delta)$	0.10	0.06	0.08	0.08	0.08	0.21	0.21	1.00	1.90	0.86	1.71	1.71		
$^+ScS(^3\Sigma^+)$	0.30	0.07	0.08	0.08	0.86	0.22	0.22	-	1.92	0.87	1.69	1.69		
$^+ScSH(^2\Delta)$	0.14	0.08	0.08	0.08	0.10	0.19	0.19	1.00	1.79	1.11	1.73	1.73	0.78	
$^+ScSH(^2\Sigma^+)$	0.28	0.09	0.08	0.08	0.93	0.20	0.20	-	1.80	1.14	1.71	1.71	0.78	

This structure strikes a balance between the lower energy Scandium $4s3d$ configuration and the $3d^2$ configuration which distorts the charge perpendicular to the sigma orbitals, effectively draining charge from the internuclear region.

The $^3\Delta$ state arises from moving the Sc $3d\sigma+\lambda 4s$ electron to a $Sc^+ 3d\delta_-$ orbital. The bonding structure doesn't change, indicating that both electrons are simply spectators. The MCSCF gross atomic charges for ^+ScS are collected in Table 6.

C. COMPARISON OF ^+ScO AND ^+ScS

In comparison to ^+ScO we find that in general the ^+ScS gross charge transferred is less as expected from the longer bond distance. We find the sigma bond composition in $^+\text{ScO } ^1\Sigma^+$ to be an O $2p\sigma$ and Sc^+ hybrid composed of the $4s$, $4p\sigma$ and $3d\sigma$ orbitals¹. Similarly, the $^+\text{ScS } ^1\Sigma^+$ sigma bond is found to be a S $3p\sigma$ plus $Sc^+ 4s$, $4p\sigma$, $3d\sigma$ hybrid with, however, the $4p\sigma$ and $4s$ contributions inverted relative to ^+ScO . In $^+\text{ScS } ^1\Sigma^+$ the $Sc^+ 4s$ orbital is much more important than the $4p\sigma$. This larger $4s$ contribution weakens the sigma bond because of the lesser overlap with the S $3p\sigma$. This greater importance is caused by the larger internuclear separation and the consequently smaller in-situ gross charge on Sc in ^+ScS . This causes a larger portion of the wavefunction to be composed of the $4s3d$ configuration relative to ^+ScO . This smaller overlap would result in a smaller charge donation to Scandium in the sigma system and hence a smaller amount of back donation in the π system as suggested in Table 5.

Table 6: MCSCF Gross Atomic Charges

System	State	Gross atomic charge		
		Sc	S	H(S)
+ScS	($1\Sigma^+$)	+1.14	-0.14	
+ScS	(3Δ)	+1.18	-0.18	
+ScS	($3\Sigma^+$)	+1.17	-0.17	
+ScSH	(2Δ)	+1.14	-0.36	+0.22
+ScSH	($2\Sigma^+$)	+1.14	-0.36	+0.22
		Sc	O	H(O)
+ScO	($1\Sigma^+$)	+1.28	-0.28	
+ScO	(3Δ)	+1.42	-0.42	
+ScO	($3\Sigma^+$)	+1.40	-0.40	
+ScOH	(2Δ)	+1.41	-0.77	+0.36
+ScOH	($2\Sigma^+$)	+1.45	-0.78	+0.33

D. DIFFERENCE DENSITY CONTOURS

The electron distribution in the $^1\Sigma^+$ and $^3\Sigma^+$ states is so different that it is easily seen at the total density level. The total density (ρ) is obtained from the MCSCF NOs with the following equation:

$$\rho(\mathbf{R}) = \langle \psi | \sum_i \delta(\mathbf{r}_i - \mathbf{R}) | \psi \rangle.$$

where r_i denotes the electron coordinates and \mathbf{R} is the field coordinate. The total density simplifies to

$$\rho(\mathbf{R}) = \sum_i n_i \phi_i^2(\mathbf{R})$$

where ϕ is a *spatial* natural orbital (NO) and n_i is the occupation of the orbital. The difference density contours (DDCs) are obtained by subtracting one density from another.

Figure 3 shows the total electron density of ^+ScO contoured in a plane containing both nuclei for these two states. The Sc atom is to the left of O. Positive contour levels are indicated by solid lines and negative contours by dashes. For both states, there is an decrease of density in the σ space relative to the ground state. This is caused by the triplet coupling of the valence sigma electrons. Dashed lines in the π space reflect the concomitant increase in π density.

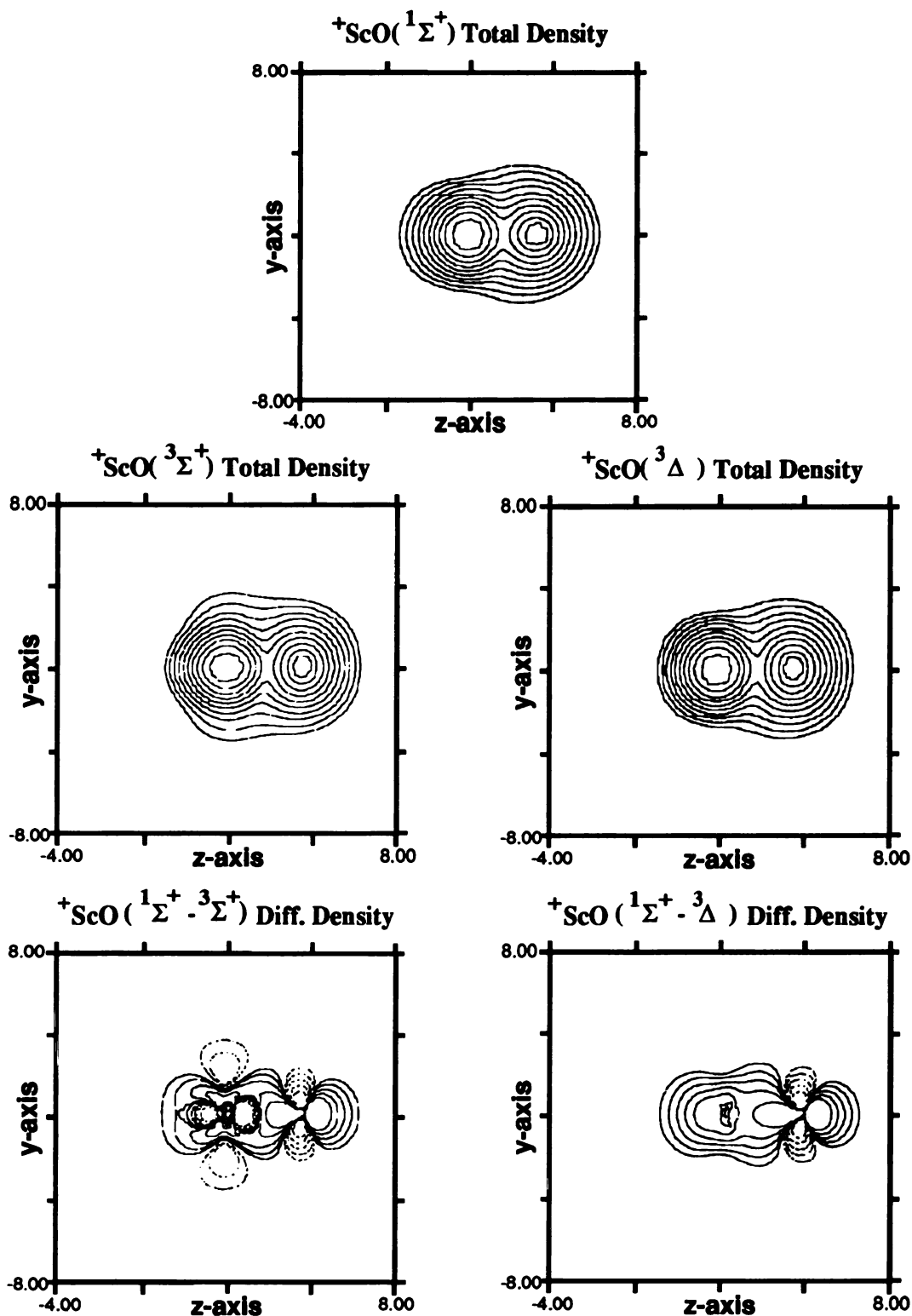
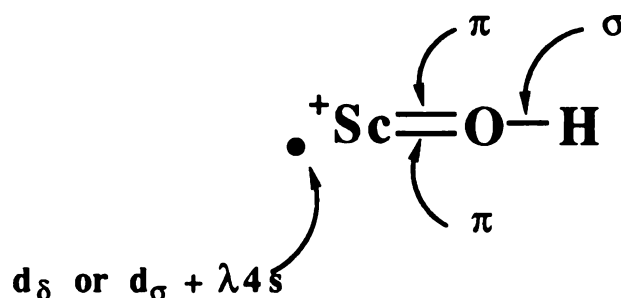


Figure 3. MCSCF Total density contours (TDCs) and difference density contours (DDCs) for the $1\Sigma^+$, 3Δ and $3\Sigma^+$ states of ${}^+ScO$. The DDCs are molecular differences where the indicated triplet state is subtracted from the ground $1\Sigma^+$ state. The triplets are at the equilibrium geometry. The contour levels range from 0.0025e to 1.28e (TDCs) and -0.04 to +0.04 (DDCs). Each level differs by a factor of 2. No zero contour is displayed and negative contours are indicated by a dashed line.

AB-INITIO CALCULATIONS OF $^+\text{ScOH}$ AND $^+\text{ScSH}$ A. $^+\text{ScOH}$

The hydroxide can be formed by adding a H atom to ^+ScO . Both the $^3\Delta$ and $^3\Sigma^+$ states have an unpaired 2p electron on oxygen and singlet coupling the H 1s electron to the oxygen electron results in the linear $^2\Delta$ and $^2\Sigma^+$ states of $^+\text{ScOH}$. These two states have the Lewis structure



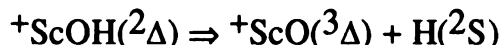
in which the unpaired electron is localized on Sc^+ in either a $d\delta$ ($^2\Delta$) or sigma orbital of mixed $d\sigma$ and 4s character ($^2\Sigma^+$). MCSCF functions which correlate the three bonds and allow all spin couplings consist of 76 CSFs in C_s symmetry for each molecular state. We optimized the $^+\text{Sc-O}$ and OH bond lengths as well as the $^+\text{Sc-O-H}$ angle at the MCSCF and MCSCF+1+2 levels. Both electronic states are linear and the total energy, bond lengths and various dissociation energies are collected in Table 7. The electron populations in the valence orbitals and the charges on each atom are collected in Tables 4 and 6.

The $^2\Delta$ state of $^+\text{ScOH}$ is calculated to be 17.2 kcal/mol lower than the $^2\Sigma^+$ state, which is very similar to the corresponding $^3\Delta$ - $^3\Sigma^+$

separation of 19.9 kcal/mol for ${}^+ScO$ (both calculated at the MCSCF+1+2 level of theory). As we see from Table 4, the H atom has little effect on the charge distribution on Sc^+ and in particular on the character of the unpaired electron.

Figure 4 shows the electron density in the ${}^2\Sigma^+$ state of ${}^+ScOH$ minus the density in the ${}^3\Sigma^+$ and ${}^1\Sigma^+$ states of ${}^+ScO$. The ${}^+ScOH({}^2\Sigma^+) - {}^+ScO({}^1\Sigma^+)$ difference density illustrates the negligible effect bonding of H to O has on the character of the Sc^+ non bonding electron. The difference density is very similar to that of ${}^+ScO({}^1\Sigma^+) - {}^+ScO({}^3\Sigma^+)$ (Figure 3) and results from a similar mixing of $d\sigma$ and $4s$ orbitals. The ${}^+ScOH({}^2\Sigma^+) - {}^+ScO({}^3\Sigma^+)$ density shows little difference in the Scandium structure, in-situ, and indicates that slightly more ${}^+Sc-O$ sigma density is present in the hydroxide.

The relative energies of ${}^+ScO$ and ${}^+ScOH$ are shown in Figure 5. Experimental values (corrected for zero point energy) are shown in parenthesis. Our calculated bond energy for free OH is 97.6 kcal/mol, approximately 10% lower than the experimental D_e (corrected to 0K) of 106.8 kcal/mol.²⁴ We have two options for the OH bond strength in ${}^+ScOH({}^2\Delta)$. First, we may break the OH bond along the Δ potential curve



which requires 139.1 kcal/mol, significantly larger than the free OH value. This enhanced OH bond strength obtains because the ${}^+Sc-O$ and O-H bonds are strongly coupled in ${}^+ScOH({}^2\Delta)$.

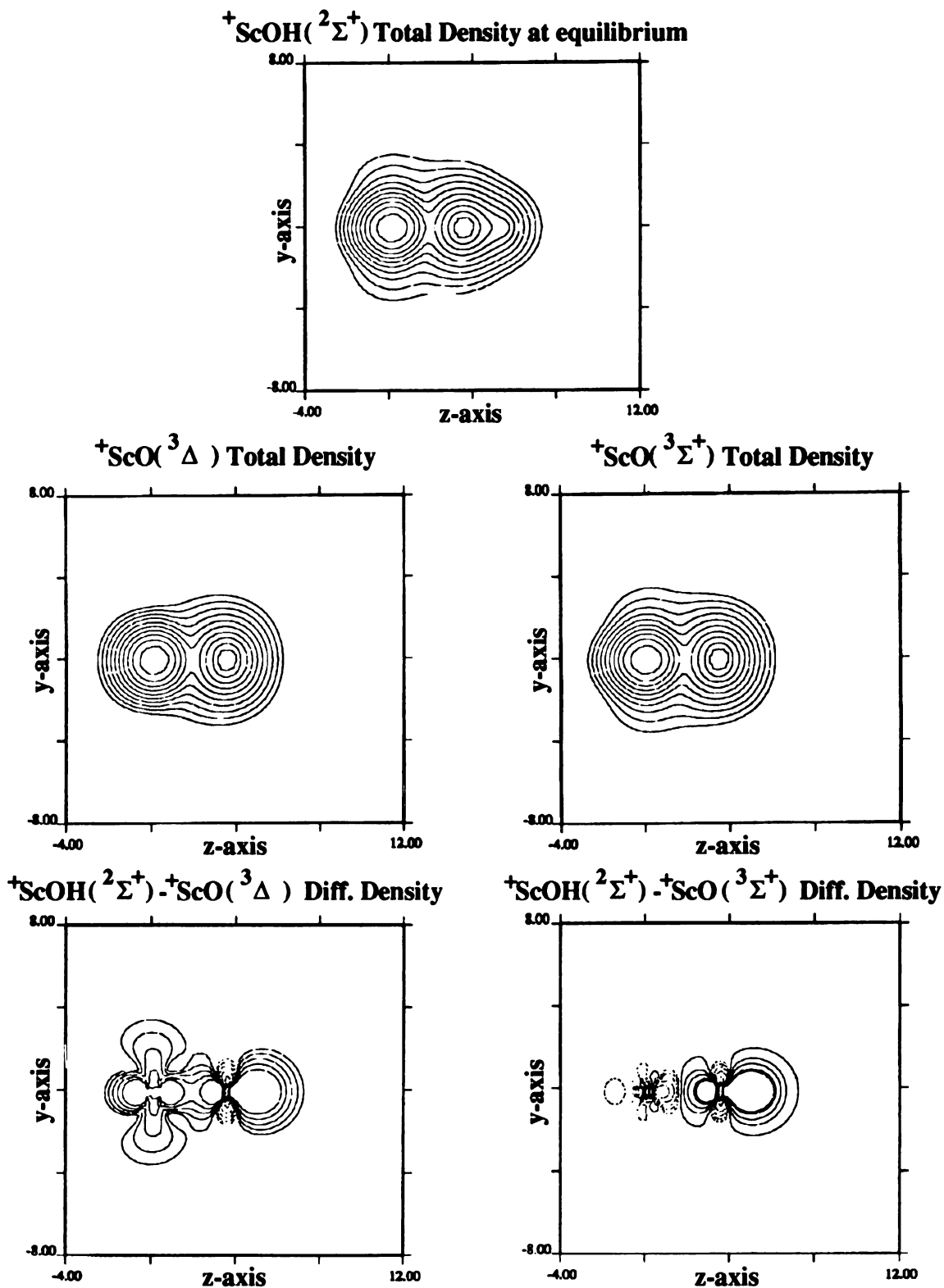


Figure 4. MCSCF total density contours (TDCs) and difference density contours (DDCs) for the $2\Sigma^+$ state of ${}^+ScOH$ and the $1\Sigma^+$ and $3\Sigma^+$ states of ${}^+ScO$. The DDCs are molecular differences where the ${}^+ScO$ states are subtracted from the ${}^+ScOH$ density. The ${}^+ScO$ states are at the equilibrium ${}^+ScOH$ (Sc-O) geometry. Contour levels range from 0.0025e to 1.28e (TDCs) and -0.04e to 0.04e (DDCs). Each level differs by a factor of 2. No zero contours are displayed and negative contours are indicated by dashes.

When H bonds to the unpaired $2p\sigma$ electron in ${}^+ScO(^3\Delta)$ the O $2s$ and $2p\sigma$ hybridize, simultaneously strengthening the OH bond and forming a dative bond in the empty σ space of Sc^+ using the companion to the O-H bond hybrid. This symbiosis also manifests itself in a stronger than expected Sc-O bond strength in ${}^+ScOH$. From Figure 5 we see that the ${}^+Sc-O$ bond strength in ${}^+ScOH$ is 108 kcal/mol, intermediate between the strength of a ${}^+ScO(^2\Delta)$ double bond (66.4 kcal/mol) and the ${}^+ScO(^1\Sigma^+)$ triple bond (146.0 kcal/mol). Our computed ${}^+Sc-OH$ bond strength (108 kcal/mol) is significantly higher than that reported⁵ by Magnera et al. (87.8 kcal/mol). These experiments determine the ${}^+Sc-OH$ energy from the parent molecule, $(H_2OScOH)^+$. If the structure of this species were of the form $H_2O\cdots{}^+Sc-OH$, then the intact ${}^+Sc-OH$ would prefer to be in its ground ${}^2\Delta$ state in-situ. The ${}^2\Delta$ state positions the Sc non-bonding electron in a $3d\delta_-$ orbital perpendicular to the internuclear axis and would minimize the repulsions to an electrostatically bound H_2O molecule. The energy of the ${}^2\Sigma^+$ state of ${}^+ScOH$ is 17 kcal/mol (MCSCF+1+2, Table 7) higher than the ${}^2\Delta$. While an H_2O molecule should still be able to electrostatically bind to the Sc atom, there should be more repulsion between H_2O and the now *in-axis* $3d\sigma$ electron. This would likely increase the ${}^2\Sigma^+ \leftarrow {}^2\Delta$ separation and could possibly account for the 20 kcal/mol discrepancy.

The second option for the OH bond breakage is the thermodynamically lowest path



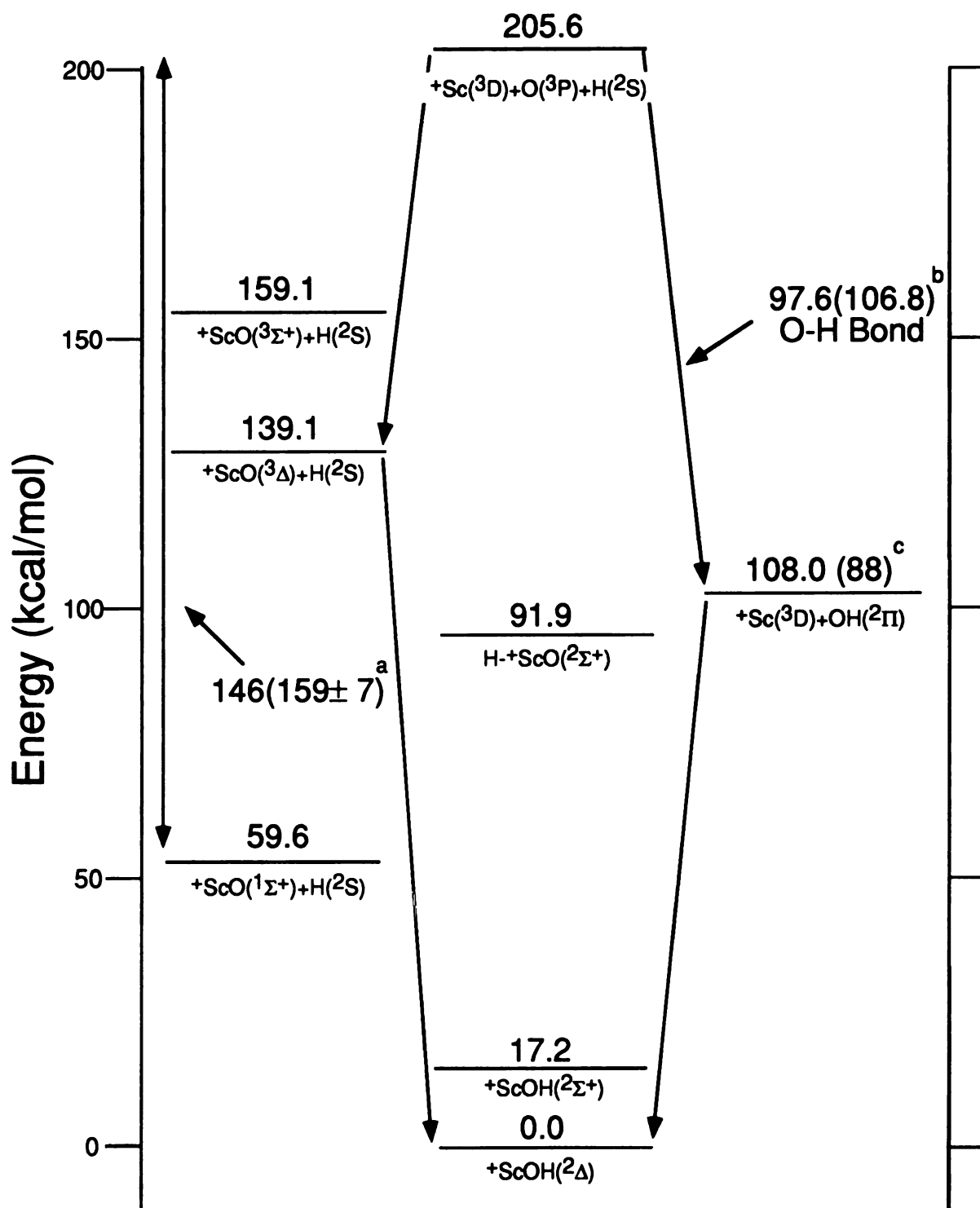
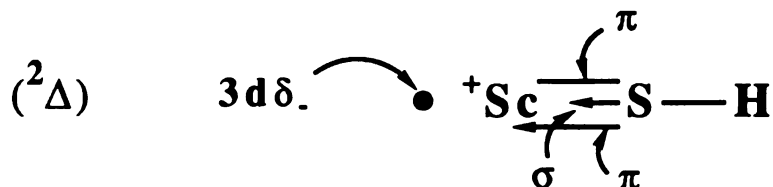


Figure 5. MCSCf+1+2 relative energies (kcal/mol) (numbers in parenthesis are experimental values)
^a Ref (3), ^b Ref (24) Value given as D_e corrected to 0K, ^c Ref (5).

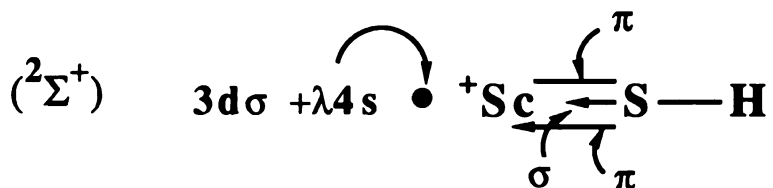
which requires 59.6 kcal/mol. This is much lower than the free OH bond strength, reflecting the differentially stronger ^+Sc-O bond in $^+ScO(^1\Sigma^+)$ compared to $^+ScOH(^2\Delta)$.

B. ^+ScSH

^+ScSH states of $^2\Delta$ and $^2\Sigma^+$ symmetry can be formed when a H atom bonds to the S $3p\sigma$ electron in $^+ScS\ ^3\Delta$ and $^3\Sigma^+$, respectively. This gives rise to the Lewis structures



and



The $^2\Delta$ MCSCF wavefunction was constructed to correlate the 3 bonds in a GVB way, followed by all spin couplings, and results in 76 CSFs. The $^2\Sigma^+$ MCSCF was constructed to correlate the two π bonds in a GVB way and three valence sigma orbitals. All spin couplings on this function result in 144 CSFs. All calculations were performed under the C_{2v} point group. The MCSCF+1+2 wavefunctions were

constructed by allowing all valence single and double substitutions from the MCSCF functions and results in 138,529 CSFs for the ${}^2\Delta$ and 149,312 CSFs for the ${}^2\Sigma^+$. The Sc^+ $3d\delta_+$ orbitals were eliminated from all ${}^+\text{ScSH } {}^2\Sigma^+$ calculations to prevent collapsing to the lower energy ${}^2\Delta(\delta_+)$ state. The total energy, optimized geometries and bond dissociation energies are collected in Table 7.

The ${}^2\Delta$ state is calculated to be 14.2 kcal/mol (MCSCF+1+2) lower in energy than the ${}^2\Sigma^+$. This is similar to the (MCSCF+1+2) ${}^+\text{ScS } {}^3\Delta - {}^3\Sigma^+$ difference of 12.6 kcal/mol and slightly smaller than the corresponding ${}^+\text{ScOH}$ difference of 17.2.¹

The MCSCF electron distributions for the ${}^+\text{ScSH } {}^2\Sigma^+$ and ${}^2\Delta$ states are collected in Tables 5 and 6. We find the bonding of H to ${}^+\text{ScS}$ has little effect on the ${}^+\text{Sc-S } \pi$ bonding structure. Analysis of the natural orbitals (NOs) and populations does, however, reveal significant changes in the sigma structure. In both states the S $3s$ and $3p\sigma$ orbitals are hybridized, one hybrid bonding to H and the other interacting with the Sc^+ $4s + 3d\sigma$ orbitals.

The strength of the Sc^+ to SH sigma dative interaction can be estimated by examining the bond energies from Tables 2, 3 and 7. Our calculated SH (${}^2\Pi$) bond strength (D_0) of 77.0 kcal/mol ($D_e=78.0$ kcal/mol) is approximately 6% lower than the experimental value of 81.4 kcal/mol.²⁴

If the ${}^+\text{ScSH } ({}^2\Delta)$ S-H bond is broken along the Δ potential curve

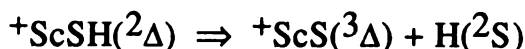


Table 7: ^+ScSH and ^+ScOH Equilibrium Energies (au), Equilibrium Bond Lengths (au) and Dissociation Energies (kcal/mol)

State	^+ScSH								
	Energy	MCSCF		MCSCF+1+2					
		$r_e(Sc-S)$	$D_e(Sc-S)$	$r_e(S-H)$	$D_e(S-H)$				
2Δ	-1157.71187	4.359	43.3	2.540	31.5(87.9) ^a	4.353	56.6	2.535	37.6(94.4) ^a
$2\Sigma^+$	-1157.70291	4.269	37.6	2.555	25.8(89.2) ^b	4.189	42.4	2.561	23.4(92.8) ^b

State	^+ScOH								
	Energy	MCSCF		MCSCF+1+2					
		$r_e(Sc-O)$	$D_e(Sc-O)$	$r_e(O-H)$	$D_e(O-H)$				
2Δ	-835.15522	3.509	101.8	1.848	57.4(136.7) ^c	3.505	108.0	1.821	59.6(139.2) ^c
$2\Sigma^+$	-835.13583	3.505	89.7	1.829	45.3(140.2) ^d	3.481	90.8	1.836	42.4(141.8) ^d

^a Values in parenthesis are for separation to $^+ScS(^3\Delta)+H$; ^b Values in parenthesis are for separation to $^+ScS(^3\Sigma^+)+H$.

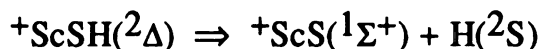
^c Values in parenthesis are for separation to $^+ScO(^3\Delta)+H$; ^d Values in parenthesis are for separation to $^+ScO(^3\Sigma^+)+H$.

we obtain an MCSCF+1+2 ΔE of 94.4 kcal/mol, 16.4 kcal/mol greater than the free (MCSCF+1+2) SH bond strength. Dissociating ^+ScSH along the path



requires 56.6 kcal/mol and is, as required, 16.5 kcal/mol larger than the $^+ScS(3\Delta)$ bond strength of 40.1 kcal/mol. These enhanced bond strengths are the result of bond formation to H. As the S to H bond is formed, using the S 3s and 3p σ orbitals, the companion 3s \pm 3p σ hybrid orbital interacts with Scandium causing a simultaneous strengthening of the Sc^+ to SH bond. This is half that found for ^+ScOH where a stabilization energy of 43 kcal/mol was observed (MCSCF+1+2).¹

$^+ScSH(2\Delta)$ can also dissociate along the adiabatic pathway

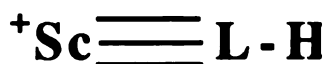


and requires 37.6 kcal/mol. This is significantly less than the free SH dissociation energy and reflects the differentially stronger bond in $^+ScS(1\Sigma^+)$ relative to $^+ScSH(2\Delta)$.

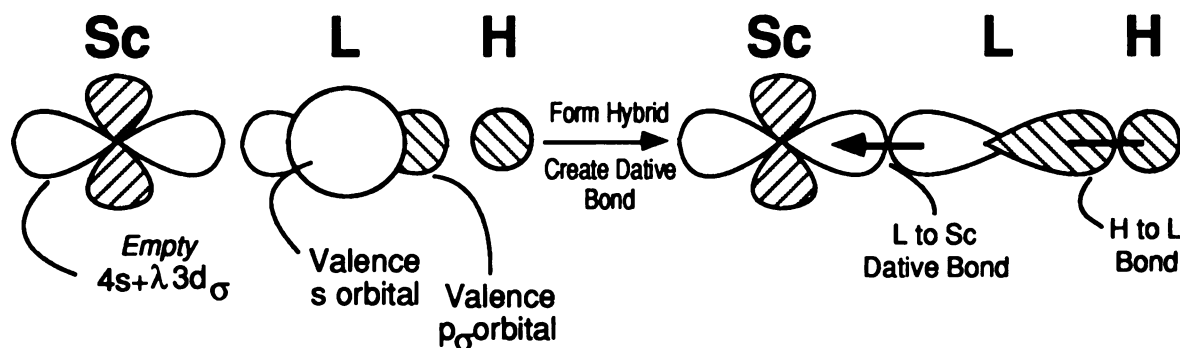
The gross atomic charges are collected in Table 6 and indicate that bonding H to ^+ScS does not change the charge on Sc but increases the anionic character on the Sulfur. The increase in S charge relative to the ^+ScS molecule is approximately 0.2 electrons.

C. COMPARISON OF $^+\text{ScNH}$, $^+\text{ScOH}$ AND $^+\text{ScSH}$

The species $^+\text{ScNH}$,⁶ $^+\text{ScOH}$ and $^+\text{ScSH}$ can all be described with the Lewis structure



where if $\text{L} = \text{O}$ or S both the σ and one π bond are dative bonds while for N only the σ bond is formally dative. The bonding of H to L causes the ligand's valence s and $p\sigma$ orbitals to mix as suggested below.



For $\text{L} = \text{N}$ and O this results in a sigma dative bond that stabilizes the Sc-L interaction by 43 kcal/mol. Since the S atom is larger than either O or N the bond length is longer than in either ^+ScO or ^+ScN . Moreover, the larger size also decreases the amount of stabilization afforded by formation of the sigma dative bond to 16.6 kcal/mol. The increased Sc to S bond length also affects the detailed structure of the spectator electron density. In $^+\text{ScOH}$ the Scandium spectator electron is composed of (in order of decreasing importance) the Sc^+

$3d\sigma, 4s, 4p_z$ with the 4s contributing up to 44% of the charge density ($^2\Sigma^+$ state). In $^+\text{ScSH}$, the mixing also goes as $\text{Sc}^+ 3d\sigma, 4s, 4p_z$, but with the 4s only contributing around 23% of the charge density ($^2\Sigma^+$ state). This is indicative of the amount of Scandium 4s available for the sigma dative bond. In particular, the 4s contribution to the dative bond is greater in $^+\text{ScSH}$ than in $^+\text{ScOH}$. The structure of the dative bond and the similarity in the $^+\text{ScOH}$ and $^+\text{ScSH}$ structures is illustrated in the MCSCF difference density contours displayed in Figures 4 and 6. In both Figures the $^2\Sigma^+ ^+\text{Sc-SH}$ ($^+\text{Sc-OH}$) total density at a geometry near equilibrium has the fragment ^+ScS (^+ScO) triplet state density subtracted from it. The $^+\text{Sc-L}$ molecule is maintained at the $^+\text{ScLH}$ geometry. This clearly indicates which orbitals are used in constructing both the sigma dative bond and the π bonds. Specifically, the $^+\text{ScSH}(^2\Delta) - ^+\text{ScS}(^3\Delta)$ difference density (Figure 6) shows a much increased density in the Sc-S sigma system relative to $^+\text{ScS}(^3\Delta)$. The MCSCF+1+2 bond dissociation energies for several states of $^+\text{ScSH}$, $^+\text{ScOH}$ and $^+\text{ScNH}$ have been collected in Table 8.

REACTION PRODUCTS

A. H- ^+ScO

If we bond to the unpaired electron on Sc in the $^3\Delta$ or $^3\Sigma^+$ states of ^+ScO we form $\text{H-}^+\text{ScO}(^2\Sigma^+)$. The Sc-H bond strength, relative to the $^3\Delta$ state of ^+ScO is calculated to be 47.2 kcal/mol (MCSCF+1+2 level), a typical²⁵ Sc-H bond strength.

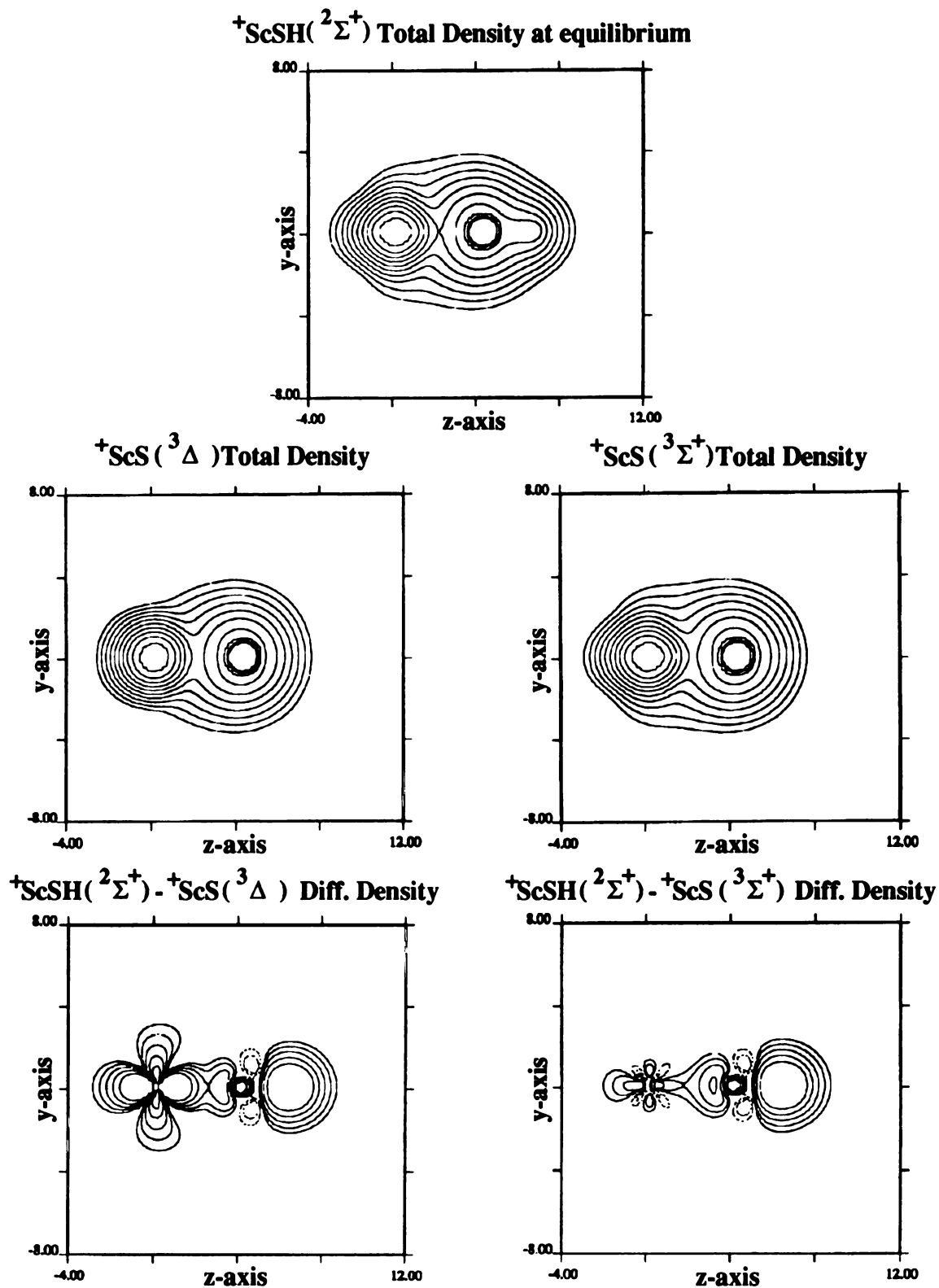


Figure 6. MCSCF total density contours (TDCs) and difference density contours (DDCs) for the $2\Sigma^+$ state of ${}^+ScSH$ and the $1\Sigma^+$ and $3\Sigma^+$ states of ${}^+ScS$. The DDCs are molecular differences where the ${}^+ScS$ states are subtracted from the ${}^+ScSH$ density. The ${}^+ScS$ states are at the equilibrium ${}^+ScSH$ (Sc-S) geometry. Contour levels range from 0.0025e to 1.28e (TDCs) and -0.04e to 0.04e (DDCs). Each level differs by a factor of 2. No zero contours are displayed and negative contours are indicated by dashes.

Table 8: Summary of MCSCF+1+2 Sc^+ + SH and OH fragment energies (kcal/mol)

System	Energy	System	Energy
$\text{SH}(^2\Pi) \Rightarrow \text{S} + \text{H}$	78.0	$\text{OH}(^2\Pi) \Rightarrow \text{O} + \text{H}$	97.6
$^+\text{ScS}(^1\Sigma^+) \Rightarrow \text{Sc}^+ + \text{S}$	96.9	$^+\text{ScO}(^1\Sigma^+) \Rightarrow \text{Sc}^+ + \text{O}$	146.0
$^+\text{ScS}(^3\Delta) \Rightarrow \text{Sc}^+ + \text{S}$	40.1	$^+\text{ScO}(^3\Delta) \Rightarrow \text{Sc}^+ + \text{O}$	66.4
$^+\text{ScS}(^3\Sigma^+) \Rightarrow \text{Sc}^+ + \text{S}$	27.6	$^+\text{ScO}(^3\Sigma^+) \Rightarrow \text{Sc}^+ + \text{O}$	46.5
$^+\text{ScSH}(^2\Delta) \Rightarrow ^+\text{ScS}(^1\Sigma^+) + \text{H}$	37.6	$^+\text{ScOH}(^2\Delta) \Rightarrow ^+\text{ScO}(^1\Sigma^+) + \text{H}$	59.6
$^+\text{ScSH}(^2\Delta) \Rightarrow ^+\text{ScS}(^3\Delta) + \text{H}$	94.4	$^+\text{ScOH}(^2\Delta) \Rightarrow ^+\text{ScO}(^3\Delta) + \text{H}$	139.1
$^+\text{ScSH}(^2\Delta) \Rightarrow ^+\text{Sc} + \text{SH}(^2\Pi)$	56.6	$^+\text{ScOH}(^2\Delta) \Rightarrow ^+\text{Sc} + \text{OH}(^2\Pi)$	108.0
$^+\text{ScSH}(^2\Sigma^+) \Rightarrow ^+\text{ScS}(^1\Sigma^+) + \text{H}$	23.4	$^+\text{ScOH}(^2\Sigma^+) \Rightarrow ^+\text{ScO}(^1\Sigma^+) + \text{H}$	42.4
$^+\text{ScSH}(^2\Sigma^+) \Rightarrow ^+\text{ScS}(^3\Sigma^+) + \text{H}$	92.8	$^+\text{ScOH}(^2\Sigma^+) \Rightarrow ^+\text{ScO}(^3\Sigma^+) + \text{H}$	141.8
$^+\text{ScSH}(^2\Sigma^+) \Rightarrow ^+\text{Sc} + \text{SH}(^2\Pi)$	42.4	$^+\text{ScOH}(^2\Delta) \Rightarrow ^+\text{Sc} + \text{OH}(^2\Pi)$	90.8
$^+\text{ScNH}(^1\Sigma^+) \Rightarrow ^+\text{ScN}(^2\Sigma^+) + \text{H}$	106.0 ^a	$^+\text{ScN}(^2\Sigma^+) \Rightarrow ^+\text{Sc}(^3D) + \text{N}(^4S)$	63.1 ^a

44

^a ref(6).

B. ${}^+\text{ScOH}_2$

There are three isomers with this empirical formula: the two electrostatic complexes,



and

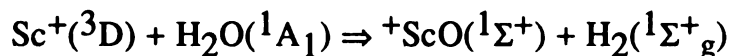


and the insertion product



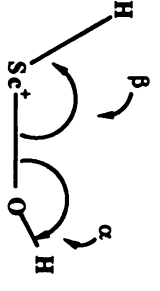
The electrostatic complex involving intact H_2O was studied by Rosi and Bauschlicher.⁷ The $\text{Sc}^+\cdots\text{OH}_2$ complex is bound, relative to the ground state products, by 36.2 kcal/mol with a Sc^+ to OH_2 distance of 4.296 au. The H_2O was constrained to the SCF geometry.

We will focus on the two remaining isomers. Consider first the electrostatic complex involving intact H_2 . It is easily seen that this will be an exoergic product of the reaction of Sc^+ with H_2O . It requires 219 kcal/mol (ΔE) to dissociate H_2O into its atoms²⁴ and we regain 103 kcal/mol (ΔE) when H_2 is formed²⁴ and 159 ± 7 kcal/mol when ${}^+\text{ScO}(1\Sigma^+)$ is formed³. ΔE for the reaction



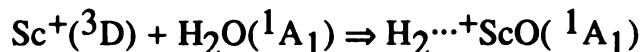
is at least 36 kcal/mol exothermic. Detailed calculation at the MCSCF and GVB+1+2 levels result in the energies collected in Table 9. Our explicitly calculated ΔE for the above reaction is 32.6 kcal/mol at the GVB+1+2 level.

Table 9: H_2^+ScO and H^+ScOH Equilibrium Energies (au), Bond Lengths (au) and Angles (deg).

State	$1A1$	$1A$
Structure		
Energy(au)	MCSGF -835.71753	MCSGF -835.72224
	MCSGF+1+2 -835.79674	MCSGF+1+2 -835.80464
$r_e(\text{H-H})$	1.4603	$r_e(\text{H-Sc})$ 3.5320
$r_e(\text{H}_2\text{-Sc})$	5.2020	$r_e(\text{Sc-O})$ 3.4414
$r_e(\text{Sc-O})^a$	3.1	$r_e(\text{O-H})$ 1.8486
		β 117.4
		α 162.7

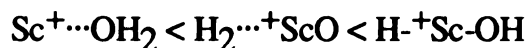
^a Constraint. Minimum occurs between 3.2 and 3.0 au.

The electrostatic complex is bound by an additional 2.5 kcal/mol, making our calculated $\Delta E = -35.1$ kcal/mol for the reaction



The insertion product may be formed from either the $^2\Delta$ or $^2\Sigma^+$ states of $^+\text{ScOH}$ by coupling the second H atom to the unpaired electron on Sc^+ . The resulting molecule has 4 formal electron pairs (a $^+\text{Sc-H}$, O-H and two $^+\text{Sc-O}$ bonding pairs), and an MCSCF function which correlates each (in the left-right GVB sense) and includes all spin couplings consists of 150 CSFs. The bond lengths and bond angles for the planar structure were optimized and the results are shown in Table 9. Also listed is the optimal geometry and associated energy obtained from a CI wave function which includes all single and double excitation relative to an 8 configuration (4 pair) GVB function (which generates 112,088 CSFs of ^1A symmetry). The single particle basis for this CI were the natural orbitals from the MCSCF function. This calculation places the insertion product ~ 5 kcal/mol lower than the electrostatic complex.

The errors in these calculations increase in the order



and improved calculations should favor the insertion product, suggesting that it is the global ground state. The $^+\text{Sc-H}$ bond length is 3.50 au and the bond energy is calculated to be 50 kcal/mol

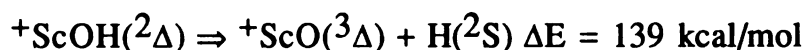


which is remarkably similar to the 3.52 au and 50.7 kcal/mol calculated by Alvarado-Swaisgood and Harrison²⁵ for $^+\text{ScH}(^2\Delta)$.

The computed ΔE for removing the O-H hydrogen

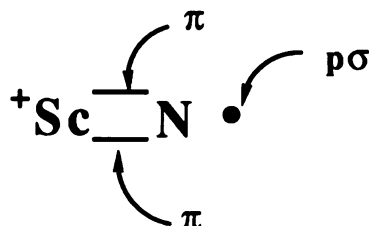


is 141 kcal/mol, virtually the same as that computed for



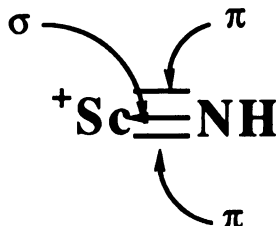
C. COMPARISON WITH THE $\text{Sc}^+ + \text{NH}_3$ SYSTEM

It is interesting to compare these results with those reported recently for the $\text{Sc}^+ + \text{NH}_3$ system.⁶ The ground state of ^+ScN is of $^2\Sigma^+$ symmetry and has a calculated bond energy (D_e) of 63.1 kcal/mol. The molecule has two π bonds and no σ bond. Its Lewis structure is



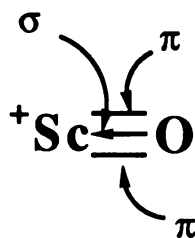
When the N atom bonds to an H atom, its 2s and $2p\sigma$ orbitals hybridize - one component reaching out to bond the H atom while

the companion component forms a dative bond in the empty valence σ space of Sc^+ .

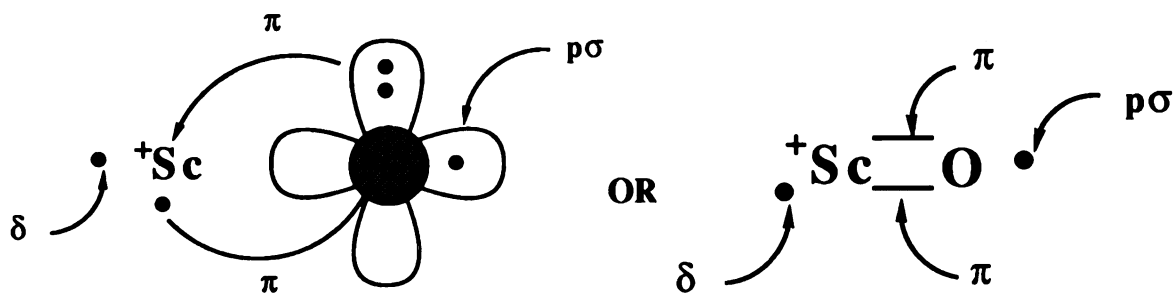


The resulting $^+\text{Sc-NH}$ bond is calculated to be 106 kcal/mol, some 43 kcal/mol stronger than the Sc-N bond in ^+ScN .

The ground state of $^+\text{ScO}(^1\Sigma^+)$ has a triple bond



with no unpaired electron on O. However, the $^3\Delta$ state is a π, π state, similar to ^+ScN , except that it has been formed formally from a dative interaction in the π system

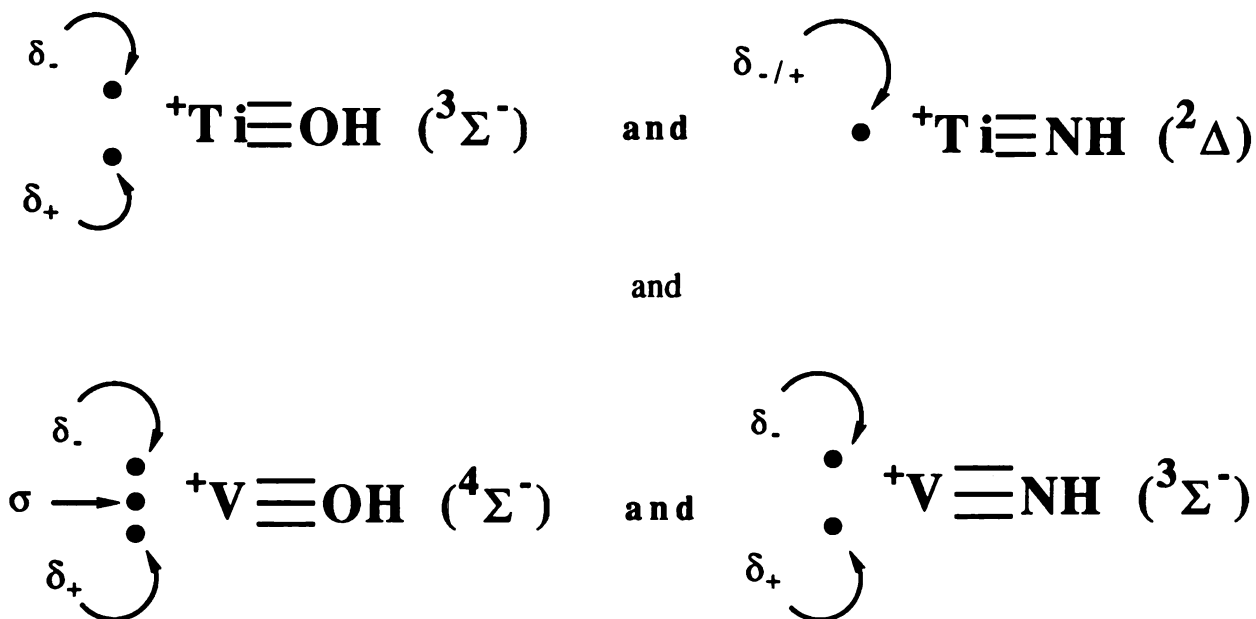


where we show both π bonds as being equivalent, of course. When the O atom is approached by an H, it will also hybridize its 2s and 2p σ orbitals forming a covalent bond to H and a second dative bond (in the σ system) to Sc⁺.



The ⁺Sc-O bond strength in this molecule is calculated to be 109 kcal/mol, 43 kcal/mol higher than in ⁺ScO(³ Δ) and essentially the same as the Sc-N bond strength in ⁺ScNH. It is interesting that the σ dative interaction has stabilized both the ⁺Sc-O and ⁺Sc-N bonds to the same extent, 43 kcal/mol.

This suggests that the ⁺M-L bond energies in the pairs



will be similar. Indeed, Armentrout et al.²⁶ have determined D_0 for the ^+V-L pairs and finds 100 kcal/mol for ^+V-OH and 102 kcal/mol for ^+V-NH . Since these two bond strengths are similar, the unpaired σ electron in ^+VOH must not interfere with the σ dative bond. It would be very interesting to know the detailed atomic orbital composition of this electron. Finally, The ^+Ti-L bond strengths were previously found to be essentially the same with ^+TiOH $D_0=113$ kcal/mol and ^+TiNH $D_0=111$ kcal/mol.^{5,27}

D. Sc⁺-SH₂

The MCSCF wavefunctions for the 3A_1 and 3A_2 states were constructed under the C_s point group by pairing, in a GVB way, the two S-H bonds and in-out correlating the out of plane S $3p\pi^2$ orbital. The Scandium 4s and 3d orbitals were maintained singly occupied. All spin couplings from this GVB function result in a 126 CSF MCSCF. The MCSCF+1+2 functions were constructed from all valence single and double substitutions from the 8-configuration GVB function (3 GVB pairs and 2 singly occupied orbitals), using the optimized MCSCF NOs as the orbital basis. This results in 216,530 CSFs for the 3A_2 state and 221,182 CSFs for the 3A_1 . A MCSCF+1+2 function constructed from the full MCSCF reference space was not possible. It was found, however, for the $Sc^+ + OH_2$ studies¹ that the GVB correlation plus all valence single and double substitutions using the MCSCF NO basis accounts for almost all of the energy. In particular, the MCSCF+1+2 functions for ^+ScOH using both the MCSCF and GVB basis results in a total energy difference of only 2 kcal/mol.²⁸ In all

calculations the SH₂ geometry was constrained to that optimized with a 37 CSF MCSCF function and a planar geometry was selected. This technique was previously shown to be adequate for the electrostatic ⁺Sc-OH₂ systems.⁷

The ³A₂ and ³A₁ states differ only in location of the 3d electron on Scandium. In the ³A₂, the electron occupies a 3dδ₋ orbital while in the ³A₁ it occupies a 3dδ₊ orbital. In both states the companion electron is in a 4s orbital. This subtle difference results in nearly degenerate states with the ³A₂ only 1.8 kcal/mol lower in energy than the ³A₁. The near degeneracy arises from the large ⁺Sc to SH₂ distance in the molecule.

We find the ³A₂ MCSCF+1+2 interaction energy to be 11.39 kcal/mol and the ³A₁ to be 11.38 kcal/mol. The optimized ³A₂ ⁺Sc-SH₂ distance becomes 5.454 au while the ³A₁ distance is the same at 5.456 au. The optimized geometries and total energies are collected in Table 10 as are the corresponding ⁺ScOH₂ values.

The interaction energy of the electrostatic species Sc⁺SH₂ arises primarily from the charge-dipole term in the energy. The experimental dipole moment of SH₂ is 0.97 D²⁴ while that of H₂O is 1.85 D.²⁴ The simple charge-dipole energy expression is $E=q\mu/R^2$ with μ the dipole moment of SH₂, $q=1$ and R is the distance from Sc⁺ to the center of charge on SH₂. Using this expression the interaction energy of Sc⁺ + SH₂ should go as

$$E(\text{Sc}^+\text{SH}_2) \cong E(\text{Sc}^+\text{OH}_2) * (\mu_{\text{SH}_2}/\mu_{\text{OH}_2}) * (R_{\text{Sc-OH}_2}/R_{\text{Sc-SH}_2})^2.$$

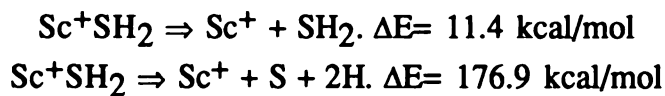
Table 10: 3A_2 and 3A_1 states of Sc^+SH_2 . Optimized Geometries, Total Energies.

	MCSCF	MCSCF+1+2		MCSCF	MCSCF+1+2
Energy(au)	-1158.28051	-1158.35311	Energy(au)	-1158.28050	-1158.35310
$r_{Sc-S}(au)$	5.608	5.459	$r_{Sc-S}(au)$	5.609	5.456

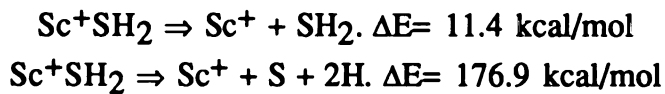
For all calculations the SH_2 geometry was constrained to $\beta(deg)=90$
and $r_{S-H}(au)=2.60$.

Energetics (CI)

3A_2 state



3A_1 state



This simple expression suggests that $E(\text{Sc}^+\text{SH}_2) \cong E(\text{Sc}^+\text{OH}_2) \cdot 0.33$. Using the $E(\text{Sc}^+\text{OH}_2)$ value³ of 36.9 kcal/mol yields $E(\text{Sc}^+\text{SH}_2) = 12$ kcal/mol, only 5% larger than our determined MCSCF+1+2 value of 11.39 kcal/mol.

E. H₂-ScS⁺

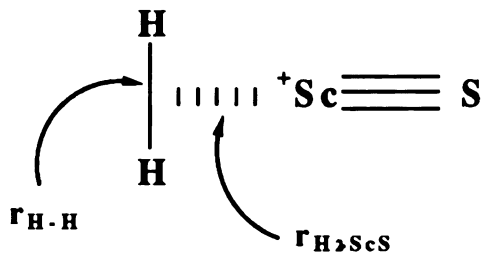
This molecule is characterized as intact H₂ electrostatically bound to ground state $^+\text{ScS}(^1\Sigma^+)$. A MCSCF function that is composed of 4 GVB pairs describing the 4 bonds in the molecule plus all spin couplings results in 74 CSFs under C_{2v} symmetry. The MCSCF+1+2 function was constructed as all valence single and double substitutions from a 16 CSF GVB function using the optimized MCSCF NOs as the basis. This results in 107,832 CSFs. The H-H and H₂- ^+ScS distances were optimized with the Sc-S distance constrained to 4.00 au which is close to the minimum energy (between 3.9 and 4.1 au). The optimized geometries and total energies are collected in Table 8. The MCSCF+1+2 interaction energy is determined to be 3.5 kcal/mol while the reaction product, H₂-ScS⁺, is exoergic, relative to Sc⁺+SH₂, by 34.5 kcal/mol.

The formation of H₂⋯ ^+ScS from Sc⁺ + SH₂ requires dissociation of SH₂ (165 kcal/mol MCSCF+1+2, Table 2), followed by formation of H₂ and $^+\text{ScS}(^1\Sigma^+)$ with a small contribution from the electrostatic interaction. Formation of $^+\text{ScS}(^1\Sigma^+)$ recovers 97 kcal/mol (MCSCF+1+2, Table 3) while the H₂ D_e was determined to be 105 kcal/mol (MCSCF+1+2, Table 2). This suggests that the reaction energy should be around 37 kcal/mol. Detailed MCSCF+1+2

calculations result in an energy of 34.5 kcal/mol with the electrostatic interaction accounting for 3.5 kcal/mol. The computed interaction energy of 3.5 kcal/mol is similar to that found for $\text{H}_2 \cdots {}^+\text{ScO}$ (2.50 kcal/mol, Table 8) and also that for the ${}^+\text{Cr} \cdots \text{H}_2$ system (3.58 kcal/mol).¹⁴ The optimized geometry and energetics are collected in Table 11.

F. H^+ScSH

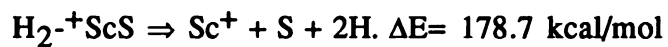
The H^+ScOH molecule was determined to be the ground state reaction product of $\text{Sc}^+ + \text{H}_2\text{O}$. Using simple bond additivity arguments and a $D_e({}^+\text{Sc-H})$ of 50 kcal/mol (a typical ${}^+\text{Sc-H}$ bond strength)²⁵ suggests that H^+ScOH is exoergic by only 1-2 kcal/mol or even isoergic with the reaction products. Including the dative bond stabilization energy of 43 kcal/mol, however, drives this product to the final reaction ground state. By analogy, the H^+ScSH product without stabilization would be exoergic relative to the products by around 3 kcal/mol. Inclusion of the 16.6 kcal/mol stabilization energy does indeed lower the total energy but not enough to compete for the ground state. Furthermore, this structure does not seem to be a minimum on the reaction energy surface. The linear structure is a saddle point on the molecular surface with a MCSCF energy, relative to $\text{Sc}^+ + \text{H}_2\text{S}$, of 4 kcal/mol. Bending the two hydrogens to either the trans or cis conformation results in a marked decrease in energy. In particular, the structure with both hydrogens 90 degrees from the internuclear line and in the cis conformation drives the MCSCF energy to around 16 kcal/mol below $\text{Sc}^+ + \text{H}_2\text{S}$.

Table 11: $\text{H}_2 \cdots {}^+\text{ScS}$ Optimized geometry, Total Energy and Dissociation Energies.

	MCSCF	MCSCF+1+2
Energy(au)	-1158.31501	-1158.38999
$r_{\text{H-H}}(\text{au})$	1.462	1.444
$r_{\text{H}_2\text{-ScS}}(\text{au})$	5.210	5.063

$r_{\text{Sc-S}}(\text{au})$ was constrained to 4.0 au for all calculations.

Dissociation Energies (CI)



This lies below the optimized Sc^+SH_2 product. Our results indicate the transition from H^+ScSH to $\text{H}_2\cdots^+\text{ScS}$ is an energetically favorable process with no apparent barrier. This process is illustrated in Figure 7, where the minima correspond to the optimized ground state products and the saddle point refers to the insertion product.

CHEMISTRY-PREDICTIONS

Recent theoretical studies of $\text{Sc}^+ + \text{H}_2\text{O}$ suggests the ground state reaction product is the insertion product, H^+ScOH , and while the experimental work of Magnera et al.⁵ didn't rule out that possibility, it was suggested that the product was the electrostatic $^+\text{Sc}\cdots\text{O H}_2$ species. The discrepancy between the expected experimental and the theoretical result is caused by a breakdown of bond additivities resulting from the induced sigma dative bond in $^+\text{ScOH}$ stabilizing the system by 43 kcal/mol. In the $\text{Sc}^+ + \text{SH}_2$ reaction we find the induced sigma bond stabilization energy to be only 16.6 kcal/mol, with the consequence of drastically changing the relative energies of the reaction products. Therefore, while in the $\text{Sc}^+ + \text{H}_2\text{O}$ reaction the products order in total energy as



in $\text{Sc}^+ + \text{SH}_2$ they order as



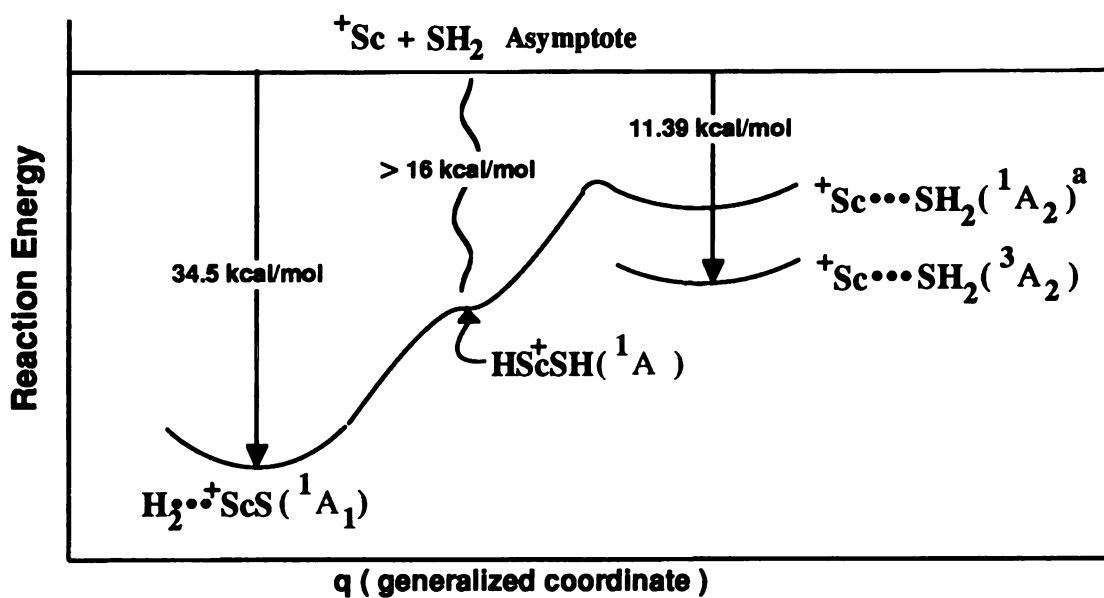


Figure 7. Illustration of the energetics amongst the $Sc^+ + SH_2$ reaction products. Minima on the curve are MCSCF+1+2 optimized values. q is a generalized coordinate.

^aEnergy Expected from the $Sc^+ \ ^1D \leftarrow \ ^3D$ separation of approximately 7 kcal/mol (ref (15)).

These results are collected into Figures 8 and 9, which depict the relative energies of the studied products; the energetics are also summarized in Table 12.

In summary, the ground state reaction products of Sc^+ with SH_2 and OH_2 can be understood using three physical properties.

- 1) Dipole moment of the ligand.
- 2) ground state ^+ScL D_e (L is the ligand atom that bonds to Sc^+).
- 3) The stabilization obtained when H bonds to ^+ScL to form $^+\text{Sc-L-H}$.

These estimates are sufficient to predict the order of the ground state reaction products. This analysis is expected to be applicable to ligands such as SeH_2 .

CONCLUSIONS

1. The ground state of ^+ScO is of $^1\Sigma^+$ symmetry. Our computed D_0 of 144.4 kcal/mol compares favorably with the experimental value of 159 ± 7 kcal/mol.
2. A major factor contributing to the strength of the $^+\text{Sc-O}$ bond is the dative bond formed between the $2p\sigma$ electron pair on O and the empty σ valence orbitals on Sc^+ . This suggests that the ground state of ^+TiO will be of $^2\Delta$ symmetry ($\cdot^+\text{Ti}\equiv\text{O}$) while ^+VO will be $^3\Sigma^-$ ($:\cdot^+\text{V}\equiv\text{O}$) (as observed).²⁹ When the metal valence σ orbitals are not empty the σ dative structure will compete with a structure having a singlet coupled oxygen-metal σ bond and a dative bond in the π system. In ^+CrO for example, the σ dative structure

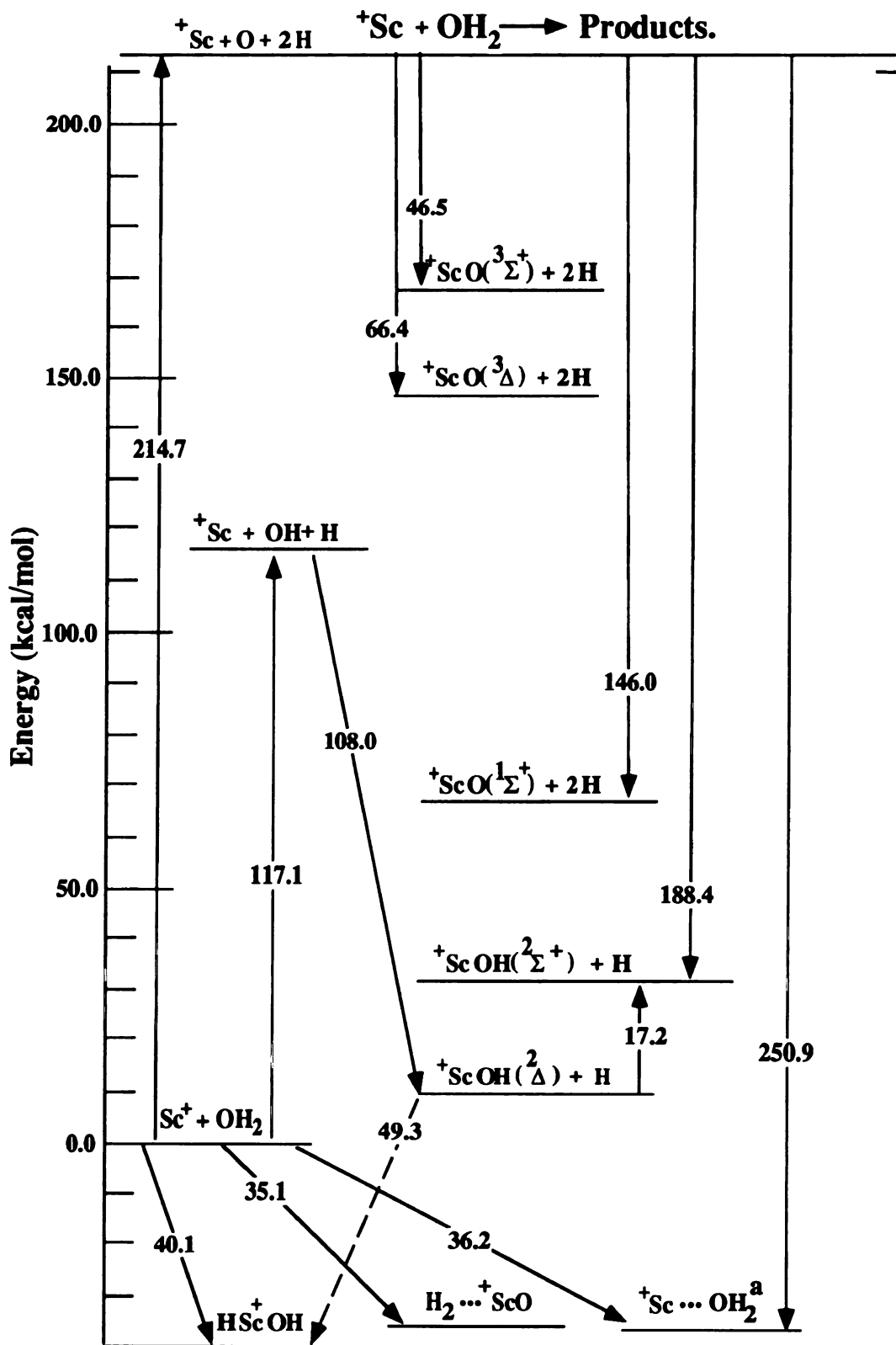


Figure 8. MCSCF+1+2 relative energies of the $Sc^+ + SH_2$ reaction.
^a ref (7).

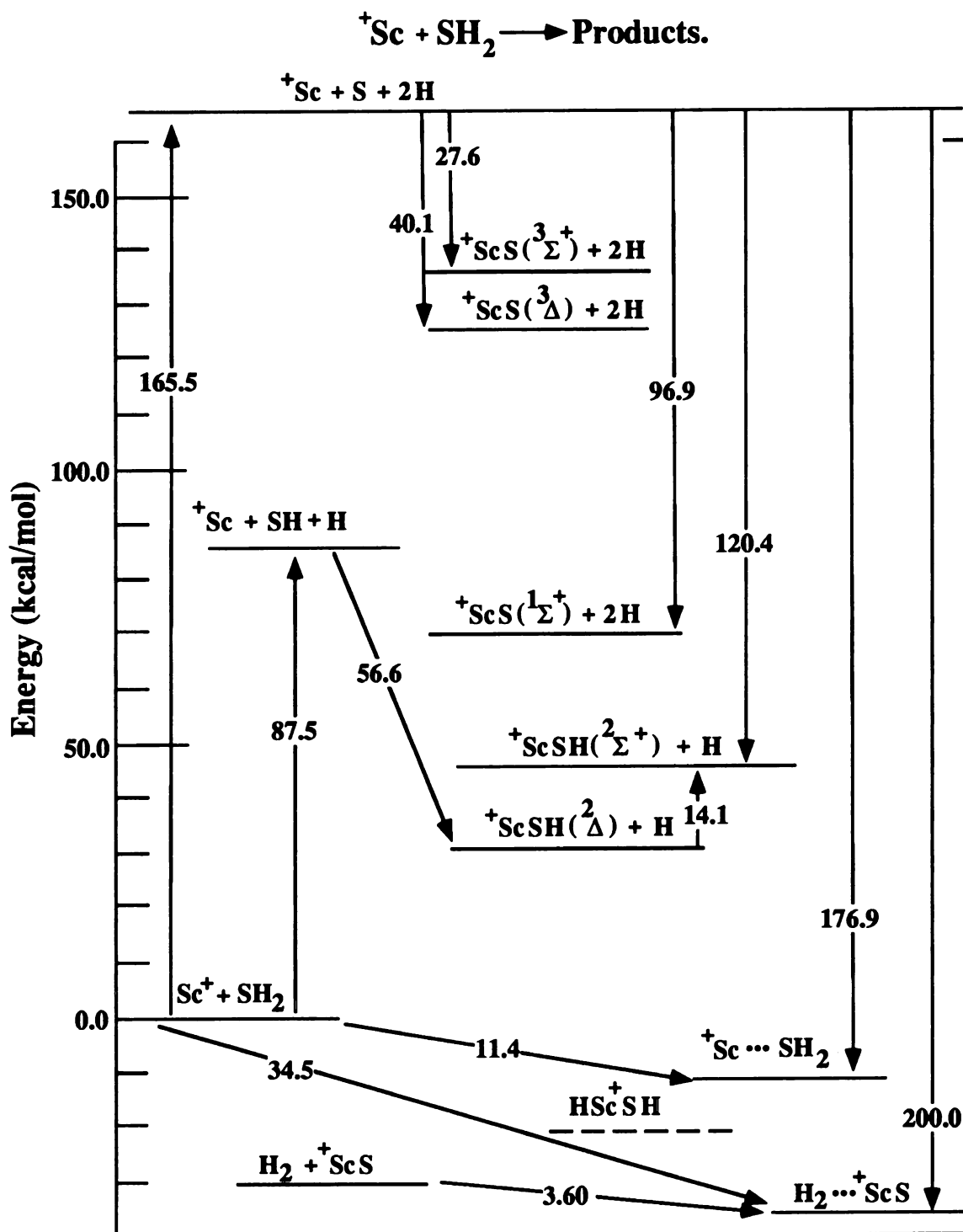
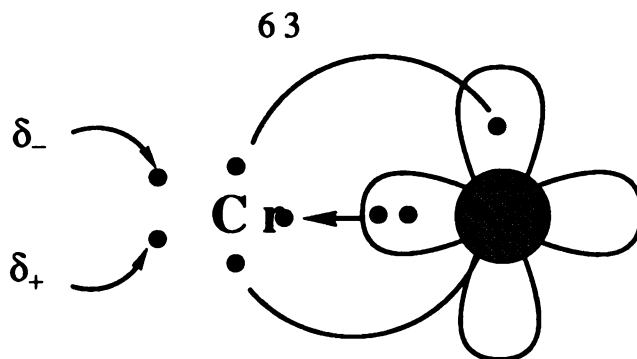


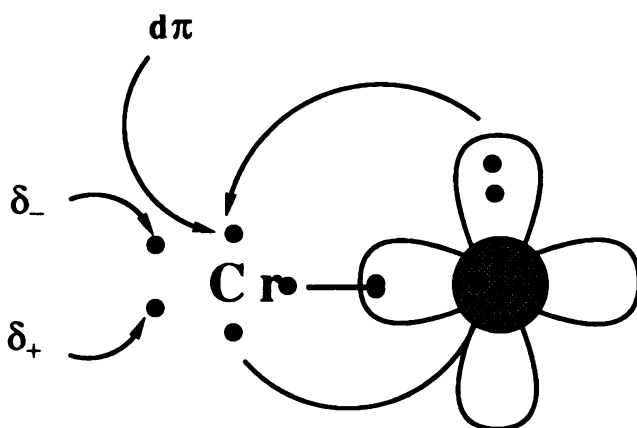
Figure 9. MCSCF+1+2 relative energies of the $\text{Sc}^+ + \text{SH}_2$ reaction.

Table 12: MCSCF+1+2 Dissociation Energies (D_e , kcal/mol).

System	Energy	System	Energy
${}^+ScSH_2({}^3A_2) \Rightarrow {}^+Sc + SH_2({}^1A_1)$	11.4	${}^+ScOH_2({}^3A_2) \Rightarrow {}^+Sc + OH_2({}^1A_1)$	36.2 ^a
${}^+ScSH_2({}^3A_1) \Rightarrow {}^+Sc + SH_2({}^1A_1)$	11.4	$H_2{}^+ScO({}^1A_1) \Rightarrow {}^+Sc + OH_2({}^1A_1)$	35.1
$H_2{}^+ScS({}^1A_1) \Rightarrow H_2 + {}^+ScS({}^1\Sigma^+)$	3.6	$H_2{}^+ScO({}^1A_1) \Rightarrow H_2 + {}^+ScO({}^1\Sigma^+)$	2.5
$H_2{}^+ScS({}^1A_1) \Rightarrow {}^+Sc + SH_2({}^1A_1)$	34.5	$H{}^+ScOH({}^1A) \Rightarrow {}^+Sc + OH_2({}^1A_1)$	40.1



is of $^4\Sigma^-$ symmetry, while the σ singlet coupled oxygen-metal electron pair structure



is of $^4\Pi$ symmetry.³⁰ We calculate that these two states are separated by only 7 kcal/mol and that the lower, the $^4\Pi$, has a calculated bond energy of 57 kcal/mol. This is significantly less than the triply bonded $^+\text{ScO}(^1\Sigma^+)$ but comparable to the doubly bonded $^+\text{ScO}(^3\Delta)$.

3. The $^+\text{Sc-O}$ bond in $^+\text{ScOH}$ is 108 kcal/mol or 43 kcal/mol stronger than the bond in $^+\text{ScO}(^3\Delta)$. This is due, primarily, to the dative interaction with Sc^+ of the O $2s+2p\sigma$ hybrid induced on O when

bonded to H. This is in substantial disagreement with the recent⁵ experimental value of 88 kcal/mol.

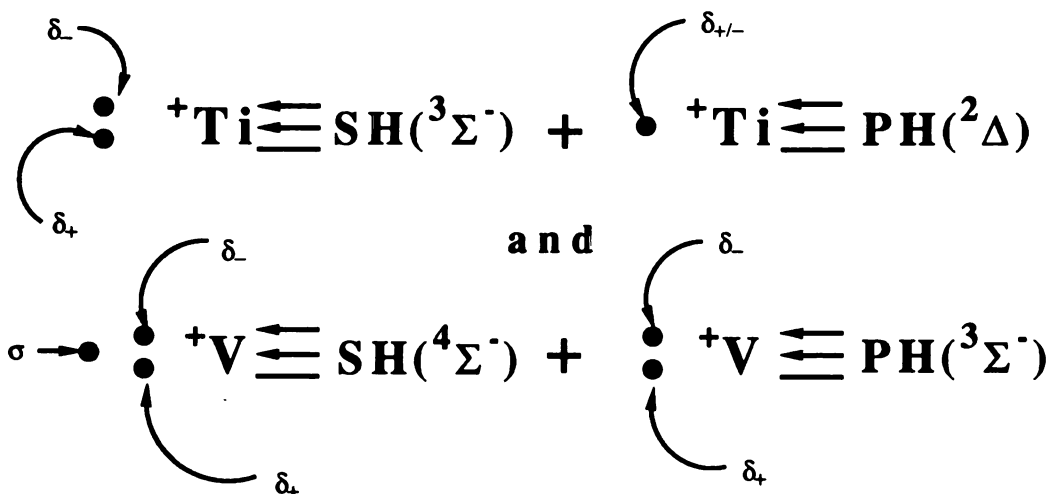
4. We calculate three exothermic products of the reaction of $\text{Sc}^+ + \text{H}_2\text{O}$. The ion dipole complex $\text{Sc}^+\cdots\text{H}_2\text{O}$, the oxide - H_2 complex $\text{H}_2\cdots^+\text{ScO}$, and the insertion product, $\text{H}-^+\text{Sc}-\text{OH}$. The oxide product is a consequence of the very strong bond in $^+\text{ScO}(^1\Sigma^+)$ which is due, in large measure, to the O lone pair forming a dative bond to Sc^+ . The oxide will not be nearly so exothermic with any other first row transition element. The insertion product is calculated to be the global ground state, although by only 3 kcal/mol. The stability of this product is due, in large measure, to a dative bond between the O $2s+2p\sigma$ hybrid on OH and Sc^+ . As this bond strength is decreased, the exothermicity of the insertion product will decrease.

5. A consequence of the strong $^+\text{Sc}-\text{OH}$ bond is that the calculated global minimum in the $\text{Sc}^+ + \text{H}_2\text{O}$ system is the insertion product $\text{H}-^+\text{Sc}-\text{OH}$, while the calculated global minimum in the $\text{Sc}^+ + \text{NH}_3$ system is the electrostatic complex $^+\text{Sc}\cdots\text{NH}_3$. This situation obtains because the $^+\text{ScNH}_2$ bond strength is calculated to be 78 kcal/mol, substantially smaller than the $^+\text{ScOH}$ bond strength of 107 kcal/mol. Since the Sc-H bond energy is similar in both systems (46 kcal/mol in $\text{H}-^+\text{ScNH}_2$ and 47 kcal/mol in $\text{H}-^+\text{Sc}-\text{OH}$) the insertion product in $\text{H}-^+\text{Sc}-\text{NH}_2$ lies ~ 24 kcal/mol above the electrostatic complex while in $\text{H}-^+\text{ScOH}$ it lies at least 3 kcal/mol below the $\text{Sc}^+\cdots\text{H}_2\text{O}$ complex.

6. The ${}^+ScS$ ground state is a triply bonded species of ${}^1\Sigma^+$ symmetry with a D_e of approximately 97 kcal/mol. The two lowest triplet excited states are π,π bonded species of ${}^3\Delta$ and ${}^3\Sigma^+$ symmetries with calculated D_e s of 40 and 28 kcal/mol, respectively.

7. The ground state product for the gas-phase reaction, $Sc^+ + H_2S$ is expected to be the electrostatic species $H_2\cdots{}^+ScS$ ($\Delta E = 34.5$ kcal/mol) with the next nearest product, ${}^+Sc\cdots SH_2$, 23 kcal/mol higher at 11.4 kcal/mol. The energy of the insertion product, HSc^+SH , is intermediate to $H_2\cdots{}^+ScS$ and ${}^+Sc\cdots SH_2$ but is not a minimum on the reaction surface.

8. Previous work on ${}^+ScOH$ and ${}^+ScNH$ indicates the slight difference in size of the ligand has little effect on the Sc-LH bond strength. Those results suggests that the ${}^+Sc-SH$ and ${}^+Sc-PH$ bond energies should be comparable. This also suggests that the M-L bond energies in the pairs



will also be similar.

REFERENCES

REFERENCES

- 1 J.L.Tilson, J.F. Harrison, *J. Phys. Chem.*, 95, 5097 (1991).
- 2 J.L.Tilson, J.F. Harrison, *J. Phys. Chem.*, 96, 1667 (1992).
- 3 a) E.J. Murad, *J. Geophys. Res.*, 83, 5525 (1978).
b) H. Kang and J.L. Beauchamp, *J. Am. Chem. Soc.*, 108, 5663 (1986).
c) N. Aristov and P.B. Armentrout, *J. Am. Chem. Soc.*, 106, 4065 (1984).
- 4 a) E. Murad, *J. Chem. Phys.*, 73, 1381 (1980).
b) H. Kang and J.L. Beauchamp, *J. Am. Chem. Soc.*, 108, 7502 (1986).
c) C.J. Cassady and B.S. Freiser, *J. Am. Chem. Soc.*, 106, 6176 (1984).
- 5 T.F. Magnera, D.E. David and J. Michl, *J. Am. Chem. Soc.*, 111, 4100 (1989).
- 6 A. Mavridis, K. Kunze, J.F. Harrison and J. Allison, "Bonding Energetics In Organometallic Compounds", T.J. Marks Ed., ACS Symposium Series 428, American Chemical Society, Washington DC, 1990, Chap. 18.
- 7 a) M. Rosi and C.W. Bauschlicher Jr., *J. Chem. Phys.*, 92, 1876 (1990).
b) M. Rosi and C.W. Bauschlicher Jr., *J. Chem. Phys.*, 90, 7264 (1989).
- 8 A.J.H. Wachters, *J. Chem. Phys.*, 52, 1033 (1970).
- 9 T.H. Dunning Jr., private communication.
- 10 P.J. Hay, *J. Chem. Phys.*, 66, 4377 (1977).
- 11 R.C. Raffinetti, *J. Chem. Phys.*, 58, 4452 (1973).
- 12 F.B. Duijneveldt, "IBM Technical Research Report No. RJ-945", IBM Research Laboratory, San Jose, CA, 1971.

- 13 S. Huzinaga, "Approximate Atomic Functions II", Research report; Division of Theoretical Chemistry, Department of Chemistry, The University of Alberta, 1971.
- 14 M. Rivera, J.F. Harrison and A. Alvarado-Swaisgood, *J. Phys. Chem.*, 94, 6969 (1990).
- 15 C.E. Moore, *Natl. Stand. Ref. Data. Ser., Natl. Bur. Stand. No. 35*.
- 16 The ARGOS integral program was developed by R.M. Pitzer (Ohio State University)
- 17 The GVB164 program was written by R. Bair (Argonne National Laboratory).
- 18 A description of the UEXP program is given in R. Shepard, J. Simons and I. Shavitt, *J. Chem. Phys.*, 76, 543 (1982).
- 19 H. Lischka, R. Shepard, F.B. Brown and I. Shavitt, *Int. J. Quant. Chem. Symp.*, 15, 91 (1981).
- 20 R. Shepard, I. Shavitt, R.M. Pitzer, D.C. Comeau and M. Pepper, *Int. J. Quant. Chem. Symp.*, 22, 149 (1988) and references therein.
- 21 J.L. Dunham, *Phys. Rev.*, 41, 721 (1932).
- 22 a) W.A. Goddard III, T.H. Dunning Jr., W.J. Hunt and P. Hay, *J. Acc. Chem. Res.*, 6, 368 (1973).
b) W.A. Goddard III and L.B. Harding, *Annu. Rev. Phys. Chem.*, 29, 363 (1978).
- 23 R.S. Mulliken, *J. Chem. Phys.*, 23, 1833, 1841, 2338, and 2343 (1955). For a critique see J.O. Noell, *Inorg. Chem.* 21, 11 (1982).
- 24 adapted from "CRC Handbook of Chemistry and Physics", R.C. Weast, Ed., CRC Press, Boca Raton, Fl., 63rd ed., 1982.
- 25 A.E. Alvarado-Swaisgood and J.F. Harrison, *J. Phys. Chem.*, 89, 5198 (1985).
- 26 P.B. Armentrout, "Bonding Energetics In Organometallic Compounds", T.J. Marks Ed., ACS Symposium Series 428, American Chemical Society, Washington DC, 1990, Chap. 2.

- 27 D.E. Clemmer, L.S. Sunderlin and P.B. Armentrout, *J. Phys. Chem.*, 94, 3008 (1990).
- 28 J.L. Tilson and J.F. Harrison, unpublished results.
- 29 J.M. Dyke, B.W.J. Gravenor and A. Morris, *J. Phys. Chem.*, 89, 4613 (1985).
- 30 J.F. Harrison, *J. Phys. Chem.*, 90, 3313 (1986).

CHAPTER III

CHAPTER III
THE ELECTRONIC AND GEOMETRIC STRUCTURES OF
 ^+ScSe AND ^+ScSeH

INTRODUCTION

The ^+ScSe and ^+ScSeH molecules were investigated by determining the Multiconfiguration self consistent field (MCSCF) and configuration interaction (MCSCF+1+2) wavefunctions for the $^1\Sigma^+$, $^3\Delta$ and $^3\Sigma^+$ states of ^+ScSe and the $^2\Delta$ and $^2\Sigma^+$ states of ^+ScSeH . The ground state ^+ScSe is a triply bonded species of $^1\Sigma^+$ symmetry with a bond strength of 84 kcal/mol. The $^3\Delta$ and $^3\Sigma^+$ excited states lie higher in energy at 31 and 28 kcal/mol, respectively. The ^+ScSeH molecule has a $^2\Delta$ ground state nearly degenerate with the excited $^2\Sigma^+$ state, with both differentially stabilized by formation of the Se-H bond. This stabilization is consistent with prior work on ^+ScOH and ^+ScSH .

Our focus is on the relative energies of the molecules and the structure of the valence σ orbitals in ^+ScSeH . Previous theoretical studies on ^+ScSH ¹ and ^+ScOH ² indicate a differential stabilization resulting from an induced σ bond between Sc^+ and the ligand, L, formed in concert with the L-H bond. This differential stabilization results in theoretical predictions of the gas-phase $Sc^+ + LH_2$ reaction that differ from those based on simple bond additivity arguments. In particular for the reaction $Sc^+ + OH_2$, the ground state was predicted to be the H^+ScOH insertion product, while for the $Sc^+ + SH_2$ reaction the

electrostatic $\text{H}_2 \cdots {}^+\text{ScS}$ molecule becomes the ground state. Clearly, the ground state reaction product is very dependent on the amount of this stabilization. The results here indicates a definite trend in electronic structure and in the amount of extra stabilization for these Group VI-containing molecules.

There are no experimental results for the ${}^+\text{ScSe}(\text{H})$ molecules nor on the reaction $\text{Sc}^+ + \text{SeH}_2$. The only direct experimental data available for comparison have been the experiments of Magnera, et al.³ on the $\text{Sc}^+ + \text{OH}_2$ reaction. We find, however, definite trends in character going from O to S to Se and are confident in the predictions.

BASIS SETS

The Scandium and Hydrogen atom basis sets employed here have been used before.¹

The Selenium basis was the (13s,9p,5d) set from Dunning,⁴ augmented with a diffuse s ($\text{exp} = 0.05592$), a diffuse p ($\text{exp} = 0.0513$) and a diffuse d ($\text{exp}=0.40$) function. This set was contracted to (7s,6p,2d) following Raffenetti.⁵

MOLECULAR CODES

All ab-initio calculations were done on a Stardent TITAN computer located in the Michigan State University Chemistry Department using the Argonne National Laboratory collection of COLUMBUS⁶ codes.

All density and difference density contours were calculated with the MSUPLOT codes and all spectroscopic constants were determined by performing a Dunham⁷ analysis.

FRAGMENT ENERGIES

Sc⁺ and H

The Sc⁺ and H atom energies were calculated before¹ and are collected in Table 1.

Se

The Selenium ³P state was analyzed with MCSCF and MCSCF+1+2 wavefunctions. The MCSCF function was constructed from the in-out correlation (GVB) of the doubly occupied 4p_x orbital plus all valence spin couplings. This results in 5 CSFs of ³B₂ symmetry. Inclusion of all valence single and double substitutions (of ³B₂ symmetry) from the MCSCF reference space results in the 691 CSF MCSCF+1+2. These energies are collected in Table 1.

SeH

The ²Π state of SeH was examined by a 17 configuration ²B₁ MCSCF function. This was constructed from all spin couplings of a GVB(2/4) function (correlating the π bond and the doubly occupied Se 4p_y orbital) and a 4,146 CSF MCSCF+1+2 constructed from all valence single and double substitutions (of ²B₁ symmetry) from the MCSCF reference space. The total energies are listed in Table 1 while the dissociation energy (D_e) is collected in Table 2.

H₂Se

The energy and optimized geometry of H₂Se was computed with a 37 CSF MCSCF function constructed to correlate in a GVB way the two bonding orbitals and the Se doubly occupied out of plane orbital followed by all spin couplings. The MCSCF+1+2 function was derived from all valence single and double substitutions from the MCSCF reference space and results in 25,979 CSFs. The equilibrium energies are listed in Table 1 and the dissociation energies in Table 2.

MCSCF FUNCTION FOR ⁺ScSe

Studies of ⁺ScS¹ and ⁺ScO² indicate that the Sc⁺ ground ³D state and excited ³F states (³F ← ³D ≅ 0.59 eV)⁸ are large contributors to the wavefunctions. The ⁺ScSe ¹Σ⁺ state MCSCF function that includes contributions from both the Sc⁺ (³D) and Sc⁺ (³F) asymptotes can be constructed from all spin couplings of the GVB(3/6)⁹ function

$$\Psi \sim (\text{core})^2 (14\sigma^2 - \lambda 15\sigma^2)(6\pi_x^2 - \nu 7\pi_x^2)(6\pi_y^2 - \nu 7\pi_y^2)$$

and results in 37 configuration state functions (CSFs) under a C_{2v} point group. The core electrons have been suppressed here for brevity but are always variationally optimized. The term 14σ²-λ15σ² represents the coupling of the Se 4pσ and Sc⁺ 4s electrons into a σ bond and allows the proper separation at large internuclear distances. Similarly, the 6π_x²-ν7π_x² and 6π_y²-ν7π_y² terms represents the π bonds with separation to the Se 4pπ⁴ and Sc⁺ 3dπ¹ configurations.

Table 1: Total Fragment Energies (au)

Fragment	E_{\min} (MCSCF)	E_{\min} (MCSCF+1+2)
Sc ⁺ $^3D(4s^1 3d^1)^a$	-759.52848	-759.52906
Sc ⁺ $^3B_2(3d\pi^1 3d\delta^1)^a$	-759.48576	-759.49960
Se 3P	-2399.71554	-2399.75294
SeH $^2\Pi$	-2400.31795	-2400.36659
H ₂ Se 1A_1	-2400.92542	-2400.99459
H ₂ $^1\Sigma_g^+(3s/3p)^a$	-1.14813	-1.16652
H $^2S^a$	-0.49928	

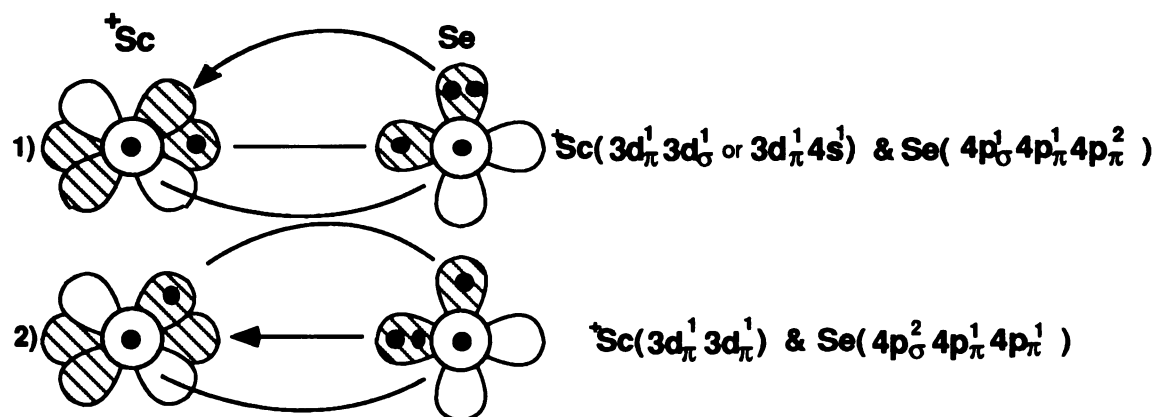
^a ref (2)

Table 2: Dissociation Energies (kcal/mol)

	MCSCF(D _e)	MCSCF+1+2(D _e)	Experimental ^a
SeH ² Π ⇒ Se ³ P + H ² S	64.3	71.8	
H ₂ Se ¹ A ₁ ⇒ SeH ² Π + H ² S	67.9	80.7	
H ₂ Se ¹ A ₁ ⇒ Se ³ P + 2H ² S	132.6	152.5	
H ₂ ¹ Σ _g ⁺ (3s/3p) ⇒ 2H ² S	93.8	105.4	103.3

^a ref (12)

The π bonds are equivalent at equilibrium but arise from formally different asymptotic occupations. This MCSCF function allows the two most important $^1\Sigma^+$ configurations to mix as illustrated below.



There are two formally covalent bonds (σ, π) and a π dative bond in structure 1), while in structure 2) there are two covalent π bonds and a σ dative bond possible.

The energy predicted by this function is shown in Figure 1 as a function of internuclear distance. The analogous $^+\text{ScO}^2$ and $^+\text{ScS}^1$ MCSCF energies are shown for comparison. The MCSCF function predicts a triply bonded species with an equilibrium separation (r_e) of 4.322 au and a dissociation energy (D_e) of 69 kcal/mol.

The energies of two low lying $^+\text{ScSe}$ triplet states were also computed and are displayed in Figure 1 as a function of internuclear distance. The $^+\text{ScSe } ^3\Delta$ state was examined with a GVB(2/4) function constructed from two π bonding pairs, one electron in an a_1 orbital and the other electron in an a_2 orbital followed by all spin couplings. This results in 25 CSFs. The predicted r_e of 4.617 au is 0.3 au longer than in the $^1\Sigma^+$ state while the D_e decreases to 16 kcal/mol.

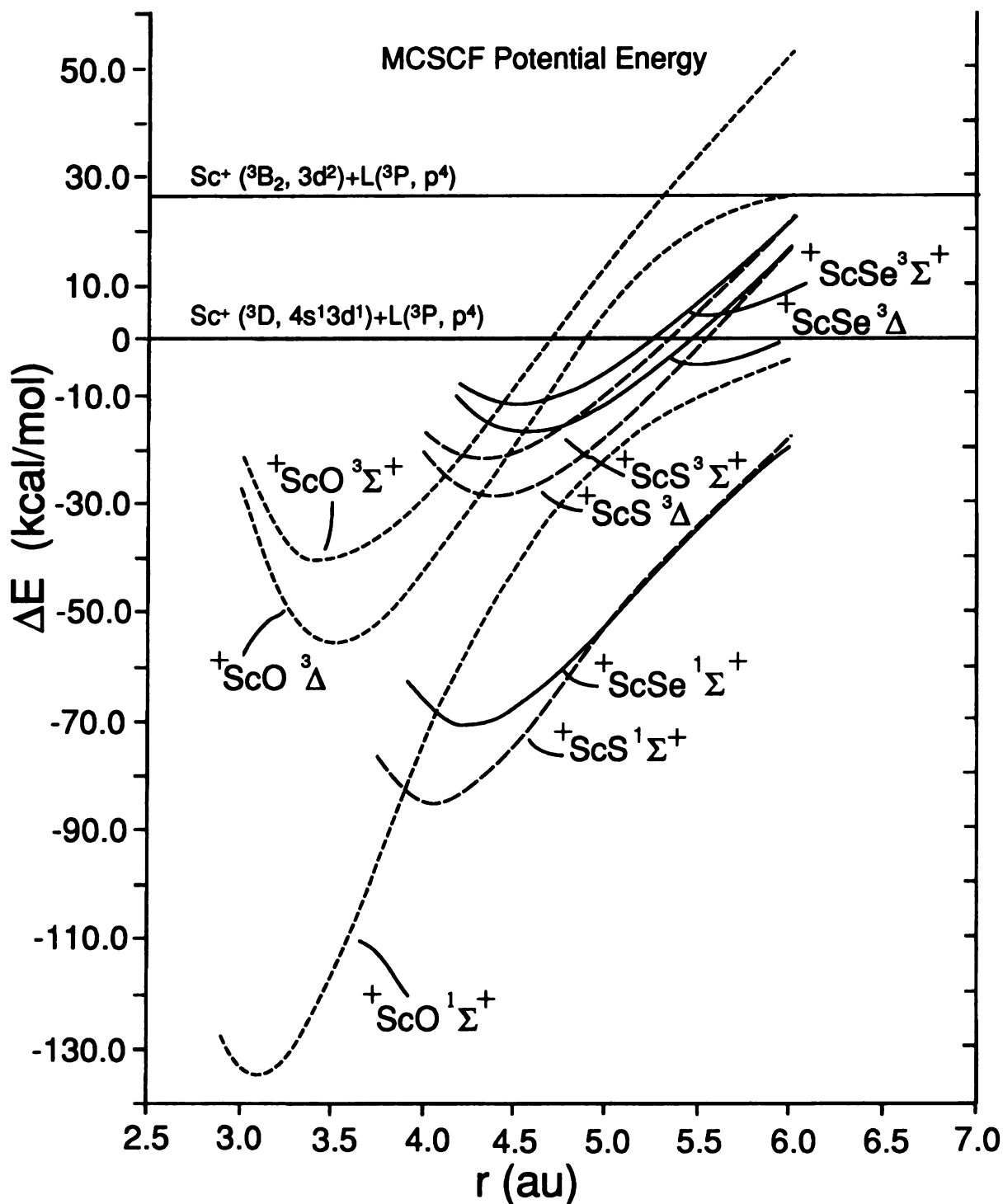


Figure 1. MScF potential energies of the $1\Sigma^+$, 3Δ and $3\Sigma^+$ states of $^+\text{ScSe}$, ^+ScS and ^+ScO relative to the ground state asymptote. Energy is in kcal/mol. The atomic structure at the asymptote is indicated by both atomic symmetry and valence configuration (L=Se, S, and O)

The structure has two π bonds, an open shell electron in a Se $4p\sigma$ orbital and another electron in a Sc^+ $3d\delta_-$ orbital. The Sc^+ $3d\delta_-$ occupation forces dissociation to the higher $^+\text{Sc}(3d\delta_-^1 3d\pi^1; ^3\text{B}_2) + \text{Se}(4s^2 4p^4; ^3\text{P})$ asymptote as indicated in fig 1.

The $^+\text{ScSe } ^3\Sigma^+$ state MCSCF function was constructed from a GVB(2/4) function with two π bonding pairs and 2 singly occupied a_1 orbitals. The Sc^+ $3d\delta_+$ orbitals were eliminated from the calculation to prevent collapse to the δ_+ component of the $^3\Delta$ state. All spin couplings of this function results in 25 CSFs. The computed D_e of 11 kcal/mol is 5 kcal/mol less than the $^3\Delta$ state and the r_e shrinks slightly to 4.542 au. The total energies, D_e s, r_e s and vibrational frequencies (ω_e) are collected in Table 3.

MCSCF+1+2 FUNCTION FOR $^+\text{ScSe}$

The configuration interaction (MCSCF+1+2) wavefunctions were constructed by taking all valence single and double substitutions from the MCSCF reference space. In particular, the $^1\Sigma^+$ MCSCF+1+2 function consists of 29,953 CSFs, the $^3\Delta$ of 36,686 CSFs and the $^3\Sigma^+$ of 32,962 CSFs. The added correlation lowers the total energies by around 61 mHartrees but has no effect on the state orderings. The energies as predicted by the MCSCF+1+2 functions are displayed in Figure 2 as a function of Sc-Se distance. The computed r_e and ω_e remain essentially unchanged while the D_e 's increased to 84 kcal/mol ($^1\Sigma^+$), 31 kcal/mol ($^3\Delta$) and 28 kcal/mol ($^3\Sigma^+$), respectively. The total energies, D_e s and some spectroscopic constants are collected in Table 3.

Table 3: $^3\text{ScSe}$, ^+ScS and ^+ScO Equilibrium Energies (E_{min} , au), Vibrational Frequencies (ω_e , cm^{-1}), Bond Lengths (r_e , au) and Dissociation Energies (kcal/mol).^a

State	Energy(E_{min} , au)		r_e (au)		ω_e (cm^{-1})		D_e (kcal/mol)	
	MCSCF	MCSCF+1+2	MCSCF	MCSCF+1+2	MCSCF	MCSCF+1+2	MCSCF	MCSCF+1+2
$^+\text{ScSe}^1\Sigma^+$	-3159.35518	-3159.41590	4.3224	4.3397	422	416	69.8	84.6
$^+\text{ScSe}^3\Delta$	-3159.26993	-3159.33073	4.6174	4.6156	333	330	16.3	31.2
$^+\text{ScSe}^3\Sigma^+$	-3159.26224	-3159.32598	4.5424	4.6496	320	213	11.4	28.2
$^+\text{ScS}^1\Sigma^+$	-1157.16247	-1157.22884	4.0477	4.0802	587	574	82.1	96.9
$^+\text{ScS}^3\Delta$	-1157.07250	-1157.13827	4.3767	4.3797	450	445	25.6	40.1
$^+\text{ScS}^3\Sigma^+$	-1157.06154	-1157.11827	4.3152	4.5611	423	358	18.8	27.6
$^+\text{ScO}^1\Sigma^+$	-834.56442	-834.63270	3.0953	3.1196	1067	1134	134.2	146.0
$^+\text{ScO}^3\Delta$	-834.43800	-834.50591	3.5008	3.4941	743	734	54.8	66.4
$^+\text{ScO}^3\Sigma^+$	-834.41312	-834.47419	3.4537	3.4361	592	622	39.2	46.5
Experimental Results ^b								
$1\Sigma^+(^+\text{ScO})^c$							159±7	
$2\Sigma^+(^+\text{ScO})$			3.153				162±3	
$2\Sigma^+(^+\text{ScS})$							113.5	
(ScSe)							91.4	

^a ^+ScS data from ref(1), ^+ScO data from ref(2), ^b ref (13), ^c ref (14)

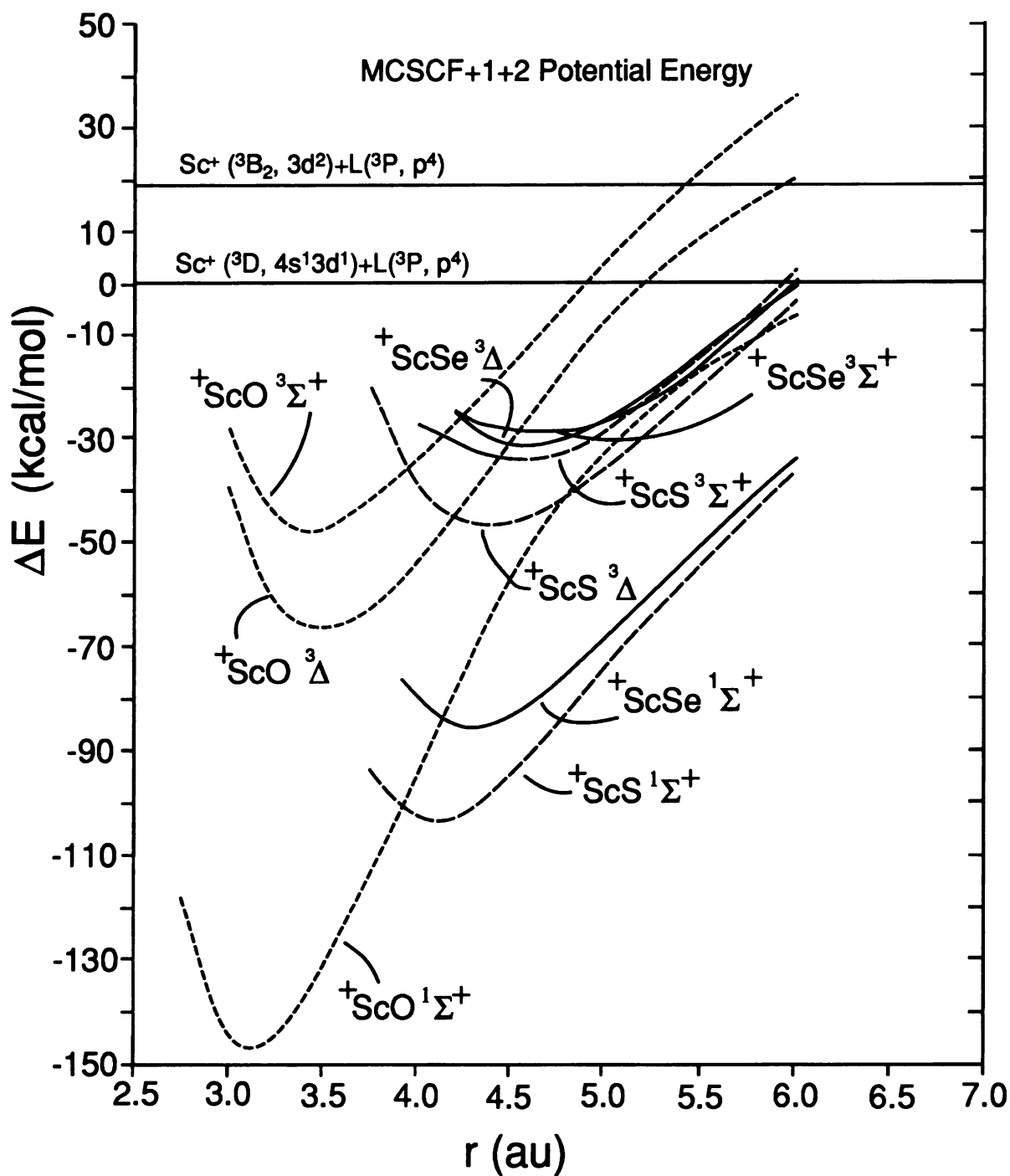


Figure 2. MCSCF+1+2 potential energies of the $1\Sigma^+$, 3Δ and $3\Sigma^+$ states of $^+\text{ScSe}$, ^+ScS and ^+ScO relative to the ground state asymptote. Energy is in kcal/mol. The atomic structure at the asymptote is indicated by both atomic symmetry and valence configuration (L=Se, S, and O)

ELECTRONIC STRUCTURE OF ^+ScSe

A Mulliken¹⁰ population analysis was performed on the MCSCF natural orbitals (NOs) of ^+ScSe and the results are collected in Table 4. The $^1\Sigma^+$ state is a triply bonded system with two π bonds and one σ bond. The π bonds are polarized towards the Scandium and are composed of, primarily, $Sc^+ 3d\pi$ and $Se 4p\pi$ orbitals. The polarization results in approximately 0.18 electrons (per π bond) being transferred to Sc^+ . The σ bond is a mixture of the $Se 4p\sigma$ and $Sc^+ 3d\sigma + \lambda 4s$ orbitals. The $Sc^+ 4s$ enters the σ bond with a weight of approximately 15%, nearly equal to that of the $3d\sigma$ orbital (20%). The σ bond is polarized towards Se and results in a transfer of 0.19 electrons from Sc^+ to Se. The gross atomic charge distribution in the $^1\Sigma^+$ state becomes $Sc^{+0.83}Se^{+0.17}$.

The $^3\Delta$ and $^3\Sigma^+$ states are both doubly bonded (π, π) species. The π bonds are composed of, primarily, $Sc^+ 3d\pi$ and $Se 4p\pi$ functions and are moderately polarized with the transfer of approximately 0.16e per π bond to Se. There are also two non-bonding electrons in these systems. One electron populates a $Se 4p\sigma$ orbital and the other an orbital on Sc^+ . In the $^3\Delta$ state, the Sc^+ non-bonded electron populates a pure $Sc^+ 3d\delta_-$ orbital. This is the lowest energy triplet with a bond strength of 31 kcal/mol (Table 3) and a $Sc^+ d^2$ configuration, in-situ. In the $^3\Sigma^+$ state, the Sc^+ non-bonded electron occupies an orbital of $3d\sigma + \lambda 4s$ character and is 3 kcal/mol higher (MCSCF+1+2) than the $^3\Delta$ (28 vs. 31 kcal/mol, Table 1). At intermediate separations the triplet coupled $Sc^+ 4s$ and $Se 4p\sigma$ electrons will interact repulsively.

Table 4: Valence $^+ScSe(H)$ MCSCF orbital populations at equilibrium

State	Sc^+							Se			H	
	4s	4p σ	4p x	4p y	3d σ	3d p_x	3d p_y	3d s	4s	4p σ	4p x	4p y
$^+ScSe(^1\Sigma^+)$	0.30	0.10	0.10	0.10	0.41	0.58	0.58	-	1.86	1.33	1.32	1.32
$^+ScSe(^3\Delta)$	0.13	0.09	0.10	0.10	0.09	0.24	0.24	1.00	1.85	0.83	1.66	1.66
$^+ScSe(^3\Sigma^+)$	0.27	0.10	0.11	0.11	0.94	0.23	0.23	-	1.88	0.81	1.66	1.66
$^+ScSeH(^2\Delta)$	0.13	0.09	0.09	0.09	0.10	0.20	0.20	1.00	1.75	1.15	1.71	1.71
$^+ScSeH(^2\Sigma^+)$	0.18	0.09	0.10	0.10	0.99	0.22	0.22	-	1.76	1.18	1.69	1.69

The π bonds are weak and cannot overcome this interaction. The repulsive energy increases with decreasing internuclear separation until it intersects the attractive $\text{Sc}^{++}(3d\sigma) + \text{Se}^-$ curve and finally settles into a structure with the Sc^+ open shell electron occupying an a_1 orbital of, primarily, $3d\sigma$ character.

The populations and NO structures suggests the following interpretation:

- 1) The π bonds are all composed of $\text{Sc}^+ 3d\pi$ and $\text{Se } 4p\pi$ orbitals.
- 2) The ground state $^1\Sigma^+$ σ bond is composed of a $\text{Se } 4p\sigma$ bonding to a Sc^+ orbital of equal amounts of $4s$ and $3d\sigma$.
- 3) The $^3\Delta$ and $^3\Sigma^+$ states are both π,π doubly bonded systems and each have a non-bonded electron on Sc^+ occupying a predominantly $3d$ type orbital.

The MCSCF orbital populations of $^+\text{ScS}^1$ and $^+\text{ScO}^2$ are collected in Tables 5 and 6 for comparison and reveal several trends. The Sc^+ $4s$ contribution, in the $^1\Sigma^+$ states, increases with increasing ligand size and presumably results from the longer bonding distances. The radial distribution functions (RDF) for the Sc^+ s , p and d orbitals ($1s$ not included) were plotted (Figure 3) and show that the $3d$ RDF has a maximum at approximately 1 au and decreases substantially between 2 and 4 au. The $4s$ reaches a maximum at approximately 3.0 au and decreases only slightly by 4 au.

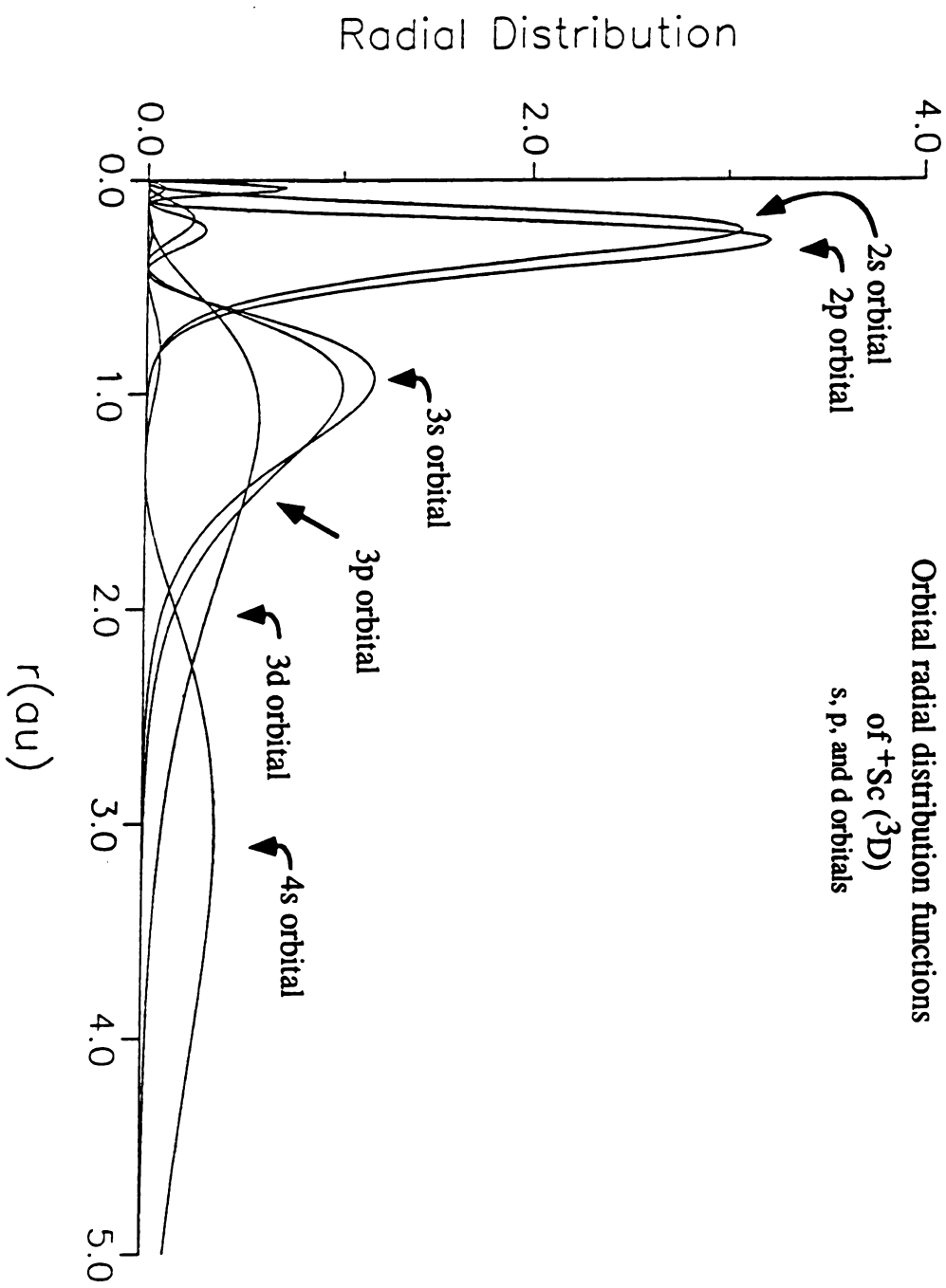


Figure 3. Radial distribution function of the ground state $^+Sc(3D)$. These are orbital radial distribution functions derived from a SCF calculation using a 5s, 4p, 10d basis set.

Table 5: Valence ^+ScS (H) MCSCF orbital populations at equilibrium^a

State	Sc^+										S			H
	4s	4p _σ	4p _x	4p _y	3d _σ	3d _{p_x}	3d _{p_y}	3d _δ	3s	3p _σ	3p _x	3p _y		
$^+ScS(^1\Sigma^+)$	0.17	0.06	0.08	0.08	0.43	0.52	0.52	-	1.94	1.42	1.39	1.39		
$^+ScS(^3\Delta)$	0.10	0.06	0.08	0.08	0.08	0.21	0.21	1.00	1.90	0.86	1.71	1.71		
$^+ScS(^3\Sigma^+)$	0.30	0.07	0.08	0.08	0.86	0.22	0.22	-	1.92	0.87	1.69	1.69		
$^+ScSH(^2\Delta)$	0.14	0.08	0.08	0.08	0.10	0.19	0.19	1.00	1.79	1.11	1.73	1.73	0.78	
$^+ScSH(^2\Sigma^+)$	0.28	0.09	0.08	0.08	0.93	0.20	0.20	-	1.80	1.14	1.71	1.71	0.78	

^a ref(1)

Table 6: Valence ${}^+ScO$ (H) MCSCF orbital populations at equilibrium^a

State	Sc^+										O			H
	4s	4p $_{\sigma}$	4p $_x$	4p $_y$	3d $_{\sigma}$	3d $_{p_x}$	3d $_{p_y}$	3d $_{\delta}$	2s	2p $_{\sigma}$	2p $_x$	2p $_y$		
${}^+ScO(1\Sigma^+)$	0.02	0.19	0.05	0.05	0.55	0.43	0.43	-	1.80	1.44	1.52	1.52		
${}^+ScO(3\Delta)$	0.02	0.09	0.04	0.04	0.07	0.16	0.16	1.00	1.88	0.94	1.80	1.80		
${}^+ScO(3\Sigma^+)$	0.40	0.07	0.04	0.04	0.67	0.19	0.19	-	1.90	0.96	1.77	1.77		
${}^+ScOH(2\Delta)$	0.03	0.10	0.03	0.03	0.10	0.12	0.12	1.00	1.74	1.37	1.83	1.83	0.64	
${}^+ScOH(2\Sigma^+)$	0.48	0.08	0.03	0.03	0.61	0.16	0.16	-	1.76	1.42	1.80	1.80	0.67	

^a ref(2)

The increase in Sc^+ 4s contribution to the σ bond at the longer bond distances reflects the favorable increase in overlap with the ligand $p\sigma$.

Secondly, as the bond length in the $^1\Sigma^+$ states is increased, the Sc^+ gross atomic charge decreases. In particular, the Sc^+ atomic charge goes from +1.28 in ^+ScO ,² to +1.14 in ^+ScS ¹ and to +0.85 in $^+\text{ScSe}$. The gross atomic charges are collected in Table 7.

The triplet states all have very similar π bonding structures with the ligand valence $p\pi$ orbitals making a lesser contribution at the longer equilibrium bond distances. A conspicuous feature of these data are the orbital population trends in the $^3\Sigma^+$ states. The π bonds are nearly identical to the corresponding $^3\Delta$ states but the Sc^+ 4s contribution to the spectator electron structure decreases with increasing bond distance.

In contrast to the $^1\Sigma^+$ states where at longer bond lengths a greater σ bond overlap occurs with inclusion of the Sc^+ 4s, the triplet coupling of the two σ non-bonded electrons requires this overlap to be a minimum. In ^+ScO ² this is accomplished by promoting the Sc^+ spectator electron to a $4s+\lambda 3d\sigma$ orbital with approximately 40% 4s character. This hybridization drains charge away from the internuclear axis. In $^+\text{ScSe}$ the $3d\sigma$ orbital is apparently small enough to not significantly interfere with Se at the large equilibrium separation and so does not hybridize as much. The ^+ScS ¹ structure is again intermediate. The orbital populations for selected valence orbitals of ^+ScL (L=O,S,Se) are displayed in Figure 4. These data are collected in a way to allow comparisons amongst the different studied states and illustrate the trends in charge transfer.

Table 7: MCSCF Gross atomic charge distribution^a

System	State	Gross atomic charge		
		Sc	Se	H
⁺ ScSe	(¹ Σ ⁺)	+0.83	+0.17	
⁺ ScSe	(³ Δ)	+1.00	+0.00	
⁺ ScSe	(³ Σ ⁺)	+1.01	-0.01	
⁺ ScSeH	(² Δ)	+1.10	-0.32	+0.22
⁺ ScSeH	(² Σ ⁺)	+1.10	-0.32	+0.22
		Sc	S	H
⁺ ScS	(¹ Σ ⁺)	+1.14	-0.14	
⁺ ScS	(³ Δ)	+1.18	-0.18	
⁺ ScS	(³ Σ ⁺)	+1.17	-0.17	
⁺ ScSH	(² Δ)	+1.14	-0.36	+0.22
⁺ ScSH	(² Σ ⁺)	+1.14	-0.36	+0.22
		Sc	O	H
⁺ ScO	(¹ Σ ⁺)	+1.28	-0.28	
⁺ ScO	(³ Δ)	+1.42	-0.42	
⁺ ScO	(³ Σ ⁺)	+1.40	-0.40	
⁺ ScOH	(² Δ)	+1.41	-0.77	+0.36
⁺ ScOH	(² Σ ⁺)	+1.45	-0.78	+0.33

^a ⁺ScS data from ref(1), ⁺ScO data from ref(2)

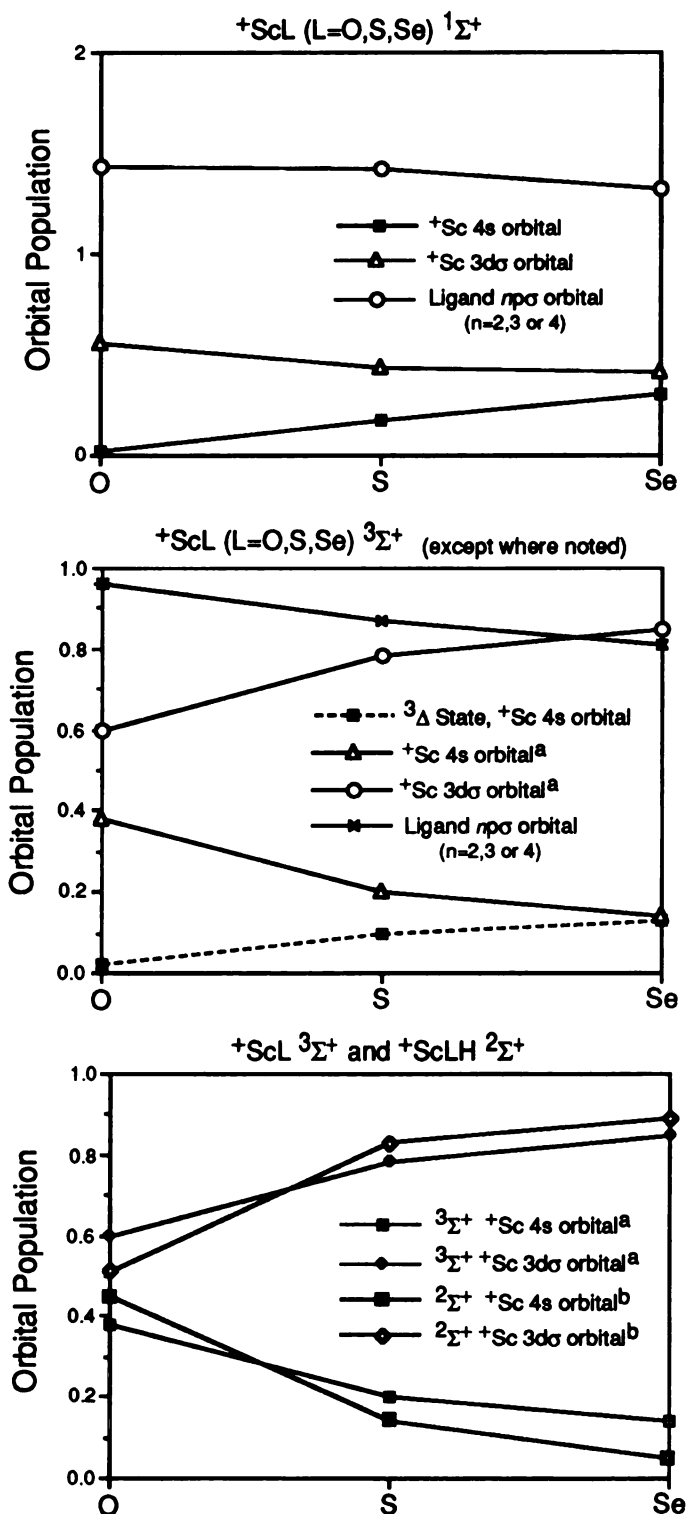


Figure 4. Orbital populations of $+ScL$ and $+ScLH$ ($L=O,S,Se$). The connection of data points is only for association and does not imply a continuous relationship. S data from Ref(1). O data from Ref(2).

^a Orbital population data relative to associated $^3\Delta$ state. ^b Orbital population data relative to associated $^2\Delta$ state.

In the studied triplets, the lowest energy state has a Sc^+ (d^2) in-situ configuration ($^3\Delta$) suggesting that in the field of the ligand the required excitation of Sc^+ to the d^2 configuration in-situ is offset by a decrease in the electron repulsions. The mixing of the Sc^+ 4s orbital into the Sc^+ spectator electron density in the $^3\Sigma^+$ states has a marked effect on the energy. We find that while the $^3\Delta$ bond energies decrease with increasing ligand size (bond length) the Sc^+ 4s contribution to the $^3\Sigma^+$ states also decreases, causing the $^3\Sigma^+ \leftarrow ^3\Delta$ separation to decrease. This separation is the least for $^+\text{ScSe}$ and results in the $^+\text{ScSe } ^3\Sigma^+$ state being more bound than the $^+\text{ScS } ^3\Sigma^+$ state. Theoretical results indicate that the $^3\Sigma^+ \leftarrow ^3\Delta$ separation decreases in the order ^+ScO (19.9 kcal/mol), ^+ScS (12.5 kcal/mol) and $^+\text{ScSe}$ (3.0 kcal/mol).

$^+\text{ScSeH}$ GENERAL CONSIDERATIONS

The $^+\text{ScSeH}$ molecule may be formed by bonding Hydrogen to either of the open shell electrons in triplet $^+\text{ScSe}$. Recent theoretical studies² have indicated that $\text{H-}^+\text{ScO}$ is less bound than $^+\text{ScOH}$ due to disruption of an induced sigma bond, and that $^+\text{ScOH}$ prefers a linear conformation. These results were applied here by examining the linear $^+\text{ScSeH}$ isomer. $^+\text{ScSeH}$ has three formal bonds (two $^+\text{Sc-Se}$ π bonds and a Se-H σ bond) and a singly occupied orbital that carries the molecular symmetry.

The $^2\Delta$ state MCSCF function was constructed by correlating the three bonds in a GVB way and placing the final valence electron in an a_2 orbital (δ_-).

$$\Psi \sim (\text{core})^2 2\delta_{-1}(14\sigma^2-\lambda 15\sigma^2)(6\pi_x^2-v7\pi_x^2)(6\pi_y^2-v7\pi_y^2)$$

All spin couplings of this function results in 76 CSFs under a C_{2v} point group. The ${}^2\Sigma^+$ state MCSCF function was constructed by correlating the two π bonds in a GVB way and allowing all occupations of the three valence σ (a_1) orbitals (Complete Active Space in the valence σ space) to insure that no limitations are imposed on the calculation. The $\text{Sc}^+ 3d\delta_+$ orbitals were eliminated from the calculation to prevent collapse to the δ_+ component of the lower energy ${}^2\Delta$ state. All spin couplings of this function result in 144 CSFs under a C_{2v} point group.

$$\Psi \sim (\text{core})^2 (14\sigma,15\sigma,16\sigma)(6\pi_x^2-v7\pi_x^2)(6\pi_y^2-v7\pi_y^2)$$

The MCSCF+1+2 wavefunction for each state was constructed by allowing all valence single and double substitutions from the MCSCF reference space. This results in 144,982 CSFs (${}^2\Delta$) and 166,770 CSFs (${}^2\Sigma^+$).

The ${}^2\Delta$ state is bound by 118.6 kcal/mol relative to the ground state atoms and is 3.2 kcal/mol lower in energy than the ${}^2\Sigma^+$ state. The optimized geometries are very similar. In particular, for the ${}^2\Delta$ state the ${}^+\text{Sc-SeH}$ bond length is 4.567 au (MCSCF+1+2) with a Se-H length of 2.760 au, while in the ${}^2\Sigma^+$ state ${}^+\text{Sc-SeH}$ bond contracts a small amount to 4.464 au and the Se-H bond lengthens to 2.774 au. The total energies and optimized geometries are collected in Table 8. Table 9 contains several computed bond energies.

Table 8: ^+ScSeH , ^+ScSH , and ^+ScOH Equilibrium energies (au), Equilibrium bond lengths (au) and Dissociation energies (kcal/mol)^a

State	Energy		^+SCLH							
	MCSCF	MCSCF+1+2	$r_e(Sc-L)$	$D_e(Sc-L)$	$r_e(L-H)$	$D_e(L-H)^{b,c}$	$r_e(Sc-L)$	$D_e(Sc-L)$	$r_e(L-H)$	$D_e(L-H)^{b,c}$
$^+ScSeH \ ^2\Delta$	-3159.89669	-3159.97035	4.568	31.5	2.769	26.5(80.0)	4.567	46.8	2.760	34.6(88.1)
$^+ScSeH \ ^2\Sigma^+$	-3159.89047	-3159.96526	4.508	27.6	2.800	22.6(80.9)	4.464	43.7	2.774	31.4(87.8)
$^+ScSH \ ^2\Delta$	-1157.71187	-1157.78806	4.359	43.3	2.540	31.5(87.9)	4.353	56.6	2.535	37.6(94.4)
$^+ScSH \ ^2\Sigma^+$	-1157.70291	-1157.76543	4.269	37.6	2.555	25.8(89.2)	4.189	42.4	2.561	23.4(92.8)
$^+ScOH \ ^2\Delta$	-835.15522	-835.22690	3.509	101.8	1.848	57.4(136.7)	3.505	108.0	1.821	59.6(139.2)
$^+ScOH \ ^2\Sigma^+$	-835.13583	-835.19948	3.505	89.7	1.829	45.3(140.2)	3.481	90.8	1.836	42.4(141.8)

^a S data from ref(1), O data from ref(2).

^b ($^2\Delta$) Values in parenthesis are for separation to $^+ScL(^2\Delta)+H$. ^c ($^2\Sigma^+$) Values in parenthesis are for separation to $^+ScL(^3\Sigma^+)+H$.

Table 9: Summary of MCSCF+1+2 Sc⁺ + H₂Se, H₂S and H₂O fragment energies (kcal/mol)

System	Energy	System	Energy ^a	System	Energy ^b
SeH(² π) ⇒ Se + H	71.8	SH(² π) ⇒ S + H	78.0	OH(² π) ⇒ O + H	97.6
+ScSe(¹ Σ ⁺) ⇒ Sc ⁺ + S	84.6	+ScS(¹ Σ ⁺) ⇒ Sc ⁺ + S	96.9	+ScO(¹ Σ ⁺) ⇒ Sc ⁺ + O	146.0
+ScSe(³ Δ) ⇒ Sc ⁺ + S	31.2	+ScS(³ Δ) ⇒ Sc ⁺ + S	40.1	+ScO(³ Δ) ⇒ Sc ⁺ + O	66.4
+ScSe(³ Σ ⁺) ⇒ Sc ⁺ + S	28.2	+ScS(³ Σ ⁺) ⇒ Sc ⁺ + S	27.6	+ScO(³ Σ ⁺) ⇒ Sc ⁺ + O	46.5
+ScSeH(² Δ) ⇒ +ScS(¹ Σ ⁺) + H	34.6	+ScSH(² Δ) ⇒ +ScS(¹ Σ ⁺) + H	37.6	+ScOH(² Δ) ⇒ +ScO(¹ Σ ⁺) + H	59.6
+ScSeH(² Δ) ⇒ +ScS(³ Δ) + H	88.1	+ScSH(² Δ) ⇒ +ScS(³ Δ) + H	94.4	+ScOH(² Δ) ⇒ +ScO(³ Δ) + H	139.1
+ScSeH(² Δ) ⇒ +Sc + SH(² π)	46.8	+ScSH(² Δ) ⇒ +Sc + SH(² π)	56.6	+ScOH(² Δ) ⇒ +Sc + OH(² π)	108.0
+ScSeH(² Σ ⁺) ⇒ +ScS(¹ Σ ⁺) + H	31.4	+ScSH(² Σ ⁺) ⇒ +ScS(¹ Σ ⁺) + H	23.4	+ScOH(² Σ ⁺) ⇒ +ScO(¹ Σ ⁺) + H	42.4
+ScSeH(² Σ ⁺) ⇒ +ScS(³ Σ ⁺) + H	87.8	+ScSH(² Σ ⁺) ⇒ +ScS(³ Σ ⁺) + H	92.8	+ScOH(² Σ ⁺) ⇒ +ScO(³ Σ ⁺) + H	141.8
+ScSeH(² Σ ⁺) ⇒ +Sc + SH(² π)	53.7	+ScSH(² Σ ⁺) ⇒ +Sc + SH(² π)	42.4	+ScOH(² Δ) ⇒ +Sc + OH(² π)	90.8
		+ScSH ₂ (³ A ₂) ⇒ +Sc + SH ₂ (¹ A ₁)	11.4	+ScOH ₂ (³ A ₂) ⇒ +Sc + OH ₂ (¹ A ₁)	36.2 ^c
		+ScSH ₂ (³ A ₁) ⇒ +Sc + SH ₂ (¹ A ₁)	11.4	H ₂ +ScO(¹ A ₁) ⇒ +Sc + OH ₂ (¹ A ₁)	35.1
		H ₂ +ScS(¹ A ₁) ⇒ H ₂ + +ScS(¹ Σ ⁺)	3.6	H ₂ +ScO(¹ A ₁) ⇒ H ₂ + +ScO(¹ Σ ⁺)	2.5
		H ₂ +ScS(¹ A ₁) ⇒ +Sc + SH ₂ (¹ A ₁)	34.5	H ⁺ +ScOH(¹ A) ⇒ +Sc + OH ₂ (¹ A ₁)	40.1

^a +ScS data from Ref(1) ^b +ScO data from Ref(2), ^c Ref (15)

ELECTRONIC STRUCTURE OF $^+\text{ScSeH}$

The $^+\text{ScSeH}$ valence orbital populations are collected in Table 2 and the gross atomic charges in Table 7. The $^2\Delta$ and $^2\Sigma^+$ states are similar, with two ($\text{Sc}^+ 3d\pi - \text{Se } 4p\pi$) π bonds, a Se-H σ bond and a non-bonded electron on Sc^+ . The π bonds are polarized towards Se with approximately 0.21e (per bond, $^2\Delta$) transferred to Se. The Se-H σ bond is also polarized and transfers 0.22e to Se from H. This H to Se charge transfer is similar¹¹ to that computed for SeH and SeH₂ and is consistent with the results of $^+\text{ScOH}^2$ and $^+\text{ScSH}^1$. The gross atomic charge distribution for the $^2\Delta$ and $^2\Sigma^+$ states becomes $\text{Sc}^{+1.10}\text{Se}^{-0.32}\text{H}^{+0.22}$.

The non-bonded electron in the $^2\Delta$ ground state occupies a pure $^+\text{Sc } 3d\delta_-$ orbital and indicates that, as with the $^+\text{ScSe}$ triplet states, $^3F^+\text{Sc } (3d^2)$ is the preferred in-situ configuration. The $^2\Sigma^+$ state non-bonded electron is primarily in a $^+\text{Sc } 3d\sigma$, and the $^2\Sigma^+ \leftarrow ^2\Delta$ separation is 3.2 kcal/mol.

In comparison to the MCSCF populations of $^+\text{ScSH}^1$ and $^+\text{ScOH}^2$ (Tables 5 and 6, respectively) we find that as the equilibrium $^+\text{Sc-LH}$ bond length increases, the amount of $^+\text{Sc } 4s$ mixed into the non-bonded electron orbital decreases. This trend is consistent with the triplet ^+ScL results. When H is bonded to the ligand atom, L (L=O,S,Se), the π bonds become slightly more polarized with from 0.2e (^+ScS) to 0.5e ($^+\text{ScSe}$) additional charge transferred to L from ^+Sc . The bonding of H to L causes L to become more negatively charged and causes an increased polarization of the ^+Sc atom.

Selected valence orbital populations of the ${}^+ScLH$ ${}^2\Sigma^+$ states are collected in Figure 4.

The similarities in π bond and non-bonded electron structures are illustrated in the DDCs (Figures 5,6 and 7). These contours were generated by computing the MCSCF total density for the ${}^+ScLH$ molecules at the equilibrium geometry and subtracting from this the total density of the indicated ${}^+ScL$ triplets superimposed at the ${}^+ScLH$ geometry. Positive contours are indicated by solid curves and negative contours by dashes. In all plots, Sc is at the origin. The lack of π contours in the DDCs indicates that the π density in the triplet ${}^+ScL$ and doublet ${}^+ScLH$ states are nearly equivalent. The non-bonding Sc^+ σ electron has a $d\sigma+\lambda 4s$ shape (${}^2\Sigma^+ - {}^3\Delta$ images) with relatively more density perpendicular to the bonding axis in ${}^+ScOH$. The bonding of H to ${}^+ScL$ introduces more charge density to the σ space (${}^2\Sigma^+ - {}^3\Sigma^+$ images).

The structure of the Sc^+ spectator electron in the ${}^2\Sigma^+$ state is also illustrated in the contours of the valence NO amplitudes (Figure 8). The large Sc^+ 4s component and its effect on ${}^+ScOH$ is evident. In these systems the Sc^+ spectator electron density is seemingly next to the ligand atom core. In ${}^+ScOH$ this core is only 3.5 au from Sc^+ and a large 4s component is introduced to allow perpendicular displacement. In ${}^+ScSeH$, the longer bond length allows significantly more population of the Sc^+ 3d σ orbital.

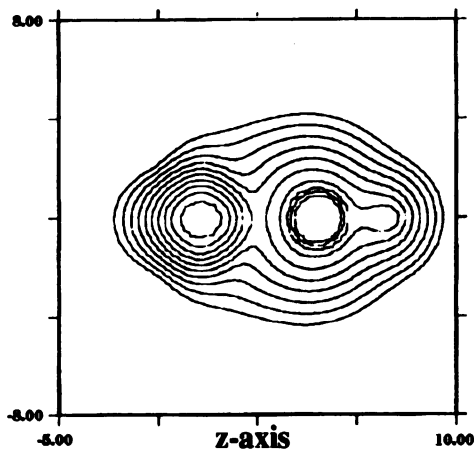
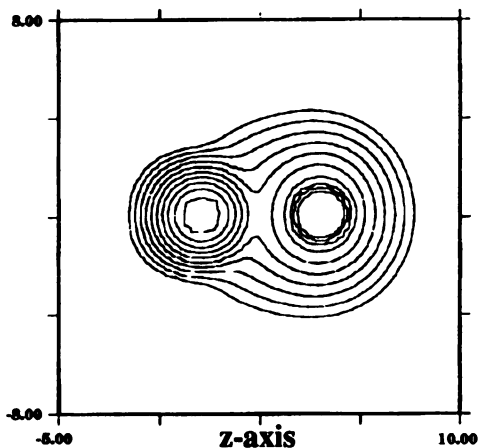
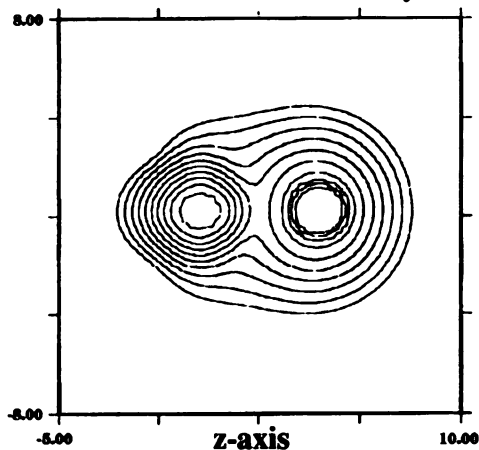
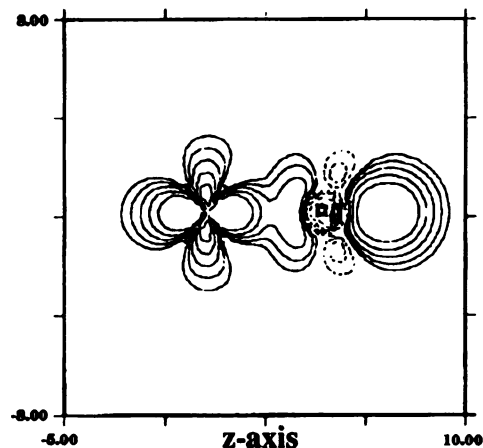
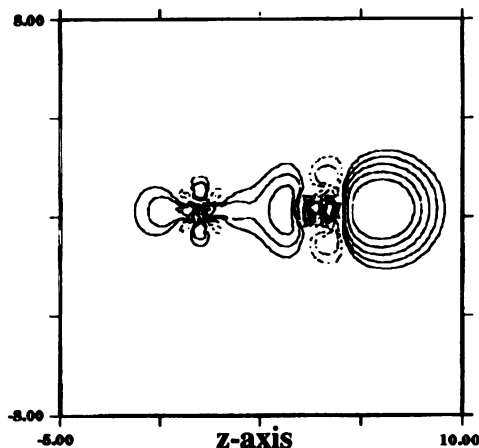
$^+ScSeH(2\Sigma^+)$ Total Density at equilibrium

 $^+ScSe(3\Delta)$ Total Density

 $^+ScSe(3\Sigma^+)$ Total Density

 $^+ScSeH(2\Sigma^+) - ^+ScSe(3\Delta)$ Diff. Density

 $^+ScSeH(2\Sigma^+) - ^+ScSe(3\Sigma^+)$ Diff. Density


Figure 5. MCSCF total density contours (TDCs) and difference density contours (DDCs) for the $2\Sigma^+$ state of ^+ScSeH and the $1\Sigma^+$ and $3\Sigma^+$ states of ^+ScSe . The DDCs are molecular differences where the ^+ScSe states are subtracted from the ^+ScSeH density. The ^+ScSe states are at the equilibrium ^+ScSeH (Sc-Se) geometry. Contour levels range from 0.0025e to 1.28e (TDCs) and -0.04e to 0.04e (DDCs). Each level differs by a factor of 2. No zero contours are displayed and negative contours are indicated by dashes.

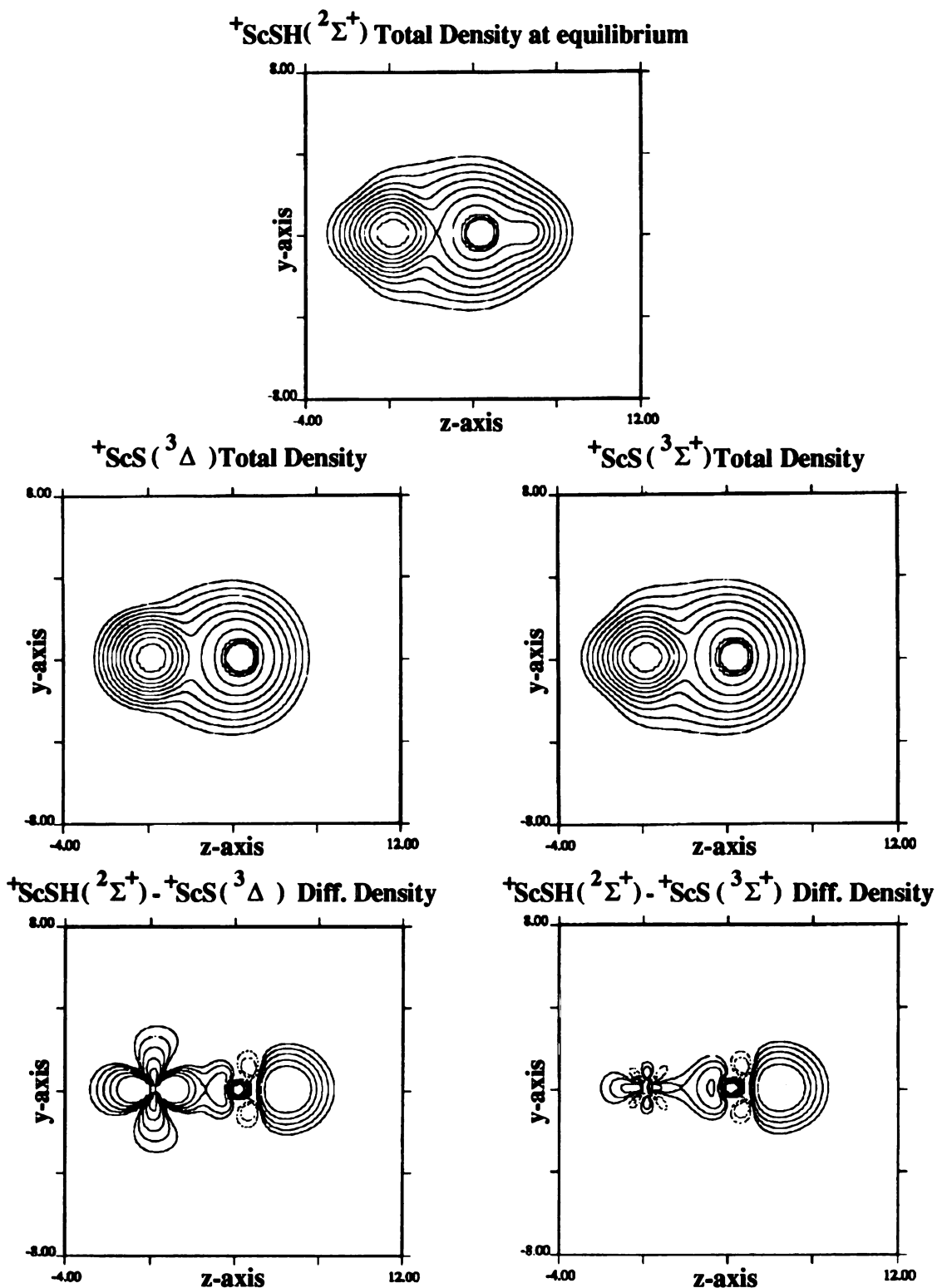


Figure 6. MCSCF total density contours (TDCs) and difference density contours (DDCs) for the ${}^2\Sigma^+$ state of ${}^+ScSH$ and the ${}^1\Sigma^+$ and ${}^3\Sigma^+$ states of ${}^+ScS$. The DDCs are molecular differences where the ${}^+ScS$ states are subtracted from the ${}^+ScSH$ density. The ${}^+ScS$ states are at the equilibrium ${}^+ScSH$ (Sc-S) geometry. Contour levels range from 0.0025e to 1.28e (TDCs) and -0.04e to 0.04e (DDCs). Each level differs by a factor of 2. No zero contours are displayed and negative contours are indicated by dashes.

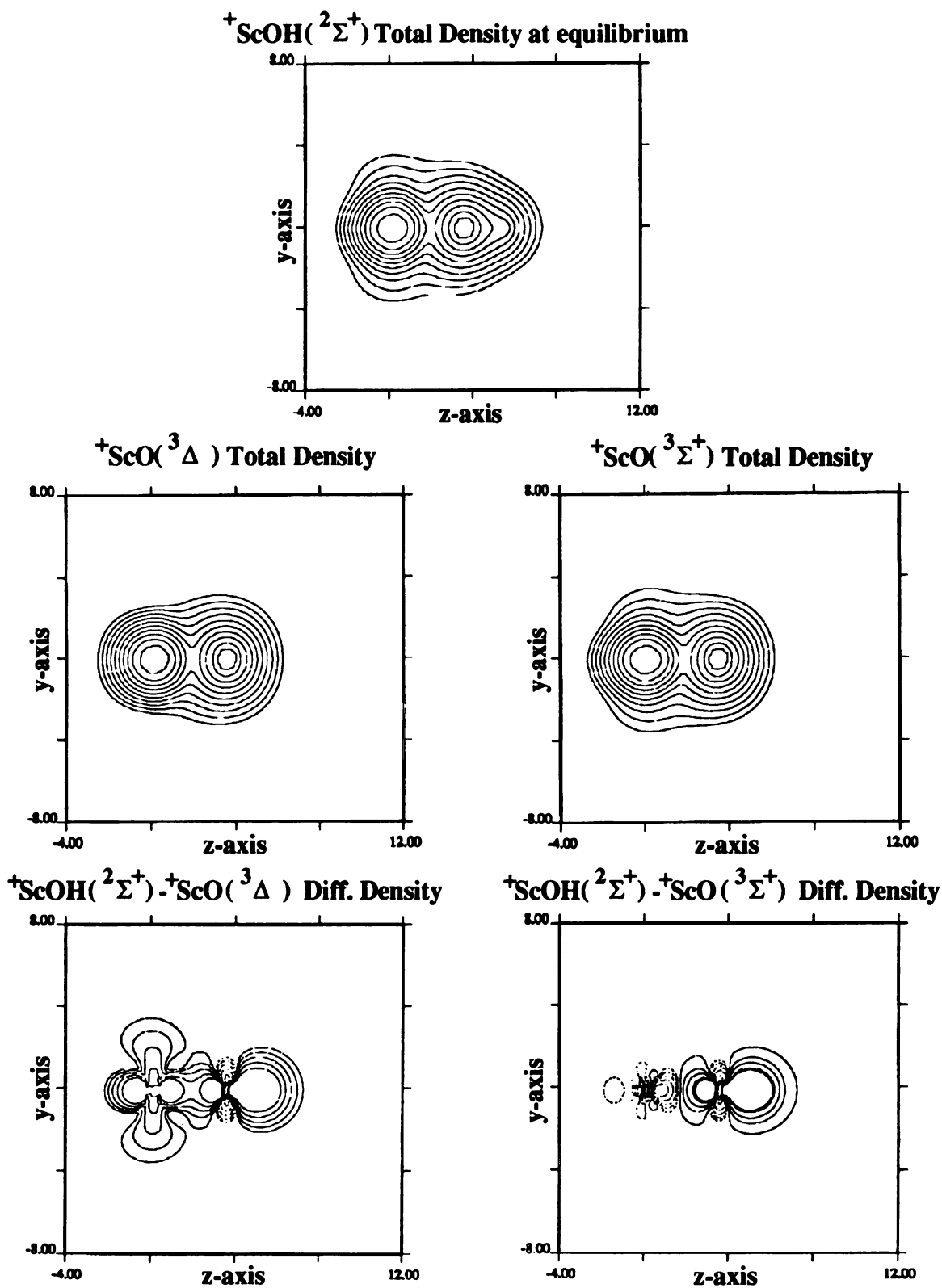


Figure 7. MCSCF total density contours (TDCs) and difference density contours (DDCs) for the ${}^2\Sigma^+$ state of ${}^+ScOH$ and the ${}^1\Sigma^+$ and ${}^3\Sigma^+$ states of ${}^+ScO$. The DDCs are molecular differences where the ${}^+ScO$ states are subtracted from the ${}^+ScOH$ density. The ${}^+ScO$ states are at the equilibrium ${}^+ScOH$ (Sc-O) geometry. Contour levels range from 0.0025e to 1.28e (TDCs) and -0.04e to 0.04e (DDCs). Each level differs by a factor of 2. No zero contours are displayed and negative contours are indicated by dashes.

Amplitudes of the valence sigma natural orbitals for the indicated species.
 $L=0$, S and Se

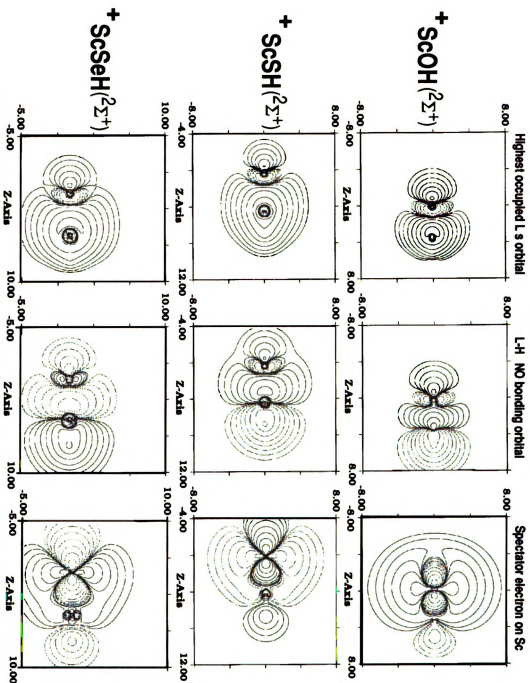


Figure 8. Contours of the valence natural orbitals for the $2\Sigma^+$ states of $+ScLH$ at equilibrium. The orbitals contoured include the Sc^+ spectator electron, the L-H bonding orbital and the highest doubly occupied orbital on L. The contours range from -0.04e to +0.04e and each contour level differs by a factor of 2. Negative contours are indicated by dashes. No zero contours are displayed. Sc is at the origin with L-H to the right. S data from Ref(1). O data from Ref(2).

THERMOCHEMISTRY

Figures 9-11 illustrate the energy relationships for the ^+ScSeH , ^+ScSH and ^+ScOH systems. The ^+ScLH (L=O,S,Se) $^2\Delta - ^2\Sigma^+$ energy separation decreases in going from O to S to Se, becoming 3.2 kcal/mol for L=Se. This is consistent with the triplet results and indicates the Scandium spectator electron has little influence on the bonding.

An induced σ bond causes a differential stabilization of these systems and this stabilization decreases for increasing ligand size. For example, ^+ScLH (L=O,S,Se) may dissociate to $^+ScL + H$ along the character-conserving paths:



If bond additivities were applicable to these systems one might expect that, since the open shell electron on Scandium isn't involved in bonding, these energies would be the same for a given L and moreover that these energies would be equal to the L-H bond strength. In fact, we find a consistent enhancement of the $^+ScL-H$ energies relative to L-H, with the greatest amount of stabilization in ^+ScOH .² The MCSCF+1+2 stabilization was found to be 42 kcal/mol for ^+ScOH ,² 16.5 kcal/mol for ^+ScSH ¹ and 15.6 kcal/mol for ^+ScSeH .

This stabilization is caused by a σ dative bond formed between ^+Sc and L. Bonding of H to L introduces charge density into the ^+Sc-L σ space (Figures 5, 6 and 7). In ^+ScOH ² this σ bond is strong (≈ 42 kcal/mol) and composed of primarily an O $2s+\lambda 2p\sigma$ hybrid

orbital bonding to a ^+Sc $3d\sigma+4p\sigma$ hybrid orbital (Table 4; $^2\Delta$). The O $2s+\lambda 2p\sigma$ hybrid is the companion orbital to the O-H bond. In ^+ScSeH the Se-H bond is mostly Se $4p\sigma + H$ $1s$; therefore the charge available for bonding to ^+Sc is primarily from the Se $4s$. This $4s$ donates charge into a ^+Sc $4s+3d\sigma+4p\sigma$ orbital and results in an induced σ bond significantly weaker than in ^+ScOH . The ^+ScSH results are intermediate. This is illustrated in Figure 8 where the orbital amplitude contours corresponding to the spectator electron on Scandium, the L-H bonding orbital and the highest doubly occupied s orbital on L for the $^2\Sigma^+$ states are presented.

The induced σ stabilization has large effects on the chemistry of these systems. In the gas phase reaction of $Sc^+ + H_2O$ the ground state reaction product was computed to be the inserted H^+ScOH species exoergic by 40 kcal/mol.² In the reaction $Sc^+ + H_2S$, we calculated an induced σ bond stabilization of 16.5 kcal/mol for ^+ScSH and determined the ground state reaction product should be the electrostatic species $H_2\cdots^+ScS$, exoergic by 34.5 kcal/mol.¹ H_2 is the intact molecule interacting electrostatically with the ground $^1\Sigma^+$ state of ^+ScS . The ^+ScSe work presented here suggests that due to the small induced stabilization in ^+ScSeH , the ground state of the gas phase reaction $Sc^+ + SeH_2$ should also be the $H_2\cdots^+ScSe$ species. The reaction energy can be estimated using the computed H_2 bond strength of 105.4 kcal/mol (Table 2), the calculated ^+ScSe $^1\Sigma^+$ bond strength of 84.6 kcal/mol (Table 3), and the SeH_2 dissociation energy of 152.5 kcal/mol (Table 2). These values indicate the $H_2\cdots^+ScSe$ reaction product is exoergic by approximately 37.5 kcal/mol.

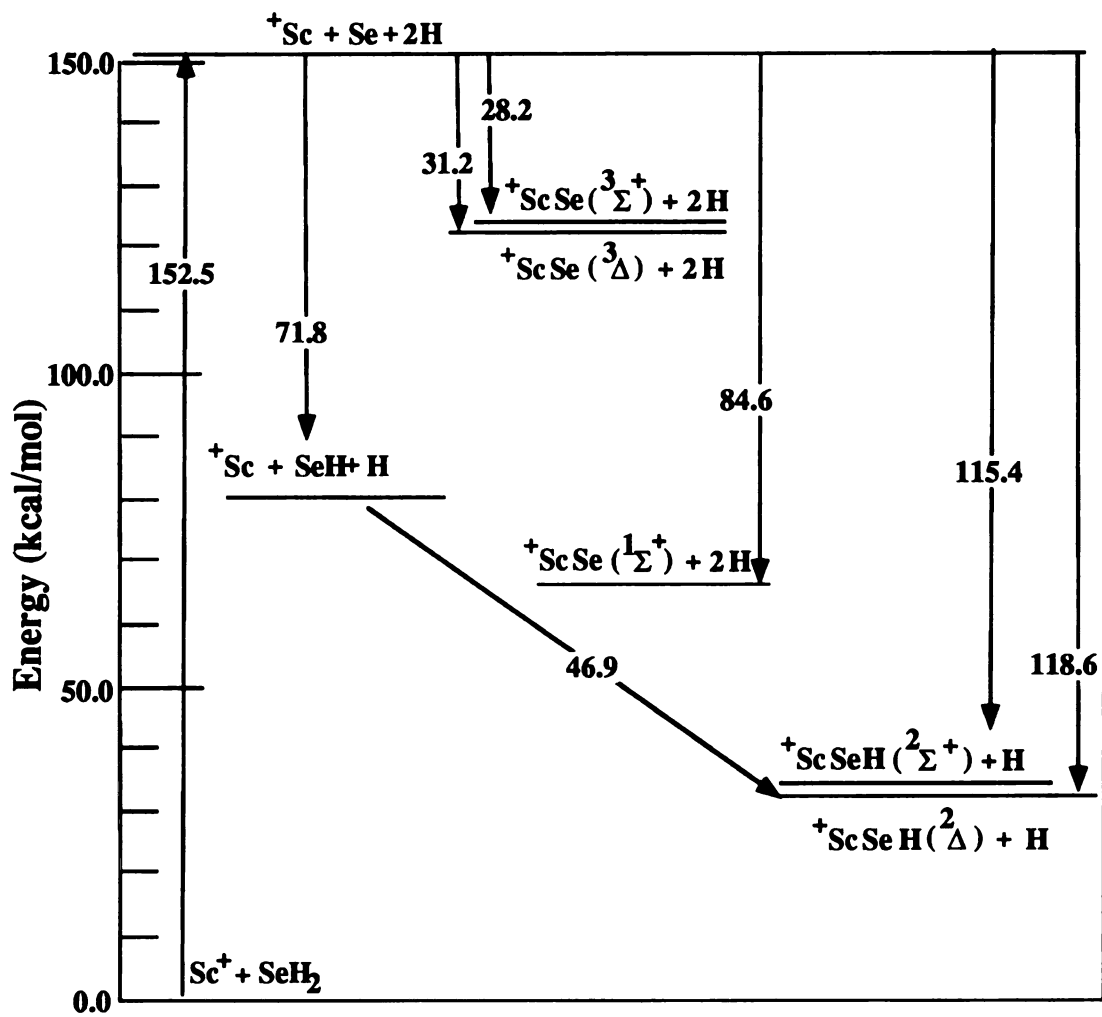


Figure 9. MCSCF+1+2 relative energies (kcal/mol) of selected $\text{Sc}^+ + \text{SeH}_2$ products.

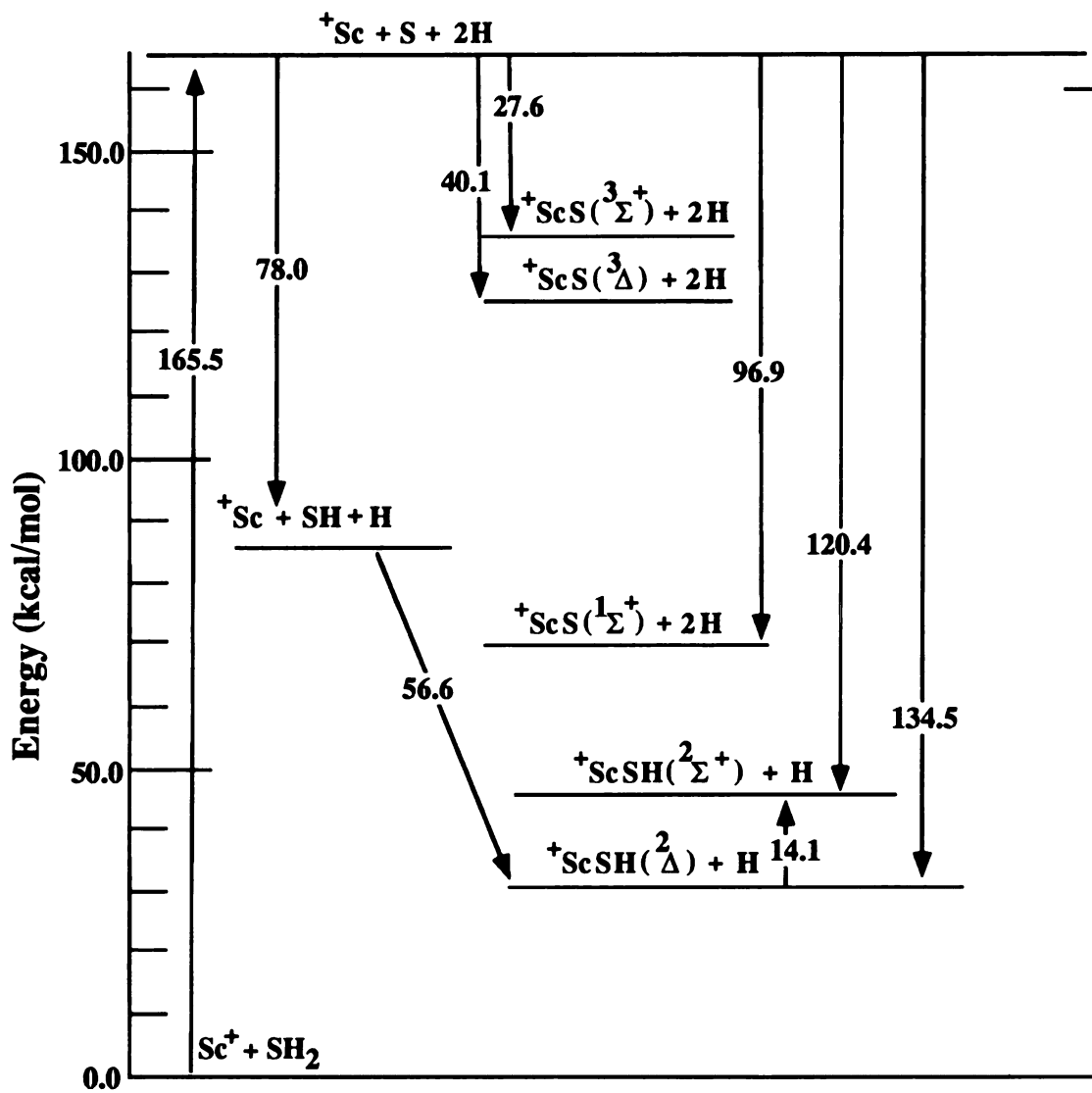


Figure 10. MCSCF+1+2 relative energies (kcal/mol) of selected $\text{Sc}^+ + \text{SH}_2$ products. Data from Ref(1).

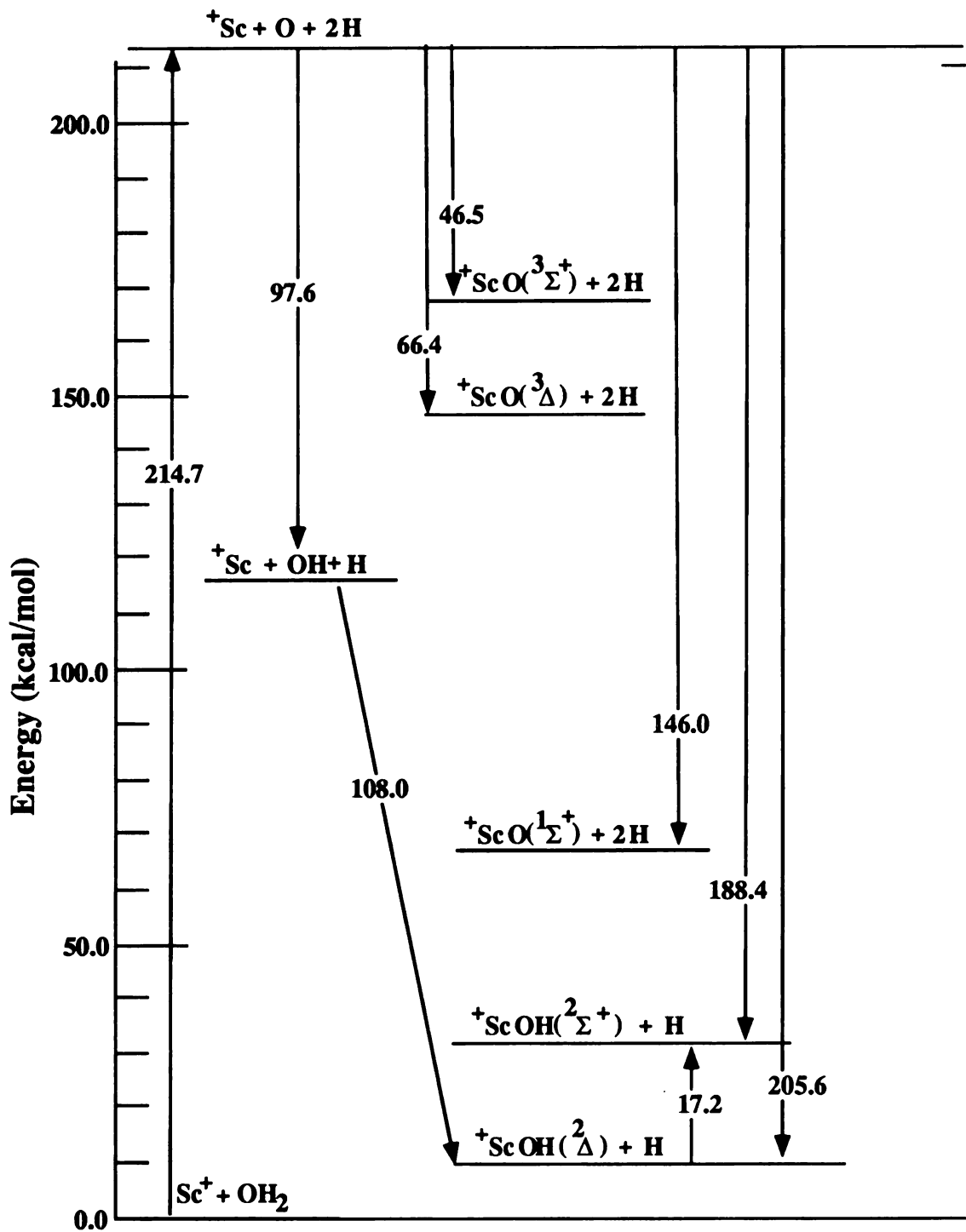


Figure 11. MCSCF+1+2 relative energies (kcal/mol) of selected $\text{Sc}^+ + \text{SH}_2$ products. Data from Ref(2).

The interaction energy for the other significant electrostatic species, $^+Sc \cdots SeH_2$, is expected to be approximately equal to that computed for $^+Sc \cdots SH_2$ (11.4 kcal/mol)¹ and is not expected to be the ground state. This is based on similarities of the (MCSCF) dipole moments¹¹ computed for SH_2 (1.27 D, experimental value¹² is 0.97 D) and SeH_2 (1.09 D) and the similar structures of SH_2 and SeH_2 .¹¹

SUMMARY

1) The ground state of ^+ScSe is the triply bonded $^1\Sigma^+$ state with a bond strength of 84.6 kcal/mol. The lowest triplet state is the $^3\Delta$ with two π bonds and a bond energy of 31.2 kcal/mol, while the $^3\Sigma^+$ state is also a π, π doubly bonded species with a bond energy of 28.7 kcal/mol.

2) The ^+ScSeH ground state is of $^2\Delta$ symmetry with a formation energy of 118.6 kcal/mol and a ^+Sc-SeH bond strength of 47 kcal/mol. The $^2\Sigma^+$ state differs only in the structure of the Sc spectator electron and has a formation energy of 115.4 kcal/mol. The formation of the $^+ScSe-H$ bond induces a Sc-Se σ dative bond, which stabilizes the species by 15 kcal/mol. This stabilization is due to the Se 4s orbital interacting with Sc^+ .

3) The small induced σ stabilization energy computed for ^+ScSeH (15 kcal/mol) suggests the gas phase reaction $Sc^+ + SeH_2$ will yield the product $H_2 \cdots ^+ScSe$, exoergic by approximately 37.5 kcal/mol.

REFERENCES

REFERENCES

- 1 J.L.Tilson, J.F. Harrison, J. Phys. Chem., 96, 1667 (1992).
- 2 J.L.Tilson, J.F. Harrison, J. Phys. Chem., 95, 5097 (1991).
- 3 T.F. Magnera, D.E. David and J. Michl, J. Am. Chem. Soc., 111, 4100 (1989).
- 4 T.H. Dunning, Jr., J. Chem. Phys., 66, 1382 (1977).
- 5 R.C. Raffenetti, J. Chem. Phys., 58, 4452 (1973).
- 6 R. Shepard, I. Shavitt, R.M. Pitzer, D.C. Comeau and M. Pepper, Int. J. Quant. Chem. Symp., 22, 149 (1988) and references therein.
- 7 J.L. Dunham, Phys. Rev., 41, 721 (1932).
- 8 C.E. Moore, Natl. Stand. Ref. Data. Ser., Natl. Bur. Stand. No. 35. Averaged over Mj values.
- 9 a) W.A. Goddard III, T.H. Dunning Jr., W.J. Hunt and P. Hay, J. Acc. Chem. Res., 6, 368 (1973).
b) W.A. Goddard III and L.B. Harding, Annu. Rev. Phys. Chem., 29, 363 (1978).
- 10 R.S. Mulliken, J. Chem. Phys., 23, 1833, 1841, 2338, and 2343 (1955). For a critique see J.O. Noell, Inorg. Chem. 21, 11 (1982).
- 11 J.L. Tilson and J.F. Harrison, unpublished results.
- 12 adapted from "CRC Handbook of Chemistry and Physics", R.C. Weast, Ed., CRC Press, Boca Raton, Fl., 63rd ed., 1982.
- 13 K.P. Huber and G. Herzberg, "Molecular Spectra and Molecular Structure", Van Nostrand Reinhold, New York, 1979.

- 14 E.J. Murad, *J. Geophys. Res.*, **83**, 5525 (1978).
- 15 a) M. Rosi and C.W. Bauschlicher Jr., *J. Chem. Phys.*, **92**, 1876 (1990).
b) M. Rosi and C.W. Bauschlicher Jr., *J. Chem. Phys.*, **90**, 7264 (1989).

APPENDIX A

APPENDIX A

ELECTRONIC STRUCTURE THEORY: TECHNIQUES

INTRODUCTION

This appendix is included to briefly illustrate and discuss those quantum mechanical techniques used throughout this work. It is not intended to be a rigorous and complete study, but rather a general outline with the appropriate references. The systems of interests are small molecules and techniques useful in their analysis will be discussed. In particular self consistent field^{1,2}(SCF) and some higher order techniques will be discussed.³⁻⁶ All reported calculations of molecular structure are of the ab-initio type. This means all results are from first principles without resort to experimental evidence with the exception of the nuclear charge. The electronic structure of molecules can be interpreted as the distribution of electrons in a system whose atoms are physically close enough to experience significant and, often, non-classical interactions. These interactions are generally in addition to the "classical" interactions of electrostatics and magnetostatics, and result specifically from the small physical sizes and distances. An example of such interactions would be the formation of bonds.

The fundamental equation used throughout this thesis is the Schroedinger equation⁷ (wave mechanics)

$$\mathcal{H}\Psi = i\hbar \frac{\partial}{\partial t} \Psi$$

and its equivalent Heisenberg formulation⁷ (matrix mechanics) where \mathcal{H} is the hamiltonian and Ψ is called the wavefunction. Ψ represents all the characteristics of the system. In general, both \mathcal{H} and Ψ have an explicit time dependence.

HAMILTONIAN

The hamiltonian is an operator that contains all the possible interactions upon the system and in an isotropic and homogenous space its eigenvalues may be identified with the total energy.⁸ If the hamiltonian contains no "explicit" time dependence, e.g., impinging electric fields, the time dependence may be separated out and for stationary states⁷ may be ignored. This is done, for example, by application of an integrating factor. When the time dependence has been separated out the Schroedinger equation reduces to

$$\mathcal{H}\Psi = E\Psi$$

where E is the total energy of the system represented by the wavefunction, Ψ , and is the response to the *actions* contained in the hamiltonian \mathcal{H} . The energy is a constant.

The hamiltonian operator for any atomic or molecular system may be written as

$$\mathcal{H} \equiv - \sum_{i=1}^n \frac{1}{2} \nabla_i^2 - \sum_{k=1}^{\lambda} \frac{1}{2M_k} \nabla_k^2 + \sum_{i=1}^n \sum_{j>i}^n \frac{1}{r_{ij}} + \sum_{k=1}^{\lambda} \sum_{p>k}^{\lambda} \frac{Z_p Z_k}{R_{kp}} - \sum_{i=1}^n \sum_{k=1}^{\lambda} \frac{Z_k}{r_{ik}} + \mathcal{V}(t)$$

Here r_i denotes the coordinates of the i^{th} electron, R_k denotes the k^{th} nuclear coordinate and Z_k the k^{th} nuclear charge. The terms⁹ $-\frac{1}{2}\nabla_i^2$ and $-\frac{1}{2M_k}\nabla_k^2$ represents the kinetic energy of the i^{th} electron and k^{th} nucleus, respectively. The masses are in atomic units (au) with m_e (the electron mass) = 1 au. $\frac{1}{r_{ij}}$, $\frac{Z_p Z_k}{R_{kp}}$, and $\frac{Z_k}{r_{ik}}$ represent the electron-electron, nuclear-nuclear and electron-nuclear coulomb interactions, respectively, and $\mathcal{V}(t)$ contains all other possible interactions, e.g., multipole, relativistic, and external fields.

The typical electronic structure calculation begins by eliminating all presumably irrelevant or negligible terms from the hamiltonian. Since most molecular calculations are for determination of quantities relative to the separated atoms or fragments, e.g., bond energies, many interactions common to both the molecular and atomic regimes cancel out and can be ignored. This often means relativistic terms are not included. The remaining hamiltonian becomes

$$\mathcal{H} \equiv -\sum_{i=1}^n \frac{1}{2}\nabla_i^2 - \sum_{k=1}^{\lambda} \frac{1}{2M_k}\nabla_k^2 + \sum_{i=1}^n \sum_{j>i}^n \frac{1}{r_{ij}} + \sum_{k=1}^{\lambda} \sum_{p>k}^{\lambda} \frac{Z_p Z_k}{R_{kp}} - \sum_{i=1}^n \sum_{k=1}^{\lambda} \frac{Z_k}{r_{ik}}.$$

The analytical solution of $\mathcal{H}\Psi = E\Psi$ would yield the exact electronic structure of any non-relativistic, gas-phase molecular system. Unfortunately, this expression is impossible to solve directly. A still further approximation is the Born-Oppenheimer^{1,2} (BO) approximation. Here the nuclear motion is presumed to be infinitely slow, relative to the electrons, allowing the electron distribution to be

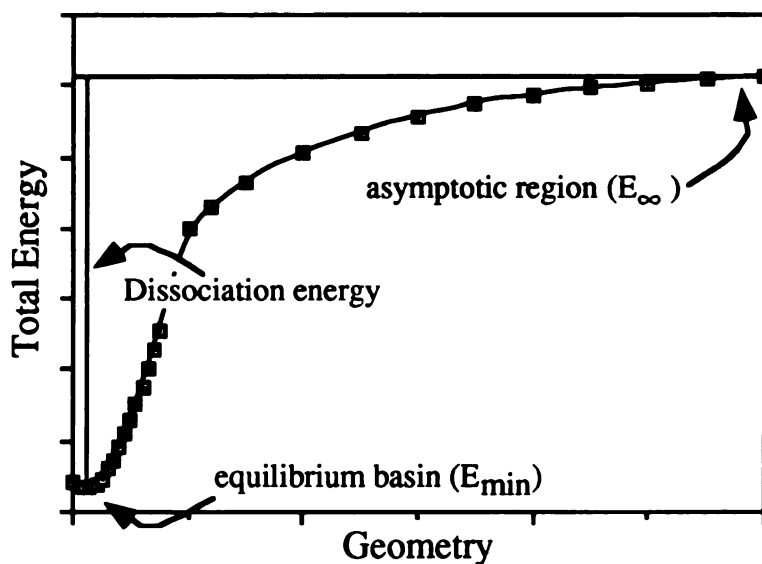
optimal for all geometries. This adiabatic¹¹ approximation assumes the nuclear and electronic motions are, essentially, independent of one another and that the wavefunction can, therefore, be written as a product of terms, viz.,

$$\Psi(\{r\};\{R\})\Phi(\{R\}).$$

Ψ represents the electronic wavefunction and is a function of the set of electron coordinates, $\{r\}$, and the set of geometry parameters, $\{R\}$. $\Phi(\{R\})$ is a nuclear function describing the vibrations and rotations of the system. This adiabatic approximation is useful but can fail for even fairly small systems.¹² The BO approximation is further simplified with the clamped-nuclei¹⁰ approximation where the kinetic energy of the nuclei is set identically to zero. The hamiltonian under these conditions becomes.

$$\mathcal{H} \equiv -\sum_{i=1}^n \frac{1}{2} \nabla_i^2 + \sum_{i=1}^n \sum_{j>i}^n \frac{1}{r_{ij}} + \sum_{k=1}^{\lambda} \sum_{p>k}^{\lambda} \frac{Z_p Z_k}{R_{kp}} - \sum_{i=1}^n \sum_{k=1}^{\lambda} \frac{Z_k}{r_{ik}} \quad (1)$$

and the Schroedinger equation becomes $\mathcal{H}\Psi = E\Psi$ where E is now a function of the nuclear geometry, i.e., $E = E(\{R\})$ or simply $E(R)$. This hamiltonian is that typically used in theoretical studies of isolated molecules and results in the notion of a potential curve.



In the above example, the total energy, $E(R)$, is plotted relative to a nuclear coordinate. The lowest energy (E_{\min}) is relative to the given coordinate while the asymptotic region corresponds to the separated atom limit (E_{∞}). The electronic dissociation energy (D_e) is defined as

$$D_e = E_{\infty} + E_{\min}$$

The hamiltonian, \mathcal{H} , contains one and two body interactions. The one body interactions are simply the hamiltonians for a one-electron system, viz

$$-\sum_{i=1}^n \frac{1}{2} \nabla_i^2 - \sum_{i=1}^n \sum_{k=1}^{\lambda} \frac{Z_k}{r_{ik}}$$

These hamiltonians have analytical solutions which are known.¹⁰

The electron-electron terms, $\sum_{i=1}^n \sum_{j>i}^n \frac{1}{r_{ij}}$, are two body interactions

describing the inter-electron (Coulomb) forces. The two body nuclear-nuclear interactions, $\sum_{k=1}^{\lambda} \sum_{p>k}^{\lambda} \frac{Z_p Z_k}{R_{kp}}$, are by construction a

parameter of the electronic wavefunction and so may be excluded from the hamiltonian and simply specified for a given molecular

geometry. The electronic hamiltonian, \mathcal{H}_e , is written as the sum $\mathcal{H}_e \equiv \hat{h}(1) + \hat{g}(1,2)$ where $\hat{h}(1)$ contains the hydrogenic (one body) terms and $\hat{g}(1,2)$ the (two body) electron-electron repulsion terms. For a hamiltonian in this form the total electronic (BO) energy may be written as

$$E(\mathbf{R}) = E_e + \sum_{k=1}^{\lambda} \sum_{p>k}^{\lambda} \frac{Z_p Z_k}{R_{kp}} \quad (2)$$

where E_e is the solution of $\mathcal{H}_e \Psi = E_e \Psi$ and the nuclear-nuclear terms are added to the total energy ad-hoc. Unless otherwise specified, the nuclear-nuclear terms will be assumed folded into the total energy for the remainder of this discussion.

CONSTRUCTION OF THE WAVEFUNCTION

The electronic hamiltonian, \mathcal{H}_e , contains all the information of the molecular system under study. If the electronic Schrodinger equation, $\mathcal{H}_e \Psi = E_e \Psi$, could be solved (or equivalently the hamiltonian matrix diagonalized) the wavefunction Ψ would tell us the exact electronic distribution and energy, the excited states, and allow us to determine the equilibrium geometry. Unfortunately this cannot be directly done. The inability to solve the Schrodinger equation is caused by the two-body electron-electron terms in the hamiltonian.

If, for example, $\hat{g}(1,2)$ were zero and electron spin were not considered, $\mathcal{H}_e \Psi = E_e \Psi$ would become

$$\left(-\sum_{i=1}^n \frac{1}{2} \nabla_i^2 - \sum_{i=1}^n \sum_{k=1}^{\lambda} \frac{Z_k}{r_{ik}} \right) \Psi = E_e \Psi$$

and the exact solution (Ψ) would be a simple product of hydrogenic wavefunctions of the form

$$\Psi = (\phi_1(1)\phi_2(2)\dots\phi_n(n)).$$

This is a rigorous result with ϕ an atomic or molecular orbital (MO). In this example, the *spin-less* electrons move independently of one another. Obviously, this approximation does not describe the electron correlation effects known to be important to most molecules. The addition of the $g(1,2)$ term allows for electron motion that is correlated, but also precludes an analytic solution. Since the hamiltonian of interest cannot be solved, the solution must be approximated in some way.

The energy of the Schrodinger equation, $\mathcal{H}_e \Psi = E_e \Psi$, can be expressed as

$$E = \frac{\langle \Psi | \mathcal{H}_e | \Psi \rangle}{\langle \Psi | \Psi \rangle}.$$

Where the bra-ket notation stands for

$$\langle \Psi | \mathcal{H}_e | \Psi \rangle = \int \Psi^* \mathcal{H}_e \Psi d\tau$$

with integration assumed over all variables (τ) and over all space. Ψ^* means the complex conjugate of Ψ . The set of solution wavefunctions (Ψ in all of its possible states) are orthogonal and can be interpreted as vectors that span the space of the hamiltonian.⁷ As in a three dimensional coordinate system, it is desirable to have these independent and orthogonal vectors normalized. The normalization criterion for Ψ can be written as $\langle \Psi | \Psi \rangle = 1$. For a normalized wavefunction, the energy expression becomes $E = \langle \Psi | \mathcal{H}_e | \Psi \rangle$ and is the integral form of the Schrodinger eigenvalue equation.

The hamiltonian operator is a Hermitian operator.⁷ This property causes all eigenvalues to be real and equally important, that a variation principle¹ applies. In particular, the variation principle states that for a function Φ used as an approximation to the exact function Ψ in the equation $E^{\text{exact}} = \langle \Psi | \mathcal{H}_e | \Psi \rangle$, the energy $E^\Phi \geq E^{\text{exact}}$. This also means that if $E^\Phi = E^{\text{exact}}$ then $\Phi = \Psi$. This suggests that if an arbitrary trial function (with the proper asymptotic and topological behavior) were selected and the energy (E^{trial}) computed we would obtain $E^{\text{trial}} \geq E^{\text{exact}}$. This affords a technique for determining the true wavefunction of a species. In essence we can select a function, calculate the energy, select a new function and calculate its energy and compare the two. The function yielding the lower energy is closer to the true function.

The intrinsic spin of electrons is an experimental fact and must be incorporated into any wavefunction containing electrons. Moreover, statistical theories¹³ of identical particles indicate that wavefunctions comprised of bosons (zero or integer spin particles) must be symmetric upon the interchange of particle coordinates

(including spin coordinates) while a wavefunction comprised of fermions (e.g., electrons) must be anti-symmetric upon coordinate interchange. This intrinsic requirement for electrons is called the Pauli exclusion principle^{1,10} and has profound effects on the electronic structure of molecules. In essence, this theory prevents two identical electrons from occupying the same region of space at the same time and is responsible for electron correlation in addition to the usual Coulomb repulsions. This requirement must also be incorporated into any electronic wavefunction. Noteworthy is that a spin based mechanics is not unique. A completely spin free quantum mechanical approach has been developed by Matsen¹⁴ using permutation operators.

The hamiltonian, \mathcal{H}_e , contains two terms; $\hat{h}(1)$ and $g(1,2)$. The necessary spin conditions, not part of this hamiltonian, must be incorporated into the wavefunction ad-hoc and are justified only in the usefulness of the results. The inclusion of spin into the wavefunction is often done with spin-orbitals.^{2,10} We assume the motion of each electron is represented by a spatial function, ϕ , with a spin of $1/2$ au and a spin projection in either the up (α) or down (β) directions. The complete function for the i^{th} electron is then written as $\phi(i)\alpha$ or $\phi(i)\beta$ with $\langle\alpha|\alpha\rangle = \langle\beta|\beta\rangle = 1$ and $\langle\alpha|\beta\rangle = 0$. $\phi(i)$ will be considered a spin function (orbital) unless otherwise specified. The final wavefunction must now satisfy the statistics of fermions, viz, the Pauli principle. If the wavefunction were simply a product of spatial functions this property can be introduced by means of a Slater determinant.¹⁰ Written in this way, the function is always antisymmetric upon coordinate interchange. In particular, for an n-

electron normalized wavefunction comprised of the spin orbitals, ϕ , the Slater determinant becomes

$$\Psi \approx \frac{1}{N!} \begin{bmatrix} \phi_1(1) \phi_1(2) \dots \phi_1(n) \\ \phi_2(1) \phi_2(2) \dots \phi_2(n) \\ \cdot \quad \cdot \quad \dots \\ \cdot \quad \cdot \quad \dots \\ \phi_n(1) \phi_n(2) \dots \phi_n(n) \end{bmatrix}$$

where the brackets indicate a determinant expansion. This wavefunction is often more succinctly expressed as $\Psi \approx \mathcal{A}(\phi_1(1), \phi_2(2) \dots \phi_n(n))$, where only the diagonal terms of the determinant are displayed and \mathcal{A} is called the antisymmetrizing operator. Finally, the energy for the molecular system using a Slater determinant wavefunction becomes

$$E = \left\langle \frac{1}{N!} \begin{bmatrix} \phi_1(1) \phi_1(2) \dots \phi_1(n) \\ \phi_2(1) \phi_2(2) \dots \phi_2(n) \\ \cdot \quad \cdot \quad \dots \\ \cdot \quad \cdot \quad \dots \\ \phi_n(1) \phi_n(2) \dots \phi_n(n) \end{bmatrix} \middle| \mathcal{H}_e \middle| \frac{1}{N!} \begin{bmatrix} \phi_1(1) \phi_1(2) \dots \phi_1(n) \\ \phi_2(1) \phi_2(2) \dots \phi_2(n) \\ \cdot \quad \cdot \quad \dots \\ \cdot \quad \cdot \quad \dots \\ \phi_n(1) \phi_n(2) \dots \phi_n(n) \end{bmatrix} \right\rangle$$

with the total energy computed as

$$E = \sum_{i=1}^n \langle h_i \rangle + \sum_{i=1}^n \sum_{i=1>j}^n (2J_{ij} - K_{ij}). \quad (3)$$

$\langle h_i \rangle$ is the one electron energy, J_{ij} is the coulombic energy between electrons i and j and K_{ij} is the non-classical exchange energy between electrons i and j . This can be equivalently written as

$$E = \sum_{i=1}^n \langle i | i \rangle + \sum_{i=1}^n (2 \langle ij | ij \rangle - \langle ij | ji \rangle) \quad (4)$$

where $\langle ij | ij \rangle$ is the coulomb energy and $\langle ij | ji \rangle$ the exchange energy. This notation implies a specific electron order. In particular, for the coulomb energy

$$\langle ij | ij \rangle = \int \frac{dv(1)dv(2) \phi_i(1)\phi_j(2) \phi_i(1)\phi_j(2)}{r_{12}}$$

while for the exchange energy

$$\langle ij | ji \rangle = \int \frac{dv(1)dv(2) \phi_i(1)\phi_j(2) \phi_j(1)\phi_i(2)}{r_{12}}$$

Using the hamiltonian, the variation and the pauli-exclusion principles, the approximate wavefunction for a molecular system may now be obtained. First, if the two-body hamiltonian term, $\mathcal{g}(1,2)$, were small relative to the $\mathcal{h}(1)$ term, the n-electron wavefunction would be *almost* an antisymmetrized product of spin orbitals (MOs), i.e.,

$$\Psi \approx \frac{1}{N!} \begin{bmatrix} \phi_1(1) \phi_1(2) \dots \phi_1(n) \\ \phi_2(1) \phi_2(2) \dots \phi_2(n) \\ \vdots \quad \quad \quad \ddots \\ \phi_n(1) \phi_n(2) \dots \phi_n(n) \end{bmatrix}$$

or simply $\mathcal{A}(\phi_1(1), \phi_2(2) \dots \phi_n(n))$.

The form of these orbitals is not yet specified. The total energy is now a function of the unknown orbitals $E(\phi_1, \phi_2, \dots, \phi_n)$. The variation principle states that the lowest energy would be obtained with the exact function. This also implies that with the orbital wavefunction model (Independent Particle Model or IPM) the lowest energy will be obtained when the best orbitals are selected for Ψ . There are many ways to select these orbitals, but the best way to begin is with the Hartree-Fock^{1,2} (HF) method.

The HF method begins with the expression

$$E^{\text{trial}} = \langle \mathcal{A}(\phi_1(1), \phi_2(2) \dots \phi_n(n)) | \mathcal{H}_e | \mathcal{A}(\phi_1(1), \phi_2(2) \dots \phi_n(n)) \rangle.$$

We then perform a functional derivative of E with respect to the orbitals and set them equal to zero.

$$\frac{\partial E}{\partial \phi_n} = 0$$

This expression will be satisfied when the orbitals, ϕ_n , are the optimum orbitals. The constraints on this equation are that $\langle \phi_i | \phi_j \rangle = \delta_{ij}$ and that variations in the orbitals themselves are orthogonal to all orbitals ($\langle \delta \phi_i | \phi_j \rangle = 0$). This procedure results in the HF equation

$$\mathcal{F}\phi_i = \epsilon_i \phi_i$$

where \mathcal{F} is the Fock operator, ϕ_i is the i^{th} optimized orbital and ϵ is the i^{th} Lagrangian multiplier⁹ often associated with the orbital (one-electron) energy. Solution of this equation yields the best possible

orbitals within the given IPM ansatz. The Fock operator for a closed shell system of n electrons has the form:

$$\mathcal{F} \equiv h(1) + \sum_{j=1}^{\frac{n}{2}} 2\mathcal{J}_j(1) - \mathcal{K}_j(1).$$

$h(1)$ is called the one-electron operator and includes the kinetic energy of the electron and the interactions of this electron with all nuclei.

$$h(1) = -\frac{1}{2}\nabla^2 - \sum_{k=1}^{\lambda} \frac{Z_k}{r_k}$$

$\mathcal{J}_j(1)$ is called the coulomb operator and has the form

$$\mathcal{J}_j(1) = \int \frac{dv(2)\phi_j(2)\phi_j(2)}{r_{12}}$$

$\mathcal{K}_j(1)$ is the exchange operator and has the form

$$\mathcal{K}_j(1) = \int \frac{dv(2)\phi_j(2)\mathcal{P}_{12}\phi_j(2)}{r_{12}}$$

where \mathcal{P}_{12} is a permutation operator.

The orbitals, ϕ_i , are spatial orbitals. The explicit representation of the electron spin has been integrated out yielding the \mathcal{J}_j and \mathcal{K}_j

operators. The one electron energy is obtained from the HF equation as

$$\langle \phi_j | \mathcal{F} | \phi_i \rangle = \epsilon_i \delta_{ij}$$

Both the \mathcal{J} and \mathcal{K} operators depend upon the solution orbitals ϕ_j and therefore the equation must be solved self consistently.

SCF EQUATION

The HF equations are coupled integro-differential equations. A numerical solution of these equations would yield the exact solution called the Hartree-Fock solution or the HF limit. The non-linear character of these equations makes a numerical solution very difficult to obtain. Moreover, the results could not be used to interpret the *Chemistry* of the system. A method amenable to larger molecules is the Self Consistent Field^{1,2} method (SCF). General mathematical theorems state that a function may be expanded into a complete set of basis functions so long as the global properties are the same.⁹ For example, expansion into polynomials and exponentials are frequently used in chemical applications. More true than not, most equations used in the physical sciences tend to result from the expansion of an unknown function into something else, e.g., Hooke's law as a truncated power series expansion.

This technique is applied to the SCF approach by expanding the unknown orbitals, ϕ , into a set of basis functions (basis set). This discretizes the HF problem by specifying the form of the orbitals to

within some unknown parameters. These expansion coefficients are then to be determined self consistently. In particular we can expand the spatial orbital ϕ_i into m basis functions as

$$\phi_i = \sum_{\mu=1}^m C_{i\mu} \chi_{\mu}$$

Where χ_{μ} is the μ^{th} basis function and $C_{i\mu}$, the expansion coefficient. Substituting the orbital expansions into the HF equation and writing it in a matrix form yields

$$\mathbf{FC}_i = \epsilon_i \mathbf{SC}_i$$

Where C_i is an m component column vector containing the expansion

coefficients, $\begin{pmatrix} C_{i1} \\ C_{i2} \\ \cdot \\ \cdot \\ C_{im} \end{pmatrix}$ ϵ is the one-electron energy, S is the

(non diagonal) basis function overlap matrix, $\begin{pmatrix} \chi_{11} & \chi_{12} & \cdot & \cdot & \chi_{1m} \\ \chi_{21} & \chi_{22} & \cdot & \cdot & \chi_{2m} \\ \cdot & \cdot & \cdot & \cdot & \cdot \\ \chi_{m1} & \chi_{m2} & \cdot & \cdot & \chi_{mm} \end{pmatrix}$

and, F , is the Fock matrix with the elements $\langle \chi_m | \mathcal{F} | \chi_{m'} \rangle$.

The solution of the HF equation yields the optimized orbitals in terms of C_i . These orbitals may then be used to compute the total energy.

Specifically, the complete set into which the orbitals are expanded must be of infinite size. This is not possible in practice and so a finite size basis is selected. The truncation of the basis set causes the energy to increase relative to the HF solution. This deviation can

be minimized by judicious choice of type and size of the basis set. Many basis functions have been examined but the Gaussian Type Functions (GTF) have found the greatest use.¹⁵ The use of GTF's and the algebraic solution to the electron integrals ($\langle ij | ij \rangle$) was first outlined by Boys.¹⁶ In the GTF expansion, functions of the form $C_i N_i r^{ng} \text{EXP}(\alpha_i r^2)$ are used to approximate the orbitals. Parameters in these basis functions are the exponents (α_i) which are selected and the expansion coefficients (C_i) which are to be determined in the SCF calculation. N_i is a normalization constant and r^{ng} is used to ensure the proper radial behavior. The basis functions only depend upon the radial coordinate (r). The angular coordinates are used to partition the Fock matrix into symmetry blocks^{7,9} and to select which basis functions can be combined together. They do not explicitly enter the numerical stage of the calculation. GTF functions have been tabulated for most of the atoms, and procedures for extending these basis sets to the molecular environment have been outlined.¹⁵

EXTENSIONS

The SCF procedure is a useful and often applied technique in the determination of molecular structure. It is especially useful for systems with a closed shell structure (all orbitals doubly occupied) and that contain no transition metals. SCF theories cannot model the dissociation of bonds nor other structural correlations important to most systems. Moreover, for transition metal systems with low lying excited states, the SCF can not include the important near degeneracy

effects. There are several methods for extending beyond the SCF method. These variational techniques are based upon the same general idea.

The SCF calculation starts with a single-determinant wavefunction occupied with n electrons. The orbitals are expanded into m basis functions with usually $n < m$. Since we expand the orbitals into m basis functions and only (at most) n are occupied, there are $m-n$ unoccupied "orbitals" left over. These are called virtual orbitals. Extensions to the SCF procedure use these orbitals to include correlation in molecular problem. Instead of using a single SCF determinant wavefunction, we start with a wavefunction consisting of many determinants. In these calculations all functions must carry the correct spin and angular momentum, and while a single determinant may not have the correct symmetry, several taken together might. A collection of determinants in this way is called a configuration state function (CSF). Computationally, however, the programs can often optimize the wavefunction using either CSFs or determinants. The additional determinants (configurations) are constructed by "exciting" one or more electrons in the SCF wavefunction to virtual orbitals. For example in a system of n electrons populating n orbitals and m basis functions with $(m-n)$ virtual orbitals we can create an "excited" determinant in the following way:

$$\Psi^{\text{SCF}} = \mathcal{A}(\phi_1(1), \phi_2(2) \dots \phi_n(n)) \rightarrow \Psi^* = \mathcal{A}(\phi_1(1), \phi_{n+1}(2) \dots \phi_n(n))$$

Where now electron 2 occupies the (n+1)th orbital (virtual). This is an example of a single excitation. Multiple simultaneous excitations may also be included. The maximum excitation level is dictated by the number of electrons and the size of the basis set. A typical wavefunction with single, double, etc. excitations is shown below.

$$\Psi = \Psi_{\text{SCF}} + \sum_i C_i \Psi_i + \sum_{ij} C_{ij} \Psi_{ij} + \sum_{ijk} C_{ijk} \Psi_{ijk} + \dots$$

The wavefunction, Ψ , is an expansion in terms of electron excitation level with (typically) the SCF determinant as the first and usually dominant term. The *initial* function from which excitations are taken is often called the reference space. The additional determinants reflect the level of excitation: 1, 2, or 3 electrons, etc. These excitations can be as few as 2 up through the number of electrons in the system.

The selection of these additional determinants and choice in orbitals (MOs), called the one particle basis, is what generally distinguishes the different available ab-initio techniques. Configuration Interaction^{3,4} (CI), Generalized Valence Bond⁷ (GVB), Coupled Cluster¹⁷ (CC), etc. techniques are theoretically different procedures for adding determinants to the wavefunction. Many of these techniques require previously determined MOs from which these determinants are constructed. The variation principle is then used to optimize the expansion coefficients.

The Multiconfigurational SCF⁵ (MCSCF) technique is a procedure for optimizing the expansion coefficients and the orbitals

themselves. In practice the MCSCF requires fewer determinants relative to the CI for a given accuracy. In the limit of an infinite basis set and full excitations (all electrons) the MCSCF = CI. The inclusion of correlation is not limited to adding determinants. The success of the GVB technique is that while multiple determinants are included, the orbital basis is not initially orthogonal but can be transformed to an orthogonal set. This allows the GVB to carry fewer determinants while still properly describing important correlations in a molecule. Some workers use an orbital basis that is non-orthogonal.¹⁸

The studies performed in this thesis typically began with a MCSCF calculation. This calculation is relatively compact with only a few determinants selected and allows an interpretation in terms of orbitals. The energetics were computed with a MCSCF+1+2 function. In this configuration interaction calculation, the first term in the wavefunction expansion is not the SCF determinant but the many-determinant MCSCF (MCSCF reference space). All single and double excitations into *excited* MCSCF configurations were then selected. Finally, the GVB+1+2 calculations were constructed from all single and double excitations from a GVB reference space.

REFERENCES

REFERENCES

1. A.Szabo and N.S. Ostlund, "Modern Quantum Chemistry: Introduction to Advanced Electronic Structure Theory", Macmillan Pub. Co., Inc., New York, N. Y., 1982.
2. H.F. Schaefer III, "The Electronic Structure of Atoms and Molecules", Addison-Wesley Pub. Co., Reading, Mass., 1972.
3. I. Shavitt, "The Method of Configuration Interaction" in "Methods of Electronic Structure Theory", edited by H. F. Schaefer III, Plenum Press, New York, 1977.
4. A.C. Wahl and G. Das, "The Configuration Self Consistent Field Method" in "Methods of Electronic Structure Theory", edited by H. F. Schaefer III, Plenum Press, New York, 1977.
5. a) R. Shepard, "Ab-Initio Methods In Quantum Chemistry II," Advances in Chemical Physics, edited by K. P. Lawley, Wiley, New York, 1987.
b) T.H. Dunning, Jr., "Multiconfigurational Wavefunctions for Molecules: Current Approaches" in "Methods of Electronic Structure Theory", edited by H. F. Schaefer III, Plenum Press, New York, 1977.
6. a) F.W. Bobrowicz and W.A. Goddard III, "The Self Consistent Field Equations for Generalized Valence Bond and Open-Shell Hartree-Fock Wavefunctions" in "Methods of Electronic Structure Theory", edited by H. F. Schaefer III, Plenum Press, New York, 1977.
b) W.A. Goddard III, T. H. Dunning, Jr., W. J. Hunt, P. J. Hay, Acc. Chem. Res., 6, 368, (1973).
c) W.A. Goddard III, L. B. Harding, Ann. Rev. Phys. Chem., 29, 363, (1978).

7. E. Merzbacher, "Quantum Mechanics", 2nd. ed., John Wiley and Sons, New York, 1970.
8. J.B. Marion, "Classical Dynamics of Particles and Systems", 2nd. ed., Academic Press, Inc., New York, 1970.
9. G. Arfken, "Mathematical Methods for Physicists", 3rd. ed., Academic Press, New York, 1985.
10. I.N. Levine, "Quantum Chemistry", 2nd. ed., Allyn and Bacon, Inc., Boston, 1974.
11. a). F.T. Smith, Phys. Rev., 179, 111, (1969).
b). L.S. Cederbaum and H. Koppel, Chem. Phys. Let., 87, 14, (1982).
12. a) A.S. de Meras, M-B. Lepetit and J. P. Malrieu, Chem. Phys. Let., 172, 163, (1990).
c) L.R. Kahn and P.J. Hay, J. Chem. Phys., 61, 3530, (1974).
d) H.J. Werner and W. Meyer, J. Chem. Phys., 74, 5802, (1981).
13. D.A. McQuarrie, "Statistical Mechanics", Harper and Row, New York, 1973.
14. a) F.A. Matsen, Adv. Quantum Chem., 1, 59 (1964).
b) F.A. Matsen, J. Am. Chem. Soc., 92, 3525 (1970).
15. a) K. Faegri, Jr., H.J. Speis, J. Chem. Phys., 86, 7035 (1987) .
b) B.H. Botch, T.H. Dunning, Jr. and J.F. Harrison, J. Chem. Phys., 75, 3466, (1981).
c) P.J. Hay, J. Chem. Phys., 66, 4377, (1977).
d) R.D. Bardo and K. Ruedenberg, J. Chem. Phys., 60, 918, (1974).

- e) R.D. Bardo and K. Ruedenberg, *J. Chem. Phys.*, 59, 5966, (1972).
 - f) R.D. Bardo and K. Ruedenberg, *J. Chem. Phys.*, 59, 5956, (1973).
 - g) T.H. Dunning, Jr., *J. Chem. Phys.*, 53, 2823, (1970).
 - h) T.H. Dunning, Jr. and P.J. Hay, "Gaussian Basis Sets for Molecular Calculations" in "Methods of Electronic Structure Theory", edited by H. F. Schaefer III, Plenum Press, New York, 1977.
16. S.F. Boys, *Proc. Roy. Soc. (London)*, A200, 542, (1950).
17. a) W.D. Laidig and R.J. Bartlett, *Chem. Phys. Lett.*, 104, 424, (1984).
- b) R.J. Bartlett, *J. Phys. Chem.*, 93, 1697, (1989).
18. L. Noodelman and E.R. Davidson, *Chem. Phys.*, 109, 131 (1986).

APPENDIX B

APPENDIX B

LISTING OF PUBLICATIONS

Included here is a listing of publications resulting from this dissertation.

1. "The Electronic and Geometric Structures of Products of the $\text{Sc}^+ + \text{H}_2\text{S}$ Reaction" J. L. Tilson and J. F. Harrison, *J. Phys. Chem.*, 96,1667, (1992).
2. "The Electronic and Geometric Structures of Products of the $\text{Sc}^+ + \text{H}_2\text{O}$ Reaction" J. L. Tilson and J. F. Harrison, *J. Phys. Chem.*, 95,5097, (1991).
3. "The Electronic and Geometric Structures of $^+\text{ScSe}$ and $^+\text{ScSeH}$ " J. L. Tilson and J. F. Harrison, accepted *J. Phys. Chem.*

MICHIGAN STATE UNIV. LIBRARI



31293010330425